



NTNU – Trondheim
Norwegian University of
Science and Technology

Preparation of PVAm/PSf composite hollow fibers for flue gas applications

Petra-Kristine Johannessen

Chemical Engineering and Biotechnology

Submission date: June 2012

Supervisor: May-Britt Hägg, IKP

Co-supervisor: Marius Sandru, SINTEF

Norwegian University of Science and Technology
Department of Chemical Engineering

Declaration of compliance

I declare that this work has been done independently according to the exam regulations of the Norwegian University of Science and Technology.

Trondheim 15.06.2012

Petra-Kristine Johannessen

Petra-Kristine Johannessen

Preface

This master thesis was carried out at the Department of Chemical Engineering at the Norwegian University of Science and Technology. The work was performed in the period 20th January 2012 to 15th June 2012.

First I wish to thank Professor May-Britt Hägg for giving me the chance to work with the exciting and important field gas separation by use of membrane technology. I wish to thank my co-supervisor Dr. Marius Sandru for being so helpful, available, dedicated and easy to ask for help and advice both in the laboratory and about the report. I would like to also give a special thanks to the other members of the Memfo group for creating a positive working environment throughout the year.

I would like to thank Ola S. Hjetland for proof reading.

Abstract

Polysulfone (PSf) hollow fibres as support for Fixed-Site-Carrier (FSC) polyvinylamine (PVAm)/PSf composite membranes used for CO₂ capture were attempted optimized by increasing the air gap and take-up speed during spinning. The goal was to produce fibres with a porous structure, a high CO₂ permeance, as few macrovoids and surface defects as possible. Most of the produced fibres coated with polydimethylsiloxane (PDMS) showed high CO₂ permeance but low CO₂/N₂ selectivity. This is most likely caused by big holes and defects present on the PSf fibre surface. The reason for these defects was determined to be too much elongational stress applied to the PSf fibres during spinning as a consequence of the high air gap and take-up speed, causing the top layer to be stretched leading to defects in the surface. It is to be noted that fibres produced during this project were the results of a very first spinning using the new spinning machine. This introduced several untested factors such as new spinneret, new take-up system and other factors affecting the hollow fibres produced.

Some of the spun PSf fibres were coated with PVAm and PDMS in order to produce PVAm/PSf composite membranes. The FSC composite membranes were tested by gas permeation at different pressure and with various sweep flow rates. When the pressure was increased, a strong decrease of CO₂/N₂ selectivity was observed. A decrease in CO₂/N₂ selectivity is expected to a certain degree due to saturation of the carriers, but the large decrease was believed to be caused by reopening of surface defects due to increased pressure. This was supported by an increase in N₂ permeance when the pressure was increased. The CO₂ permeance decreased more for the PVAm/PSf composite membrane compared to the PSf fibre coated only with PDMS. The reason for this could be that PVAm penetrated into the porous structure of the PSf support, reducing the gas permeance through the membrane, caused by the large number of surface defects and holes at the surface of the PSf supports. The PVAm/PSf composite membranes did not obtain a better CO₂/N₂ selectivity than the best PVAm/PSf composite membrane from the specialization project. The best obtained results was a CO₂ permeance of 0.15 m³(STP)/(m² bar h) and a CO₂/N₂ selectivity of 88.

The PVAm concentration was increased from 0.2% to 1% in the PVAm/PSf blend during the master thesis. This was performed by introducing more of the selective material PVAm directly into the spinning dope. The desired result was an increase in effect of PVAm polymer on the separation properties of the 1% PVAm/PSf blend hollow fibres. The influence and presence of the 0.2% PVAm content in the PVAm/PSf blend membrane was detected by differential scanning calorimetry (DSC) and during gas permeation tests with humidity. The CO₂/N₂ selectivity increased with increased relative humidity in the feed, which increases the ability of the PVAm to transport CO₂ molecules by facilitated transport. The 1% PVAm/PSf blend hollow fibres showed no indication of the presence of PVAm during DSC. One reason for this result may be that PVAm and PSf had separated, because the dope solution was ready some time before the spinning rig was available. This might have caused uneven distribution of PVAm. Another reason could be that PVAm and PSf had reacted in the polymer solution. As the amount of PSf is much higher than PVAm, the DSC curve would indicate mostly PSf. This is supported by the indication of PVAm from the humidity test. The results from gas permeation tests showed that the 1% PVAm/PSf blend membrane had better separation properties than the 0.2% PVAm/PSf blend membrane. This indicates that PVAm was present in the 1% PVAm/PSf blend membrane as well, even though the DSC gave no evidence of PVAm. One of the 1% PVAm/PSf blend membranes exhibited a CO₂ permeance of 0.05 m³(STP)/(m² bar h) and a CO₂/N₂ selectivity from 57 to 133 when the sweep flow rate changes from 5 to 47 ml/min. For pressure ranging from 1.2 bar to 8 bar, the membrane had a CO₂ permeance from 0.1 to 0.07 m³(STP)/(m² bar h) and a CO₂/N₂ selectivity from 70 to 56.

Sammendrag

Hule fibre av polysulfon (PSf) som støttemembran for en polyvinylamin (PVAm)/PSf komposittmembran for CO₂-fangst, ble forsøkt optimalisert ved å øke luftgapet og opptakningshastigheten under spinning. I en slik komposittmembran er bærerne tilført av aminogruppene i PVAm-en, som selektivt transporterer CO₂, fastsatt i bestemte posisjoner. Dette kalles en "Fixed-Site-Carrier"-membran (FSC). Målet var å produsere fibre med en porøs struktur, høy CO₂-permeans, og så få hull og overflatedefekter som mulig. De fleste fibre overflatebehandlet med polydimethylsiloxan (PDMS) ga høy CO₂-permeans, men lav CO₂/N₂ selektivitet. Grunnen ble vurdert til å være for høy strekkspenning påført fibre under spinning, som en konsekvens av det høye luftgapet og opptakningshastigheten. Dette førte til at topplaget ble strukket, noe som ga defekter i overflaten. Det var første gang fibre ble spunnet på denne spinningmaskinen, og dette introduserte flere utestede faktorer som ny spinneret, nytt opptakningssystem og andre faktorer som kan påvirke de produserte fibre.

Noen av de produserte fibre ble overflatebehandlet med PVAm og PDMS for å lage PVAm/PSf komposittmembraner. Disse membranene ble testet ved ulike trykk og "sweep"-strømningsrater. Da trykket ble økt, ble det observert en sterk nedgang i CO₂/N₂-selektiviteten. En nedgang er forventet til en hvis grad på grunn av metning av bærere, men den kraftige nedgangen er antatt å skyldes gjenåpning av overflatedefekter når trykket øker. Dette underbygges videre av at N₂-permeansen økte betraktelig når trykket økte. CO₂-permeansen ble redusert mye i forhold til de PSf-fibre som bare var overflatebehandlet med PDMS. En grunn til dette kan være at PVAm har trengt inn i den porøse strukturen til PSf-støtten, og redusert gasspermeansen gjennom membranen. Denne inntrengingen av PVAm skyldes det store antall overflatedefekter i PSf-støtten. De produserte PVAm/PSf komposittmembranene oppnådde ikke så god CO₂/N₂ selektivitet som den beste PVAm/PSf komposittmembranen fra spesialiseringsprosjektet. De beste oppnådde resultatene var en CO₂-permeans på 0,15 m³(STP)/(m² bar h) og en CO₂/N₂-selektivitet på 88.

PVAm konsentrasjonen ble økt fra 0,2% til 1% i en PVAm/PSf blandingsmembran fortsatte i masteroppgaven. Dette ble gjort ved å introdusere det selektive materialet PVAm direkte i spinningløsningen. Det ønskede resultatet var en økning i effekten av PVAm på separasjonsegenskapene til 1% PVAm/PSf blandingsmembranen. 0.2% PVAm/PSf blandingsmembranen viste innhold av PVAm da den ble testet med differensiell skanningkalorimetri (DSC) og ved gasspermeasjonstesting med varierende relativ fuktighet på fødegassen. CO₂/N₂-selektiviteten økte med økt relativ fuktighet i fødegassen, da tilstedeværelse av vann øker evnen PVAm har til å transportere CO₂ ved fasilitert transport. 1% PVAm/PSf blandingsmembranen viste ingen tilstedeværelse av PVAm ved DSC- målinger, men ved relativ fuktighetstesting viste den innhold av PVAm. En grunn for disse resultatene kan være at PVAm og PSf har separert, siden spinningløsningen var klar en stund før spinninganlegget var ledig. Dette kan ha ført til områder med mer PVAm og områder med mindre eller helt uten PVAm. En annen grunn kan være at PVAm og PSf har reagert i polymerløsningen. Dette vil føre til at membranen vil få egenskaper fra begge polymerene, siden det er mye større mengde av PSf kan dette være grunnen til at DSC-resultatene gir liten indikasjon av PVAm. Resultatene fra gasspermeasjonstestene viste at 1% PVAm/PSf blandingsmembranen hadde bedre separasjonsegenskaper enn 0.2% PVAm/PSf blandingsmembranen. Dette indikerer at PVAm er tilstede i 1% PVAm/PSf blandingsmembranen, selv om DSC ikke viste noe tegn til PVAm. En av 1% PVAm/PSf blandingsmembranene hadde en CO₂-permeans på 0,05 m³(STP)/(m² bar h) og en CO₂/N₂-selektivitet fra 57 til 133 da "sweep"-strømningsraten ble endret fra 5 til 47 ml/min. For en trykkforandring fra 1,2 til 8 bar hadde den en CO₂-permeans fra 0,1 til 0,07 m³(STP)/(m² bar h) og en CO₂/N₂ selektivitet fra 70 til 56.

Index

Declaration of compliance	i
Preface	ii
Abstract	iii
Sammendrag	iv
List of figures	viii
List of tables	xii
List of symbols and abbreviations	xiii

Chapter 1	Introduction	1
1.1	Aim of the project	2
Chapter 2	Literature study	4
2.1	Polysulfone hollow fibre support	4
2.2	Mechanism for formation of macrovoids	5
2.3	Hollow fibre spinning	5
2.3.1	Dope composition	5
2.3.2	Spinning procedure	8
2.4	Coating techniques	12
2.5	Effects of coating conditions	14
2.5.1	Effect of the support membrane	14
2.5.2	Number of sequential coatings	14
2.5.3	Effect of coating solution concentration	15
2.5.4	Effect of viscosity	16
2.5.5	Effect of pH	16
2.5.6	Effect of hydrophilicity of coating materials	16
2.6	Composite membranes	16
2.7	Blend membranes	18
Chapter 3	Theory	20
3.1	Membrane definition	20
3.2	Membrane classification	20
3.2.1	Composite membranes	20
3.2.2	Polymer blend membranes	21
3.2.3	Carrier membranes	21
3.2.4	Membrane of polysulfone	22
3.3	Gas transport in membranes	22
3.3.1	Driving force	22
3.3.2	Transport in porous membranes	22
3.3.3	Transport through dense membranes	24
3.3.4	Transport through a composite membrane	26
3.3.5	Facilitated transport	26

3.4	Membrane terminology	27
3.4.1	Process parameters	27
3.4.2	Flux	28
3.4.3	Membrane selectivity	28
3.4.4	Process selectivity	28
3.4.5	Permeance	29
3.4.6	Permeate purity	29
3.4.7	Hydrophilic and hydrophobic	29
3.4.8	Complete mixing model	29
3.5	Membrane formation	30
3.5.1	Ternary system	30
3.5.2	Mechanism of membrane formation	30
3.5.3	Formation of macrovoids	31
3.6	Preparation techniques for hollow fibres	32
3.6.1	Membrane forming parameters	32
3.6.2	Spinning parameters	34
3.7	Membrane coating	34
3.7.1	Dip-coating	34
Chapter 4	Experimental	36
4.1	Materials and chemicals	36
4.2	Spinning of PVAm/PSf blend membrane	36
4.2.1	Dope preparation	36
4.2.2	Spinning	37
4.3	Making of the composite membranes	38
4.3.1	Preparation of PDMS and PVAm coating solution	38
4.3.2	Coating of hollow fibres	38
4.4	Characterization methods	40
4.4.1	Scanning electron microscopy (SEM)	40
4.4.2	Differential scanning calorimetry (DSC)	40
4.5	Gas permeation test	40
4.5.1	Module making	40
4.5.2	Testing of membrane with mixed gas permeation	41
Chapter 5	Results and discussion	43
5.1	Optimizing the PSf support	43
5.1.1	Influence of polymer concentration	44
5.1.2	The influence of air gap	45
5.1.3	The influence of take-up speed	46
5.1.4	The influence of dope and bore flow rate	48
5.1.5	Summary of effects of spinning conditions	49
5.2	Composite membranes	51
5.2.1	Gas permeation tests for the different PVAm/PSf FSC composite membranes	51
5.2.2	Comparison of the FSC composite membranes with the best obtained composite membrane made in the specialization project	59

5.3	The importance of the PSf support and the PVAm selective coating layer	62
5.4	Blend hollow fibre membranes	63
5.4.1	Preparation of blend membranes	63
5.4.2	Gas permeation tests for both hollow fibre blends	70
5.5	Comparison of the blend and composite membranes	78
5.5.1	Comparison of pressure influence	79
5.5.2	Comparison of sweep flow rate influence	82
5.5.3	Summary	84
5.6	Uncertainties	85
Chapter 6	Conclusion	88
6.1	PSf support	88
6.2	PVAm/PSf FSC composite membrane	88
6.3	PVAm/PSf blend membrane	89
Chapter 7	Further work	91
7.1	Optimizing the PSf hollow fibre support	91
7.2	Further investigation of PVAm/PSf composite membrane	91
7.3	Further investigation of PVAm/PSf blend membrane	91
Chapter 8	References	93
Appendix A	Risk assessment	I
Appendix B	SEM pictures	III

List of figures

Figure 1.1:	Robeson upper bound for the trade-off between CO ₂ permeability and CO ₂ /N ₂ selectivity [8]	2
Figure 2.3.1.1:	SEM pictures of PSf flat sheet membranes prepared with glycerol in the dope (left picture) and without glycerol in the dope (right picture) [25]	7
Figure 2.3.1.2:	SEM pictures of PSf flat sheet membranes prepared with THF in the dope (left picture) and without THF in the dope (right picture) [25].	8
Figure 2.3.2.1:	Cross section of different fibres spun at different air gaps [29]	9
Figure 2.3.2.2:	Cross section of 1% PVAm/PSf blend [11] and 0.2% PVAm/PSf blend [12]	10
Figure 2.3.2.3:	Morphology of inner skin layer of fabricated membranes with different solvent concentration in the bore fluid. (a) 0% NMP, (b) 50% NMP, (c) 70% NMP and (d) 90% NMP [34]	11
Figure 2.3.2.4:	Morphology of inner surface of fabricated membranes with different solvent concentration in the bore fluid. (a) 0% NMP, (b) 50% NMP, (c) 70% NMP and (d) 90% NMP [34]	12
Figure 2.4.1:	Equipment setup for continuous coating of hollow fibres [37]	13
Figure 2.4.2:	Equipment setup for inside coating (1) Rubber bulb (2) solution cell (3) membrane module (4) overflow indicator [38]	13
Figure 2.4.3:	(a) Spinning setup (b) schematic drawing of the spinneret. A is the coating solution channel, B is the dope solution channel and C is the bore fluid channel [40]	14
Figure 2.5.2.1:	Plot of selectivity against feed pressure for PSf fibre with one and two coatings of 5% PDMS [11]	15
Figure 2.7.1:	(a) The influence of relative feed humidity on selectivity for 0.2% PVAm/PSf blend coated two times with 5% PDMS. (b) Selectivity of % PVAm/PSf blend fibre coated two times with 5% PDMS plotted against the relative humidity of the feed. [11]	19
Figure 3.2.1.1:	Single layer composite membrane [16]	20
Figure 3.2.1.2:	Multilayer composite membrane [16]	21
Figure 3.2.4.1:	The chemical structure of polysulfone [5]	22
Figure 3.3.2.1:	Different mechanisms in a porous membrane [16]	23
Figure 3.3.3.1:	Transport through a dense membrane [16]	25
Figure 3.3.5.1:	Transport without and with carrier and uncoupled and coupled transport [5]	26
Figure 3.3.5.2:	Facilitated transport for a PVAm membrane [10]	27
Figure 3.4.1.1:	Schematic drawing of membrane module with flow descriptions [5]	28
Figure 3.5.1.1:	Schematic drawing of a ternary system [16]	30
Figure 3.5.2.1:	Ternary diagram for instantaneous demixing and delayed demixing [5]	31
Figure 3.5.1:	Schematic drawing of a dry-wet process [5]	32
Figure 3.6.1.1:	Forming of dense skin layer on the inside, the outside or on both sides of the hollow fibre [16]	33
Figure 3.7.1.1:	Schematic drawing of dip-coating [39]	35

Figure 4.3.2.1: Dip-coating procedure	39
Figure 4.5.1.1: Module with hollow fibres	41
Figure 4.5.2.1: Gas permeation set up [15]	41
Figure 5.1.1.1: SEM pictures of cross section and wall morphology. The left pictures are the 29% PSf hollow fibre and the right pictures are the 32% PSf hollow fibre.	44
Figure 5.1.2.1: SEM pictures of fibres with air gap of 61(B) and 50 cm (O)	46
Figure 5.1.3.1: SEM pictures of PSf fibres with a take-up speed of 18 m/min (W) and 20 m/min (J)	47
Figure 5.1.4.1: SEM pictures of fibres with a dope flow rate of 1 ml/min (B) and 2 ml/min (W)	48
Figure 5.1.5.1: SEM pictures of the outer surface of the different PSf hollow fibres	50
Figure 5.2.1: SEM pictures showing coating thickness for the B, J and O type PSf hollow fibre coated three times with PVAm and one times with PDMS	51
Figure 5.2.1.1: Selectivity of FSC composite membranes with B and O as the support as a function of pressure	53
Figure 5.2.1.2: Left: PSf hollow fibre B coated three times with 3% PVAm and one time with 5% PDMS Right: Uncoated PSf hollow fibre B	54
Figure 5.2.1.3: Left: PSf hollow fibre O coated three times with 3% PVAm and one time with 5% PDMS Right: Uncoated PSf hollow fibre O	54
Figure 5.2.1.4: CO ₂ and N ₂ permeance for the PVAm/PSf composite membrane with B as support as a function of the sweep flow rate	55
Figure 5.2.1.5: CO ₂ and N ₂ permeance for the PVAm/PSf composite membrane with J as support as function of the sweep flow rate	55
Figure 5.2.1.6: CO ₂ and N ₂ permeance for the PVAm/PSf composite membrane with O as support as a function of the sweep flow rate	55
Figure 5.2.1.7: Process and membrane CO ₂ /N ₂ selectivity for the PVAm/PSf composite membrane with B as support as a function of the sweep flow rate	56
Figure 5.2.1.8: Process and membrane CO ₂ /N ₂ selectivity for the PVAm/PSf composite membrane with J as support as a function of the sweep flow rate	57
Figure 5.2.1.9: Process and membrane CO ₂ /N ₂ selectivity for the PVAm/PSf composite membrane with O as support as function of the sweep flow rate	57
Figure 5.2.1.10: The CO ₂ purity of PVAm/PSf FSC composite membranes with B, J and O as support as a function of the sweep flow rate	58
Figure 5.2.2.1: CO ₂ /N ₂ selectivity for the PVAm/PSf FSC composite membranes with B and D as support as a function of pressure	60
Figure 5.2.2.2: Permeance of CO ₂ and N ₂ against sweep flow rate for the PVAm/PSf composite membrane with D and J as support	61
Figure 5.2.2.3: CO ₂ /N ₂ selectivity against sweep flow rate for the PVAm/PSf composite membrane with D and J as support	61
Figure 5.2.2.4: The CO ₂ purity of the PVAm/PSf FSC composite membranes with D and J as the support as a function of the sweep flow rate	62
Figure 5.4.1.1: DSC measurements of hollow PVAm/PSf blend hollow fibre nr 1 for three cycles.	65
Figure 5.4.1.2: DSC measurements of PVAm/PSf blend hollow fibre nr 2 for three cycles.	65

Figure 5.4.1.3: DSC measurements of dry PVAm/PSf polymer from dope solution for three cycles [11]	66
Figure 5.4.1.4: DSC measurements for pure PSf, 0.2% PVAm/PSF and 1% PVAm/PSf blends	67
Figure 5.4.1.5: DSC measurements for pure PSf, 0.2% PVAm/PSF and 1% PVAm/PSf blends	67
Figure 5.4.1.6: Cross section and wall cross section of 1% PVAm/PSf blend nr 1 spun in this project	68
Figure 5.4.1.7: Cross section and wall cross section of 1% PVAm/PSf blend nr 2 spun in this project	68
Figure 5.4.1.8: Surface of 1% PVAm/PSf blend nr 1 spun in this project	69
Figure 5.4.1.9: Surface of 1% PVAm/PSf blend nr 2 spun in this project	69
Figure 5.4.1.10: SEM pictures of the thickness of the coating layer when all the blend fibres were coated two times with 5% PDMS. The left pictures are 1% PVAm/PSf blend nr 1, the picture in the middle is the 1% PVAm/PSf blend nr 2 and the right picture is the 0.2% PVAm/PSf blend membrane	69
Figure 5.4.2.1: CO ₂ /N ₂ selectivity for the different blend membranes as a function of pressure	71
Figure 5.4.2.2: CO ₂ and N ₂ permeance for 1% PVAm/PSf blend hollow fibre nr 1 coated two times with 5% PDMS as a function of the sweep flow rate on a logarithmic scale	72
Figure 5.4.2.3: CO ₂ and N ₂ permeance for 1% PVAm/PSf blend hollow fibre nr 2 coated two times with 5% PDMS as a function of the sweep flow rate on a logarithmic scale	73
Figure 5.4.2.4: CO ₂ and N ₂ permeance for 0.2% PVAm/PSf blend hollow fibre coated two times with 5% PDMS as a function of the sweep flow rate on a logarithmic scale [11]	73
Figure 5.4.2.5: CO ₂ /N ₂ selectivity for 1% PVAm/PSf blend hollow fibre nr 1 coated two times with 5% PDMS as a function of the sweep flow rate	74
Figure 5.4.2.6: CO ₂ /N ₂ selectivity for 1% PVAm/PSf blend hollow fibre nr 2 coated two times with 5% PDMS as a function of the sweep flow	74
Figure 5.4.2.7: CO ₂ /N ₂ selectivity for 1% PVAm/PSf blend hollow fibre nr 1 coated two times with 5% PDMS as a function of the sweep flow rate [11]	74
Figure 5.4.2.8: CO ₂ purity for 1% PVAm/PSf blend hollow fibres coated two times with 5% PDMS as a function of the sweep flow rate	75
Figure 5.4.2.9: Influence of relative feed humidity on selectivity for 1% PVAm/PSf blend membrane nr 1 coated two times with 5% PDMS	76
Figure 5.4.2.10: Influence of relative feed humidity on selectivity for 1% PVAm/PSf blend membrane nr 2 coated two times with 5% PDMS	76
Figure 5.4.2.11: The influence of relative feed humidity on selectivity for 0.2% PVAm/PSf blend coated two times with 5% PDMS [11]	76
Figure 5.5.1.1: CO ₂ permeance as a function of pressure for 1% PVAm/PSf blend nr 1 and PVAm/PSf FSC composite membrane with B and D as support	79
Figure 5.5.1.2: N ₂ permeance as a function of pressure for 1% PVAm/PSf blend nr 1 and PVAm/PSf FSC composite membrane with B and D as support	80
Figure 5.5.1.3: CO ₂ /N ₂ selectivity as a function of pressure for 1% PVAm/PSf blend nr 1 and PVAm/PSf FSC composite membrane with B and D as support	81

Figure 5.5.1.4: CO ₂ purity as a function of pressure for 1% PVAm/PSf blend nr 1 and PVAm/PSf FSC composite membrane with B and D as support	81
Figure 5.5.2.1: CO ₂ permeance as a function of sweep flow rate for 1% PVAm/PSf blend nr 2 and PVAm/PSf FSC composite membrane with D and J as support	82
Figure 5.5.2.2: N ₂ permeance as a function of sweep flow rate for 1% PVAm/PSf blend nr 2 and PVAm/PSf FSC composite membrane with D and J as support	82
Figure 5.5.2.3: CO ₂ /N ₂ selectivity as a function of sweep flow rate for 1% PVAm/PSf blend nr 2 and PVAm/PSf FSC composite membrane with D and J as support	83
Figure 5.5.2.4: CO ₂ purity as a function of sweep flow rate for 1% PVAm/PSf blend nr 2 and PVAm/PSf FSC composite membrane with D and J as support	84
Figure 5.5.3.1: CO ₂ /N ₂ selectivity as a function CO ₂ permeance for the fibres from the master thesis with best separation properties compared with results from literature and Helberg's master thesis	85

Figure B.1.1: SEM pictures 1% PVAm/PSf blend hollow fibre nr1	III
Figure B.1.2: SEM pictures 1% PVAm/PSf blend hollow fibre nr 2	III
Figure B.2.1: SEM pictures of PSf fibre B	IV
Figure B.2.2: SEM pictures of PSf fibre J	IV
Figure B.2.3: SEM pictures of PSf fibre M	V
Figure B.2.4: SEM pictures of PSf fibre N	V
Figure B.2.5: SEM pictures of PSf fibre O	VI
Figure B.2.6: SEM pictures of PSf fibre P	VI
Figure B.2.7: SEM pictures of PSf fibre W	VII

List of tables

Table 2.3.1.1: Influence of the polymer concentration on gas separation properties	6
Table 2.3.1.2: Influence of non-solvent additive on gas separation properties	7
Table 2.3.1.3: Influence of volatile additive on gas separation properties	8
Table 2.5.2.1: Permeance for one and two coatings with 5% PDMS for PSf hollow fibre	15
Table 4.2.1.1: Concentration of the dope compositions for spinning 1	36
Table 4.2.1.2: Concentration of the dope compositions for spinning 2	37
Table 4.2.2.1: Spinning parameters for spinning 1	37
Table 4.2.2.2: Spinning parameters for spinning 2	38
Table 4.3.1.1: Composition of the PDMS coating solution	38
Table 4.3.1.2: Composition of PVAm coating solution	38
Table 4.3.2.1: Different coating sequences for each fibre type	39
Table 4.5.2.1: Varied parameter for the different tested fibres	42
Table 5.1.1: Different spinning conditions for the investigated fibres in this chapter	43
Table 5.1.1.1: Separation properties for a 29% PSf fibre and 32% PSf fibre coated two times with 5% PDMS	44
Table 5.1.2.1: Separation properties of PSf hollow fibres at 1.2 bar with different air gap lengths.	46
Table 5.1.3.1: Separation properties of PSf hollow fibres at 1.2 bar with different take up speed	47
Table 5.1.4.1: Outer diameter and wall thickness as a function of dope flow rate	48
Table 5.1.4.2: Separation properties of PSf hollow fibres at 1.2 bar with different dope flow rate	49
Table 5.2.1.1: Permeance for the FSC composite membranes with B and O as support	52
Table 5.2.1.2: The CO ₂ purity for the FSC composite membranes with B and O as support with different pressure	53
Table 5.2.2.1: Spinning conditions for PSf fibre B, J and D	59
Table 5.2.2.2: Permeance for the PVAm/PSf FSC composite membranes with B and D as support	59
Table 5.2.2.3: The CO ₂ purity for the FSC composite membranes with B and O as support	60
Table 5.3.1: Comparison of the separation properties of a PSf hollow fibre, J, with and without a selective PVAm coating layer	63
Table 5.4.1.1: Concentration of the dope components and the spinning condition for PVAm/PSf blend	64
Table 5.4.2.1: CO ₂ permeance of the different PVAm/PSf blend membranes for different pressure	70
Table 5.4.2.2: CO ₂ purity for the different blend membranes at different pressure	72
Table 5.4.2.3: The CO ₂ and N ₂ permeance, CO ₂ /N ₂ selectivity and CO ₂ purity for 1% PVAm/PSf blend fibre membranes with feed on the bore side	77
Table 5.5.1: Dope composition and spinning conditions for the compared fibres in this chapter	79

List of symbols and abbreviations

Symbol	Description	Unit
A	Area	m ²
c	Concentration	kmol/m ³
C	Concentration	m ³ (STP)/m ³ ,
D	Diffusion coefficient	m ² /s
dc/dx	Concentration gradient	mol/m ³ m
F _{ip,j}	Molar flow of component i	mol/s
g	Gravity	m/s ²
h _∞	Equilibrium thickness	m
J	Flux	kmol/s·m ²
l	Membrane thickness	m
L	Membrane thickness	m
M	Molecular weight	kg/kmol
N	Number of measurements	
p	Absolute pressure	bar, Pa
p	Partial pressure	bar, Pa
P	Permeability	m ³ (STP)m/m ² barh
P	Pressure	bar, Pa
q	Permeate flow	m ³ /s
\bar{r}	Average pore radius	m
r	Pore radius	m
R	Ideal gas constant	N·m/kmol·K
S	Solubility	m ³ (STP)/m ³ ·bar
S	Recovery	
T	Temperature	°C, K
T _g	Glass transition temperature	°C, K
U	Withdrawal speed	m/s
v	Coating velocity	m/s
\bar{v}	Average velocity	m/s
x	Mole fraction	
x _i	Value of measured variable	
x _{p,i}	Constant mole fraction, permeate	
x _{r,i}	Constant mole fraction, retentate	
\bar{x}	Arithmetic mean of all measured values	
y	Mole fraction	
y _{ip,j}	Permeance purity for component i	%
Greek letter	Description	Unit
A	Membrane selectivity	
α	Process selectivity	
γ _{lv}	Liquid-vapour Surface tension	N/m
ε	Porosity	
η	Viscosity	Pa·s
λ	Mean free path	m
μ	Viscosity	Pa·s
ρ	Density	kg/m ³
σ	Standard deviation	

Subscript	Description	Unit
0	Initial value	
A	Component A	
B	Component B	
f	Feed	
i	Component i	
K	Knudsen	
p	permeate	
r	retentate	

Abbreviation	Description
DSC	Differential Scanning Calorimeter
FSC	Facilitated Selective Transport
HF	Hollow Fibre
IR	Infrared
NMP	1-Methyl-2-Pyrrolidone
PAMAM	poly(amidoamine)
PDMAEMA-PEGMEA	poly(N,N-dimethylaminoethyl)-poly(ethylene glycol methyl ether acrylate)
PDMS	Polydimethylsiloxane
PEG	poly(ethylene glycol)
PPO	poly(phenylene oxide)
PSf	Polysulfone
PVAm	Polyvinylamine
SEM	Scanning Electron Microscopes
STP	Standard temperature and pressure
THF	Tetrahydrofuran

Chapter 1: Introduction

The vast majority of energy production in the world today is based on coal and other fossil fuels. Combustion of such fuels releases large amounts of CO₂ to the atmosphere, which is a major contributor to global warming. To control global warming, international measures have been made leading to the establishment of the Kyoto protocol by United Nations Framework Convention on Climate Change (UNFCCC) [1]. The protocol requires that all ratifying nations reach individual emission reduction targets of greenhouse gases. This agreement, in addition to a world that demands an ever increase in energy consumption, makes it necessary to find solutions for capture and storage of CO₂ from flue gases in power plants and other fossil fuel based facilities. The most common technology to clean CO₂ from flue gases is absorption with amines [2]. There are some drawbacks associated with this technology. Amines have a relatively small absorption capacity and require large energy inputs to be able to absorb a sufficient amount of CO₂ [3]. This energy is likely to come from fossil fuel which will be a source of extra CO₂ production. Other disadvantages with amine absorption are corrosion and potentially hazardous amine [2]. Amines can react and form nitrosamines and nitramines which are highly carcinogenic compounds. This represents a potential risk for humans and the environment close to the absorption plant. The Norwegian Institute of Public Health recommend that the total air concentration of nitrosamines and nitramines should not exceed 0.3 ng/m³ [4].

Membrane separation processes represent another technology for CO₂ separation, and has the advantage of low energy consumption, process simplicity and lack of additional chemicals [2]. Separation of large volumes of gas, as for flue gas, requires a large membrane area with a minimal foot print. Hollow fibres have a high ratio of membrane area per volume and are therefore a good choice for gas separation [5]. In addition to large volumes of gas there are other challenges related to CO₂ separation from flue gas. The concentration of CO₂ in flue gases is relatively small and usually at low pressure, which gives low driving forces for separation [6]. To achieve a successful separation with a membrane, the membrane must have high selectivity and high permeability of one component compared to the other components. Robeson, L.M showed that there is a trade-off between the permeability and the selectivity in polymeric membranes through the “Robeson upper bound” [7]. The trade-off between CO₂ permeability and CO₂/N₂ selectivity is shown in the Robeson upper bound plot in figure 1.1. High CO₂ permeance is essential to make the membrane able to treat large volumes of flue gas at reasonable membrane area. To make membranes a viable option to existing technologies for CO₂ capture, the permeance must be as high as possible and provide a specified minimum CO₂/N₂ selectivity that give the required permeate purity and recovery.

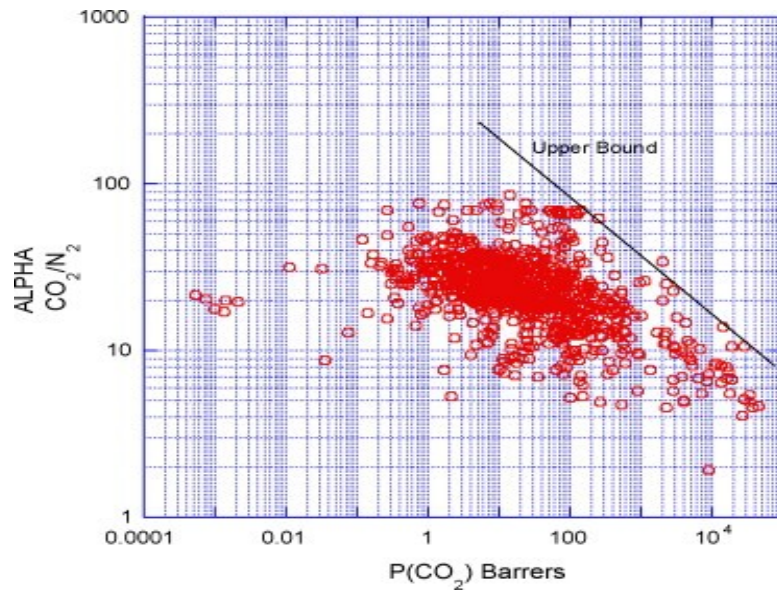


Figure 1.1: Robeson upper bound for the trade-off between CO_2 permeability and CO_2/N_2 selectivity [8]

Hollow fibre membranes are in general composite membranes which consist of a porous support membrane, coated with a thin, dense and selective top layer. Polysulfone (PSf) is a material with good properties as support, and gives mechanical strength and support to the composite membrane. The overall separation property of a composite membrane is influenced by the separation properties of the hollow fibre support [9]. The permeance and selectivity of a composite membrane can be increased by optimizing the PSf support by tailoring the spinning conditions. By fine tuning the spinning conditions the structure and wall thickness of the fibres can be optimized, while surface defects and macrovoids can be eliminated. The presence of macrovoids in membrane structure may contribute to low selectivity, weak spots in the membrane, and can make the coating procedure more difficult. PSf membranes can be coated with a selective layer such as polyvinylamine (PVAm) to increase the CO_2/N_2 selectivity. Polydimethylsiloxane (PDMS) is a highly permeable polymer film, which can be used to repair surface defects of the hollow fibres, without affecting the permeance. PVAm is a material which is selective towards CO_2 , because of CO_2 facilitated transport by the amino groups present in PVAm [10]. Other components of the feed gas, such as N_2 and CH_4 , do not react with the PVAm and are only transported by solution-diffusion mechanism [10]. This composite membrane is made in two steps. First the preparation of the PSf support and then the coating step. It is also possible to prepare blend membranes, in one step, by adding a PVAm solution into the polymer solution, which forms the PVAm/PSf hollow fibre blend membrane. This will be very time saving, as coating with PVAm is a highly time consuming process.

1.1 Aim of the project

The aim of the master thesis is to prepare hollow fibre membranes for CO_2 separation from a mixture of N_2 and CO_2 . The experimental work consists of preparing composite membranes, by coating PVAm and PDMS on a PSf support. The composite membranes prepared in the specialization project had good selectivity, but quite low CO_2 permeance [11]. To increase the CO_2 permeance, the hollow fibre support was optimized by changing the spinning conditions. The starting point was the spinning conditions for the best support from the specialization project [11]. Based on these spinning conditions and the conclusions, the air gap and take-up speed were increased. The best fibres with respect to the SEM pictures were chosen for coating with PVAm and PDMS. There were performed coatings of the chosen fibres with

PDMS as the top layer and with the PVAm layer as the intermediate layer. The selectivity and permeability was tested in a permeation rig at different pressures and sweep flow rates.

The second part of the experimental work consists of spinning a blend membrane of 32% PSf and 1% PVAm. This is a one-step procedure. This is a continuation from the specialization project and Helberg's master thesis. The results from Helberg's master thesis had promising results for a blend of 32% PSf and 0.2% PVAm [12]. Therefore in the specialization project this work was continued with a blend of 32% PSf and 1% PVAm. The performance was expected to be better for the 1% PVAm/PSf hollow fibre, but this membrane did not obtain good results [11]. The reasons for the lower separation performances was assumed to be that during the dope filtration the filter retained some PVAm from the PVAm/PSf blend solution because of filter fouling. The PVAm/PSf blend polymer solution might also have been phase separated as the solution was filtrated for 72 hours, leading to hollow fibres without PVAm content. Also, the desired spinning conditions were never obtained because the amount of filtered 1% PVAm/PSf blend solution was too small. These sources of error will be attempted eliminated, and the work of making a successful 1% PVAm/PSf blend membrane will be continued in this master thesis. The spun blend membrane was coated two times with 5% PDMS. The selectivity and permeance for the blend membranes were tested in a permeation rig at different pressures, sweep flow rates and humidity.

The PVAm/PSf blend membranes and the PVAm/PSf composite membranes were analysed by use of SEM. The blend fibre membranes spun in this project was also analysed by use of DSC. The master thesis consists also of a literature study on spinning conditions, coating techniques, coating conditions and composite membranes.

Chapter 2: Literature study

This chapter summarize specific literature concerning preparation and properties of support hollow fibres, composite membranes and blend membranes. The literature review is presented together with some of the most important results from the Specialization project written by Johannessen, P-K [11] at the Department of Chemical Engineering, NTNU. The main goal of this Specialization project was to investigate composite hollow fibre membranes and blend membranes for CO₂ capture from flue gas. The composite hollow fibre membranes were produced using polysulfone (PSf) porous hollow fibres as support which was coated with polydimethylsiloxane (PDMS) and polyvinylamine (PVAm). Two different composite membranes were produced, one having PDMS as the top layer and one with PVAm as the top layer with the other coating layer as the intermediate layer. The PVAm/PSf blend membranes were produced by introduction of PVAm in the spinning dope together with the polysulfone (PSf). The different membranes were investigated and compared with respect to structure, geometry, permeance and selectivity. This work is continued in the master thesis. The results from the Specialization project showed that the PSf support is important in the overall separation performance for a composite membrane. The composite membrane prepared presented high selectivity, but quite low permeance. In this master thesis, the focus will be on optimizing the PSf support in order to increase the permeance by investigating the spinning dope composition and the fibre spinning parameters without decreasing the selectivity significantly. A part of this literature study will also present different coating techniques and coating conditions, discussing and comparing them with the results obtained in the specialisation project on this field. After investigating the optimization of the PSf support and the coating procedure, the complete composite membrane will be considered. The last part of this literature study contains the previously obtained results from the specialization project regarding production of PSf/PVAm blend membranes.

2.1 Polysulfone hollow fibre support

It has been a common belief that the gas transport property of an asymmetric composite membrane has been determined by the thin, dense skin layer. Pinnau, I., and Koros, W. J [13] suggested that for an integrally skinned asymmetric membrane having a defect-free skin layer at a desired thickness, the porous support itself becomes an important factor for the gas transport properties of the membrane. This is supported by Clausi, D.T., et al [14] which state, by using a series resistance model, that as the skin layer thickness is reduced, the porous substructure contributes more and more to the total rate of permeation through the membrane. Results from the specialization project and from Sandru, M [15] showed that the properties of the support are important in the overall separation performance of a FSC composite membrane. The results from Johannessen, P-K [11] showed that the fibres with the fewest macrovoids and defects had the best selectivity and permeance, when the fibres were coated one and two times with 5% PDMS. The best fibre was then chosen as the support for the PVAm/PSf composite membrane. The best achieved CO₂/N₂ selectivity was 123 with a CO₂ permeance of 0.06 m³(STP)/m² bar h [11]. Sandru, M [15] report that some of the first fibres spun at NTNU research group had a CO₂/N₂ selectivity of 0.5 and a CO₂ permeance of 0.035 m³(STP)/m² bar h. The surface of the fibre contained many surface defects and the structure had a high amount of macrovoids, which made the fibre impossible to coat. The support membrane will influence the performance of a composite membrane in a negative or a positive way, depending on the support characteristics. The result of Sandru, M [15] shows that the limiting step to achieve a successful FSC composite membrane is the support itself. The support will have negative contribution to the overall separation properties if the

separation is based on Knudsen diffusion. Viscous flow will have a neutral contribution, while surface selective flow, activated diffusion and solution diffusion will have positive contribution on separation properties [16].

2.2 Mechanism for formation of macrovoids

The mechanisms for formation of macrovoids are well studied in literature. Widjojo, N., and Chung, T-S [17] have indicated that several mechanisms may occur simultaneously when macrovoids are formed, but the mechanisms proposed by Smolders, C., et al [18] and Strathmann, H., and Kock, K [19], are the most likely mechanisms for formation of macrovoids. Strathmann, H., and Kock, K [19] suggest that the formation of macrovoids most likely starts from an instability in the local surface of the membrane and imbalance of materials and stresses. The macrovoids are formed from local surface instability, skin rupture and solvent intrusion, continued by the nucleation of droplets in the polymer lean phase [23]. Smolders, C., et al [18], suggest that the formation of macrovoids are based on the two types of demixing, delayed demixing and instantaneous demixing. Demixing is explained in detail in chapter 3.5.1-3.5.2. They report that membranes without macrovoids are formed when delayed demixing occurs, except when the delay time is very short. The authors assumed that nucleated droplets of the polymer lean phase in the immersed polymer solution are responsible for the formation of macrovoids. The nucleated droplets expand when the diffusional flow of solvent from the polymer solution into the nuclei is larger than the flow of non-solvent from the nuclei into the polymer solution, and macrovoids are produced [18]. With delayed demixing the solvent from the polymer solution has the opportunity to diffuse out of the fibre into the coagulation water, before the fibre walls are sealed. In literature polymer concentration, non-solvent concentration, air gap and take-up speed are listed as factors that can affect and prevent the formation of macrovoids [18, 19, 20].

2.3 Hollow fibre spinning

The best fibre tested in the specialization project was spun again in the master thesis, and it was attempted to increase the permeance of the fibres by altering the spinning conditions.

2.3.1 Dope composition

Polymer concentration

Peng, N., et al [20] states that the critical polymer concentration for PSf is 29 % by weight, and the critical dope viscosity is 36.2 Pa·s for producing macrovoid free hollow fibres at high speed spinning processes. The critical polymer concentration exists because of intimated intermolecular interaction and significant polymer chain entanglements [20]. For chain entanglements, Bird, R.B., et al [21, 22] found that it only occurs at the concentrated long chain polymer system and the entanglements is released progressively when the solvent concentration increase. Therefore under the critical polymer concentration, polymer chains have high degree of freedom and are loosely packed. The non-solvent can then via diffusional and convective movement easily penetrate into the chain space of polymer solution and form macrovoids [20]. Wang, D., et al [23] prepared hollow fibres from a polymer concentration of 26 wt%, 28 wt% and 30 wt% PSf. The fibres prepared from a polymer concentration of 30 wt% PSf had high CO₂/N₂ selectivity, but low CO₂ permeance. The fibres with a PSf concentration of 26 wt% and 28 wt% exhibited high CO₂ permeability, but in general lower CO₂/N₂ selectivity. The selectivity was especially low for the fibre with PSf concentration of 26 wt%. Wang, D., et al [23] reported that the fibre prepared from 28 wt% PSf had the best combination of permeability and selectivity for O₂/N₂ separation. Van de Witte, P., et al [24]

claim that increasing the polymer concentration will increase the thickness of the top layer and decrease the porosity. This means that high polymer concentration leads to lower permeance compared to fibres with low polymer concentration. Table 2.3.1.1 shows the influence of polymer concentration on the gas separation properties for silicone coated hollow fibres from literature.

Table 2.3.1.1: Influence of the polymer concentration on gas separation properties [23]

Dope composition[wt%]	CO₂ permeance [*]	CO₂/N₂ selectivity
26 PSf/69.66 NMP/ 4.34 water	0.41	33
28 PSf/67.78 NMP/ 4.22 water	0.32	35
30 PSf/65.90 NMP/ 4.10 water	0.27	38

* $m^3(STP)/(m^2 \text{ bar h})$

Addition of additives

The effect on performance and morphology of a PSf flat sheet membrane by addition of non-solvent and polymeric additives was investigated by Aroon, M.A., et al [25]. Their results show that the non-solvent and the polymeric additives move the binodal curve and the curve comes closer to the dope position [25]. This means that the dope composition is close to the precipitation point, which gives an increased ideal separation factor. The sequence of how the different additives shift the binodal line is glycerol > PVP > ethanol > PEG 400. Glycerol gives the largest shift of the binodal curve because of its high affinity for NMP and weak solvent properties, and is therefore yielding the highest ideal separation factor. In addition, the CO₂ permeance is reported increased by using glycerol as an additive. This is attributed to the instantaneous demixing which is induced by having a non-solvent additive present. PVP is reported to give the second most significant shift of the binodal curve, but does not exhibit an enhanced CO₂ permeance. This is due to the coalescence between the PVP and PSf polymer chains, which make the two polymers behave as one. Adding a non-solvent additive makes precipitation easier and results in membranes with a more uniform structure, a thinner skin layer and can decrease macrovoids formation in the sub layer. The membrane containing glycerol was reported to have the thinnest skin layer as expected [25]. Van de Witte, P., et al [24] also points out that the size of the skin layer will decrease when a non-solvent is added to the polymer dope solution. Membranes with a defect free ultrathin dense top layer and a sub layer with high porosity and low resistance are suitable for gas separation application. The non-solvent additives should be miscible with the coagulant, because of its strong non-solvent power, water as a non-solvent is not recommended [25]. As reported by Smolders C., et al [18], macrovoid-free membranes are formed in situations with delayed solvent non-solvent demixing. Van de Witte, P., et al [24] suggest that before demixing, the composition of the entire solution is in the homogenous region. This period of time is called the delay time. When there is no delay time, the demixing is instantaneous and a membrane is formed immediately. The morphology is highly dependent on the demixing time, and an instantaneous demixing will give a porous top layer, which also means that the chance of forming macrovoids is higher than for delayed demixing. In figure 2.3.1.1 are the SEM pictures of PSf flat sheet membranes with and without glycerol shown.

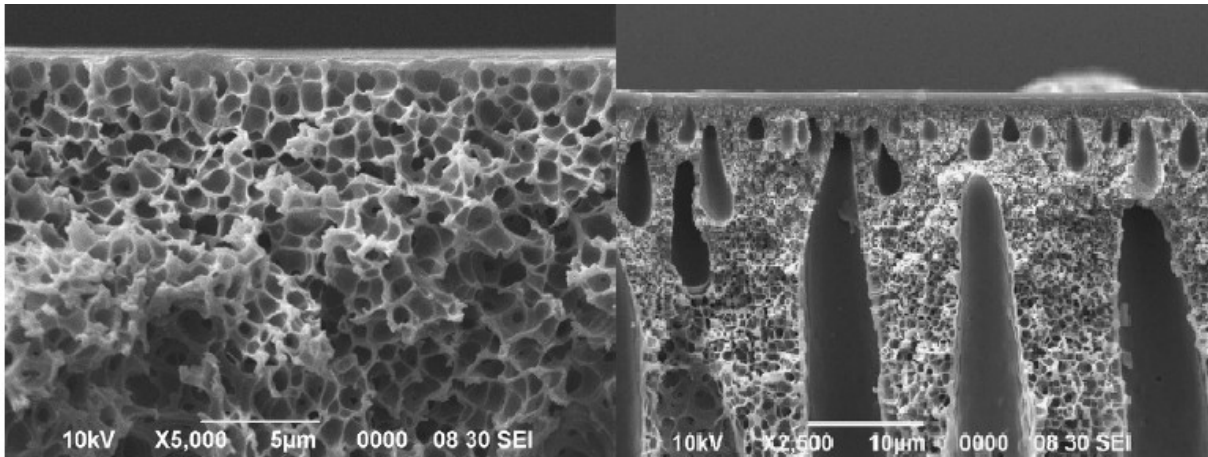


Figure 2.3.1.1: SEM pictures of PSf flat sheet membranes prepared with glycerol in the dope (left picture) and without glycerol in the dope (right picture) [25].

From the figure it can be seen that the membrane with glycerol has much less macrovoids. In table 2.3.1.2 some results from literature on how addition of non-solvent influences the flat sheet membranes performance are shown.

Table 2.3.1.2: Influence of non-solvent additive on gas separation properties [25]

Dope composition [wt%]	CO ₂ permeance [*]	CO ₂ /CH ₄ selectivity
25 PSf/ 75 NMP	0.03	2.39
25 PSf/ 10.7 glycerol/ 64.3 NMP	0.2	10.24
30 PSf/ 70 NMP	0.02	4.43
30 PSf/ 10 glycerol/ 60 NMP	0.05	15.07

*m³(STP)/(m² bar h)

The results from table 2.3.1.2 show that the permeance increases with addition of glycerol for both the membranes consisting of 25 % PSf and 30 % PSf. The selectivity increases with increasing PSf concentration and addition of glycerol. The highest reported selectivity is 15, which is much lower than the intrinsic CO₂/CH₄ selectivity of 33 for PSf [25]. This indicates that it can be defects in the skin layer.

Aroon, M.A., et al [25] suggested adding volatile tetrahydrofuran (THF) to the dope solution to increase the CO₂/CH₄ selectivity. Their results show that adding THF does increase selectivity, and this was attributed to the formation of a thicker and denser skin layer and suppressed formation of macrovoids in the membrane structure. The formation of a thicker and denser skin layer was reported to cause a decrease in permeance as the resistance for mass transfer is larger than for a polymer solution added only glycerol. THF is a volatile solvent that is miscible with water. It does not shift the binodal curve significantly, but will evaporate at a high rate from the outermost surface of the membrane. This causes rapid vitrification which gives an oriented membrane skin with few defects and pores [25]. Ding, X., et al [26] points out that adding THF has two opposite effects on the membrane performance. The first effect is an increase in solvent evaporation from the outermost surface of the membrane as mentioned earlier. In addition, the THF, as a weaker solvent of PSf than NMP, will shift the binodal curve to the polymer-solvent location and cause faster decomposition. This will increase the permeance and reduce the CO₂/CH₄ selectivity. These two effects work against each other, and an optimal concentration has to be found [26]. In figure 2.3.1.2 are the SEM pictures of a flat sheet membrane with and without 17 % THF.

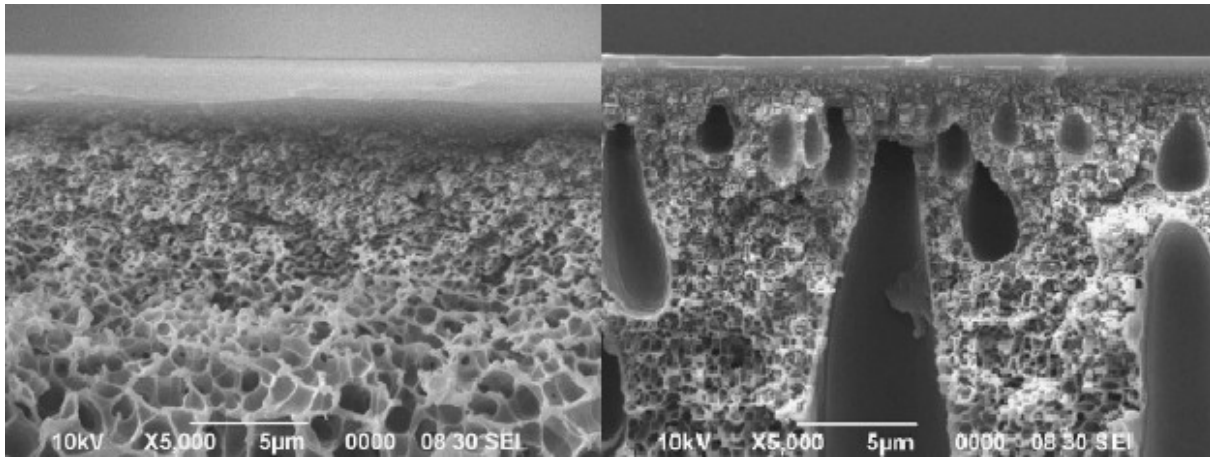


Figure 2.3.1.2: SEM pictures of PSf flat sheet membranes prepared with THF in the dope (left picture) and without THF in the dope (right picture) [25].

From the SEM pictures in figure 2.3.1.2 it can be seen that the effect of adding THF, is a membrane with a defect free skin layer and suppressed formation of macrovoids [25]. Table 2.3.1.3 shows Aron, M.A et al's results of adding THF in the dope solution.

Table 2.3.1.3: Influence of volatile additive on gas separation properties [25]

Dope composition [wt%]	CO ₂ permeance [*]	CO ₂ /CH ₄ selectivity
30 PSf/ 70 NMP	0.02	4.43
30 PSf/ 10 glycerol/ 60 NMP	0.05	15.07
30 PSf/ 10 glycerol/ 15 THF/ 45 NMP	0.02	31.65

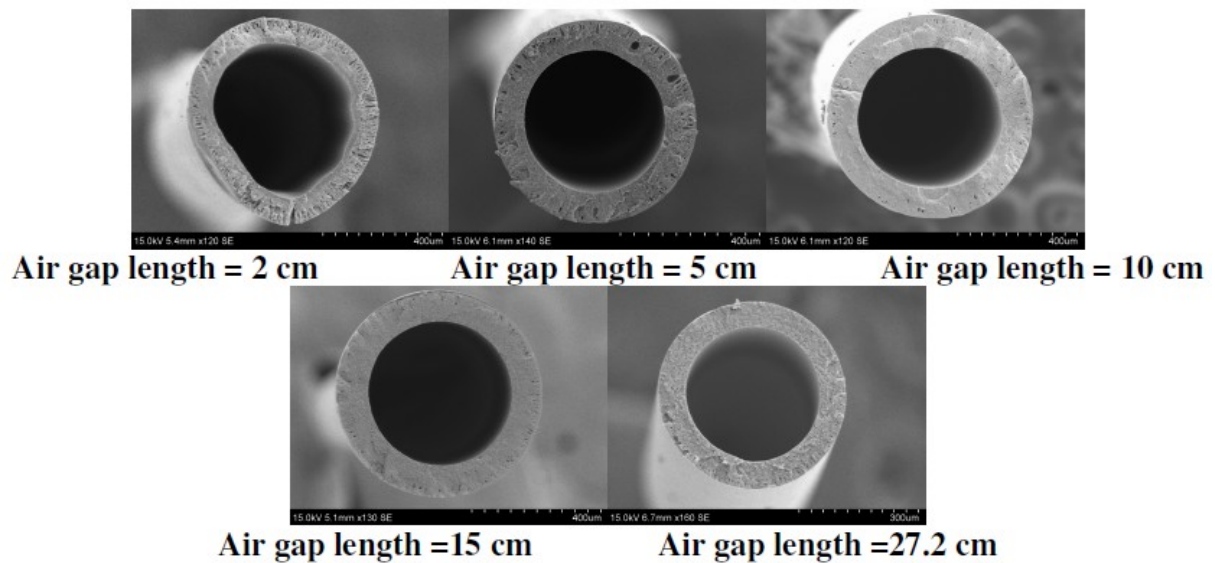
*m³(STP)/(m² bar h)

2.3.2 Spinning procedure

The spinning parameters control the geometry of the fibres, inner and outer diameters and wall thickness [27]. The porosity of the fibres is controlled by the fibre spinning parameters to a certain degree.

The influence of air gap length

Peng, N., et al [20] points out that there exists a critical air gap distance. Only above this distance can macrovoid free hollow fibres successfully be produced. The critical air gap length is 5 cm. This is explained by the fact that high elongation stretch can lead to chain packing of the polymer chains. This may lead to retarding of the penetration of external coagulant and thus suppress macrovoids. Elongation stress is induced during take-up. This stress effect on the membrane morphology needs a certain distance to fully develop. This certain distance is the critical air gap. Tsai, H.A., et al [28] concluded that macrovoids disappears, reappears and re-disappears when the air gap increases from 0 to 60 cm. An air gap above 20 cm made the macrovoids shrink in size, and at 60 cm the macrovoids no longer were observed. When entering the air gap, a transient gel will be formed. This inhibits the phase separation, and slows down the formation of macrovoids. The gel formation does not occur at longer air gaps, and macrovoids are formed until a critical air gap length is reached where the phase separation is complete. This critical air gap was proposed to be at 60 cm, but this is reduced when the air humidity is increased [28]. Helberg [29] found in her specialization project that higher air gap length suppresses the forming of macrovoids, this lead to a higher CO₂/N₂ selectivity. The CO₂ permeance increased also with higher air gap length, because of the decrease of the wall thickness. In figure 2.3.2.1 are the SEM pictures of fibres spun at 2 cm, 5 cm, 10 cm, 15 cm and 27.2 cm shown.



Conditions spinning

Dope 32 wt% PSf, 68 wt% NMP, dope flow rate 2ml/min, 1 ml/min
 Bore 80/20 NMP/Water, bore flow rate 1.3 ml/min, 0.65 ml/min
 Temperature 25 °C, 14 °C, take up speed 8 m/min

Figure 2.3.2.1: Cross section of different fibres spun at different air gaps [29]

Kapanaaidakis, G.H., et al [30] report that a longer air gap length in a humid atmosphere causes more water in the top layer. This gives a more porous structure, which leads to higher permeation rates. This means that the air gap could be considered equivalent to adding small amounts of water in the spinning dope.

During the spinning in the specialization project, the air gap was between 15 cm and 23 cm, for the spun 1% PVAm/PSf blend membrane, while the 0.2% PVAm/PSf blend membrane had an air gap of 28 cm. The 0.2% PVAm/PSf blend membrane had much less macrovoids than the 1% PVAm/PSf blend membrane [11]. The results obtained were according to results from literature.

Coagulation bath temperature

The temperature of the coagulation bath is an important factor to control during membrane formation [23]. For PSf hollow fibres with silicone coating, Wang. D., et al [23] found that the selectivity decreased when the coagulant bath temperature was reduced. As the coagulation temperature was decreased from 26-27 °C to 20 °C, the permeability increased slightly while the selectivity decreased. With further reductions of the coagulation bath temperature, the selectivity of the fibre membranes was considerably reduced. Wang. D., et al [23] suggests that the membranes prepared at a coagulation bath temperature between 10-15°C exhibit such a large surface porosity, that the membranes cannot be repaired with silicone coating. This result indicates that initial wet phase separation rate is the most important factor to control outer skin layer formation of fibre membranes [23]. Wallace. D.W., et al [31] report that an increase in temperature leads to skins that are more likely defect free, but an increase in temperature decreases the viscosity as well. Wallace. D.W., et al [31] stipulates that when the spin line remains stable and the viscosity is sufficiently high, the air gap and the temperature should be increased as much as possible. The viscosity of the dope solution is the limiting factor in raising the coagulation bath temperature, and the viscosity must have a sufficient value to be extruded through the spinneret and drawn [31].

Take-up speed

A minimum take-up speed of 50 m/min for formation of hollow fibres without macrovoids was reported by Peng, N., et al [20]. This may be related to the elongational stress experienced by the hollow fibre when it is stretched by the take-up unit. The increased elongational stress associated with an increased take-up speed gives a better morphology for several reasons. Increased elongation rates may cause chain packing, extra phase instability is created which changes the inner structure from a close-cell structure to an open-cell structure, the shrinkage of the fibre dimensions may stop the external coagulants to enter into the fibre structure and the elongation stress has reduced the wall thickness which causes faster solidification and thus a more macrovoid free structure [20].

Bore fluid and dope fluid extrusion rate

A precise control of both the inner and the outer diameter is essential when hollow fibres are to be coated, and this means that the bore fluid extrusion rate has to be tuned together with the dope fluid extrusion rate. When the dope fluid extrusion rate increases, the rate of tensile strain on a hollow fibre decreases, leading to an increase in outer diameter as stated by McKelvey, S.A., et al [27]. The inner diameter of hollow fibres will increase when the bore fluid extrusion rate increases [27]. This leads to higher permeance for the membrane as the mass transfer resistance is smaller when the membrane thickness decreases. From the specialization project of Helberg [29] it is shown that the ratio between the bore fluid extrusion rate and the dope fluid extrusion rate should be kept constant. Wallace D.W., et al [31] suggest that the bore fluid extrusion rate should be about one third of the dope extrusion rate. Qin, J., and Chung, T.S [32] reported that to obtain even demixing and reduce coupling effects, the bore fluid velocity and the dope fluid velocity should be kept as similar as possible. To obtain this, Aron M.A., et al [33] concluded that the ratio between bore fluid flow rate and dope fluid flow rate should be 0.8 times the ratio of the cross-sectional area of bore fluid and dope fluid at the spinneret outlet.

The 0.2 % PVAm/PSf blend membranes prepared by Helberg [12] and the 1 % PVAm/PSf blend membranes prepared in the Specialization project had different bore rate. The bore fluid extrusion rate during preparation of the 1 % PVAm/PSf blend fibres was higher than wanted [11]. In figure 2.3.2.2 the cross section of 1 % PVAm/PSf blend membrane and 0.2% PVA/PSf blend membrane are shown.

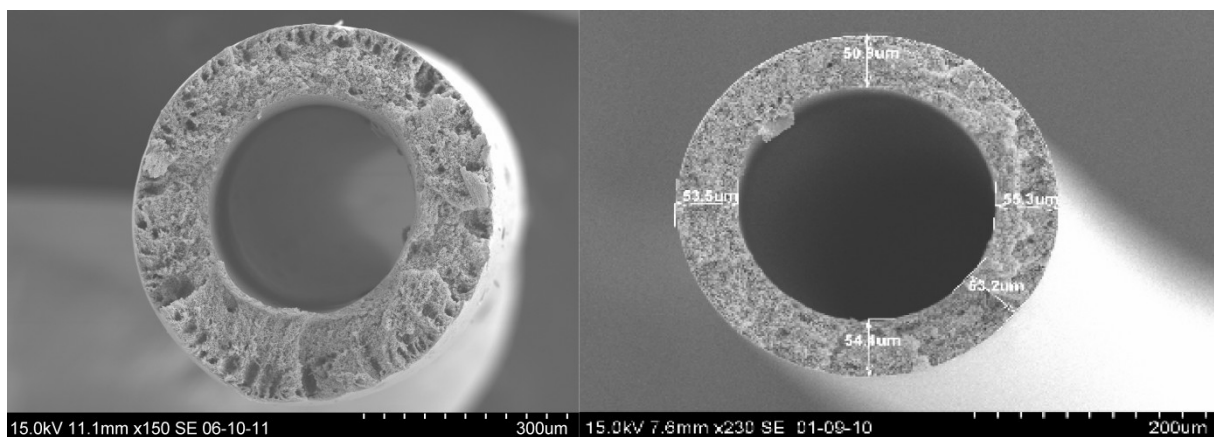


Figure 2.3.2.2: Cross section of 1% PVAm/PSf blend [11] and 0.2% PVAm/PSf blend [12]

As can be seen from figure 2.3.2.2, the 1% PVAm/PSf blend membrane wall is much thicker than the 0.2% PVAm/PSf blend membrane. The 1% PVAm/PSf blend membrane has a diameter of about 550 μm while the 0.2% PVAm/PSf blend membrane has a diameter of about 300 μm . This result is according to literature.

Composition of bore fluid

Rahbari-sisakh M., et al [34] and Qin, J-J., and Chung, T-S [35] both reported that the structure of hollow fibres is highly dependent on the composition of the bore fluid. The membrane formed with distilled water as bore fluid had finger-like macrovoids and a dense skin layer, and an increased concentration of solvent NMP in the bore fluid gave a more microporous structure with a more porous skin layer [34]. This is attributed by Rahbari-sisakh M., et al [34] to the suppressed flux of solvent from the polymer solution phase to the coagulant when the concentration of NMP in the coagulant increases. This leads to a considerable amount of NMP at the interface between polymer solution and coagulant making formation of a dense skin layer difficult. The same result was obtained by Qin, J-J., and Chung, T-S [35] who attributed the same effect to reduced mass transfer at the inner surface relative to the mass transfer at the outer surface, leading to a faster skin formation giving a decrease in the skin thickness. Both authors reported higher permeance and lower selectivity when the solvent concentration in the bore fluid was increased. In figure 2.3.2.3 the hollow fibre cross-sectional structure at different solvent concentrations is shown.

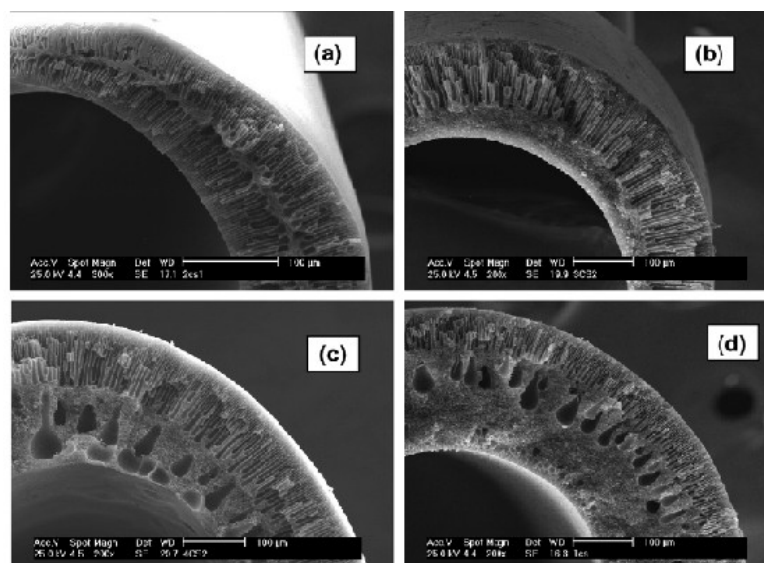


Figure 2.3.2.3: Morphology of inner skin layer of fabricated membranes with different solvent concentration in the bore fluid. (a) 0% NMP, (b) 50% NMP, (c) 70% NMP and (d) 90% NMP [34]

Figure 2.3.2.4 shows the inner surface morphology for the same hollow fibres as in figure 2.3.2.3 at different bore solvent concentrations.

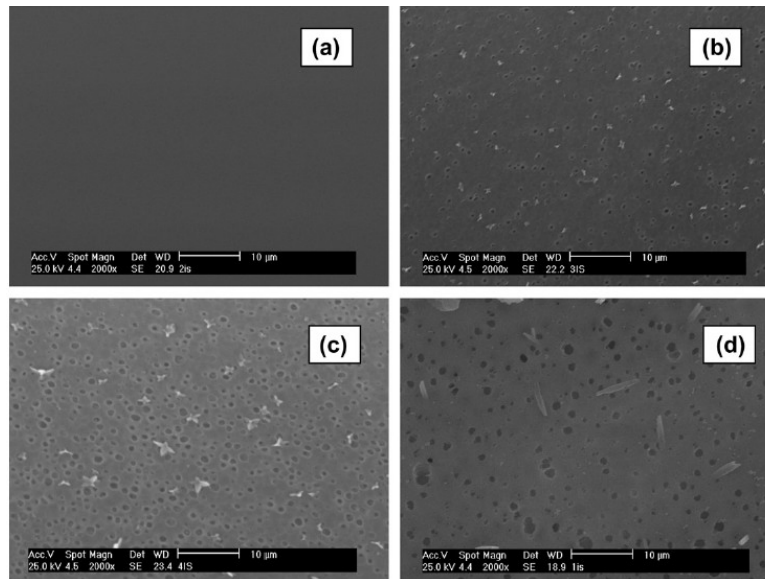


Figure 2.3.2.4: Morphology of inner surface of fabricated membranes with different solvent concentration in the bore fluid. (a) 0% NMP, (b) 50% NMP, (c) 70% NMP and (d) 90% NMP [34]

2.4 Coating techniques

The most commonly used coating technique for hollow fibre membranes is the dip coating technique. As described by Sandru. M., et al [36], the dip coating is performed by immersing the porous support membrane into a coating solution consisting of a coating material and a solvent, and pulling the fibres up from the solution at a constant speed. After being withdrawn from the coating solution, the fibres are dried vertically. The withdrawal speed will affect the coating layer thickness as an increased speed will lead to increased coating layer thickness. The dip coating technique is described in more detail in chapter 3.7.1. Interfacial polymerisation is a coating technique described Mulder, M [5]. This technique gives a thin layer upon the porous support membrane consisting of monomers that have polymerised directly on the surface. The membrane is first placed in a bath consisting of an aqueous solution containing a reactive monomer or pre-polymer. After the first bath the fibre is immersed in a second bath containing a water-immiscible solvent with another reactive monomer. The two monomers react and a dense polymeric top layer is formed. This technique gives a very thin layer thickness within the range of 50 nm [5].

Another coating technique is continuous coating of hollow fibres described by Chen. H.Z., et al [37]. This represents a more efficient and automated method which easier can be scaled up for industrial purposes. The equipment used for continuous coating consists of two glass coaters, a tubular dryer and a take-up unit. The first of the coaters contains a wetting agent which is immiscible with the coating solution, and this is used to seal the pores of the hollow fibre temporary so that the coating solution is prevented from penetrating the pores. A schematic drawing of the continuous coating equipment is shown in figure 2.4.1.

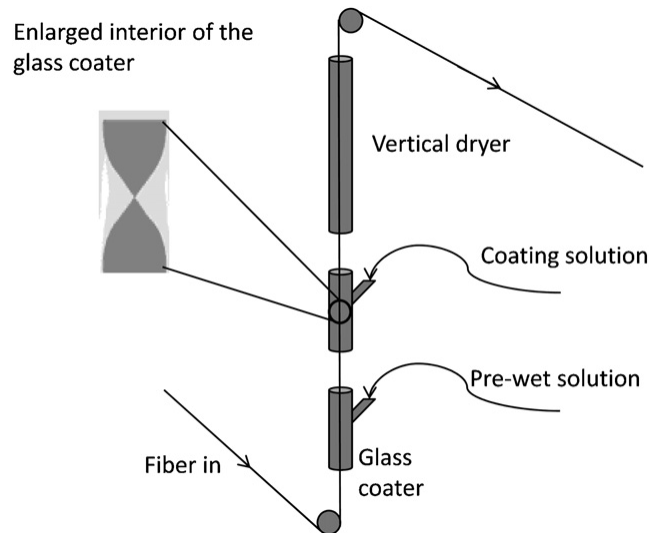


Figure 2.4.1: Equipment setup for continuous coating of hollow fibres [37]

It is also possible to coat on the bore side of the fibre. Two different techniques for inside coating are described by Sandru. M., et al [36] and He. T., et al [38]. Inside coating protects the coating layer from external effects. In this method, it is more difficult to reveal defects in the coating layer, because it is not possible to observe the coating process on the inside of the fibre [39]. The method used in [36] is to circulate the coating solution vertically inside the fibre, followed by drying. For the other option described in [38], the coating solution is raised from the bottom of the hollow fibre to the top by an air bubble. After the solution reaches the top, it is allowed to stay for 3 seconds, and then gravity drains the fibre. The fibres are dried by N_2 gas for 24 hours. A schematic drawing of the equipment setup for this method is shown in figure 2.4.2.

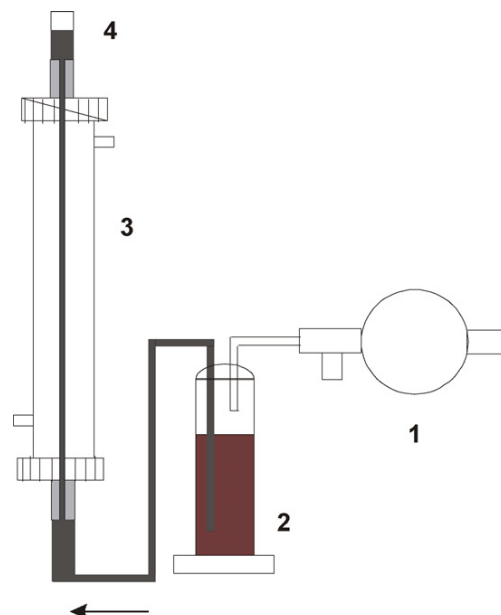


Figure 2.4.2: Equipment setup for inside coating (1) Rubber bulb (2) solution cell (3) membrane module (4) overflow indicator [38]

Co-extrusion, a coating method which includes both spinning and coating of hollow fibres in one step, is described by He, T., et al [40]. The idea behind this method is that the hollow fibre is spun in a spinneret with three separate channels, one for the bore fluid, one for the

spinning dope and one for the coating solution, and these are extruded simultaneously through the spinneret as shown in figure 2.4.3. This technique is less time consuming than the two step techniques, but the coating layer may have difficulties attaching to the support as the demixing is not fast enough to form a stable support before coating.

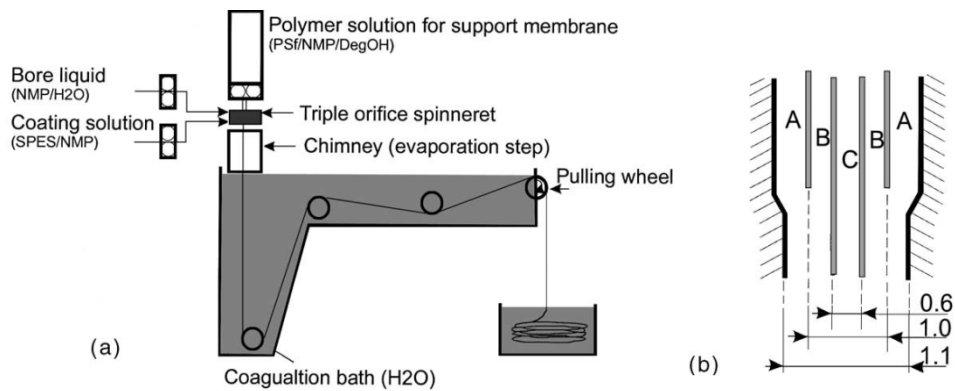


Figure 2.4.3: a) Spinning setup b) schematic drawing of the spinneret. A is the coating solution channel, B is the dope solution channel and C is the bore fluid channel [40]

2.5 Effects of coating conditions

2.5.1 Effect of the support membrane

Kim, Li and Hägg [10] point out that the pore size of the porous hollow fibre support has a significant effect on the quality of the coated membrane. Too large pore diameter in the support will cause the coating material to penetrate and plug the pores of the support, leading to a reduction in permeance. Penetration of the pores will also result in a thinner dense top layer due to loss of coating material from the surface to the support membrane. This leads to a decrease in selectivity in addition to a decrease in permeance. For the case with PVAm as the coating material, Kim, Li and Hägg [10] suggests that a reasonable difference between the average molecular weight of PVAm and the molecular weight cut-off of the support material is larger than 20,000 g/mol.

2.5.2 Number of sequential coatings

The effect on selectivity and permeance by number of sequential coatings for hollow fibre composite membranes has been investigated by Ji, P., et al [41]. Their experiment shows that the selectivity increases with increased number of coatings until a certain point when all the open pores are sealed, when it is not possible to further increase the selectivity. For each sequential coating, the coating layer thickness increases. The permeance decreases with increased coating layer thickness. The permeance continues to decrease with each sequential coating, even though the selectivity remains constant. The optimal number of coatings depends on both the support material and the coating material.

In the Specialization project PSf hollow fibres were coated one and two times with 5% PDMS. The selectivity increased for all the PSf fibres when they were coated two times with 5% PDMS, compared to one time [11]. This indicated that with two coatings, more surface defects are sealed and the membrane has an improved pressure resistance, see figure 2.5.2.1.

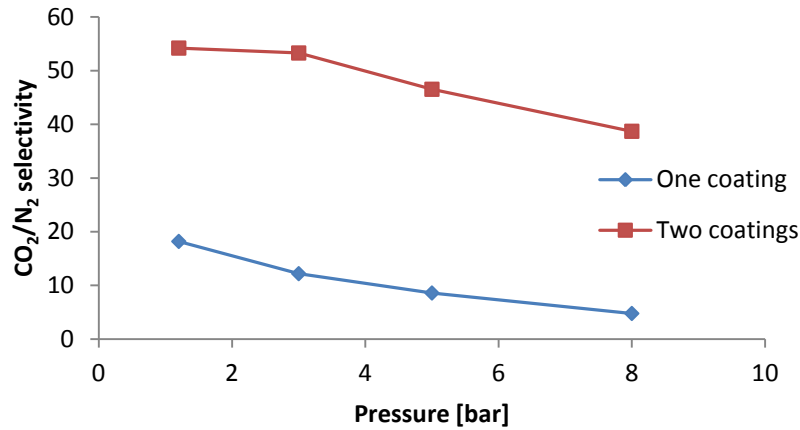


Figure 2.5.2.1: Plot of selectivity against feed pressure for PSf fibre with one and two coatings of 5% PDMS [11]

The permeance for the tested fibres was about the same for one and two coatings, even one fibre received an increase in permeance for two coatings with 5% PDMS [11]. Sandru, M., [15] points out that PDMS as a gutter layer should not affect the permeance, since PDMS have high permeance itself. It should only seal the surface defects of the membrane. An explanation for the increase in selectivity may be that the transport mechanism has changed from a situation largely influenced by Knudsen diffusion when open pores were present, to a mainly pure solution diffusion mechanism when pores were sealed. This is further supported by the fact that the N₂ permeance decreases from one to two coatings, and N₂ has both low solubility and diffusivity while CO₂ has a high solubility and therefore increases if the mechanism changes, see table 2.5.2.1.

Table 2.5.2.1: Permeance for one and two coatings with 5% PDMS for PSf hollow fibre[11]

Pressure [bar]	One coating		Two coatings	
	N ₂ [m ³ (STP)/m ² bar h]	CO ₂ [m ³ (STP)/m ² bar h]	N ₂ [m ³ (STP)/m ² bar h]	CO ₂ [m ³ (STP)/m ² bar h]
1.2	0.0020	0.090	0.0017	0.11
3	0.0019	0.087	0.0018	0.10
5	0.0019	0.078	0.0017	0.091
8	0.0029	0.074	0.0017	0.090

2.5.3 Effect of coating solution concentration

Chen, H.Z., et al [37] and Ji, P., et al [41] have investigated the effect of coating solution concentration on the coating layer and separation properties for polyethersulfone (PES) coated with poly(ethylene glycol) (PEG) and PSf coated with poly(N,N-dimethylaminoethyl)-poly(ethylene glycol methyl ether acrylate) (PDMAEMA-PEGMEA) respectively. High coating solution concentrations results in a relatively thick dense top layer, which will increase the resistance for mass transport and lead to a lower permeance. This result is reported by both Ji, P., et al [41] and Chen, H.Z., et al [37].

Using low concentrations of coating solution Ji, P., et al [41] achieved lower selectivity than desired. They suggest that the low concentration results in a coating layer that is so thin that it collapses over the pores and develops surface defects because of this. The reduction in selectivity caused by low coating solution concentrations is also noted by Shieh, J.-J., et al

[42] on a PSf hollow fibre coated with poly(4-vinylpyridine). They relate this to the non-uniform shrinkage of the coating layer when the solvent evaporates. The shrinkage causes cracks to form in the coating layer and the selectivity will be reduced. The optimal coating solution concentration will be some intermediate value, and is dependent on both the support material and the coating material.

2.5.4 Effect of viscosity

The viscosity is one of the key factors for preparation of hollow fibre membranes. Sandru, M., et al [36] shows that higher viscosity gives a thicker coating layer and almost a defect free surface leading to better selectivity. The effect of viscosity is also discussed in chapter 3.7.1.

2.5.5 Effect of pH

In cases when PVAm is used as the coating material, Sandru, M., et al [36] reported that pH should have a large effect on PVAm viscosity. Still, no clear effect of pH on coating layer thickness was observed in the coating experiments.

2.5.6 Effect of hydrophilicity of coating materials

Coating a hydrophobic porous support membrane with a hydrophilic coating material will prevent pore penetration by the coating material as reported by Sandru, M., et al [36] and Kai, T., et al [43]. Sandru, M., et al [36] further reports that when coated on a hollow fibre support membrane, the coating material has to show some affinity to the support membrane to be able to attach as the coating is performed vertically. Kai, T., et al [43] added an amphiphilic chitosan gutter layer in order to attach the hydrophilic coating material to their hydrophobic support membrane. In this study [43] relatively hydrophobic PSf was used as a support membrane and hydrophilic PAMAM (poly(amidoamine)) dendrimers as selective coating material. Chitosan, which has affinity for both materials, was used as an intermediate gutter layer to hold the support and the coating layer together.

The composite membranes made in the Specialization project consist of PSf fibres as the support, which is a slightly hydrophobic polymer with a contact angle of 64° [15]. As the PVAm used for the selective layer is hydrophilic and the coating solution is PVAm solved in water, is it difficult for the PVAm to attach to the PSf. Therefore some of the composite membranes were first coated with PDMS as an intermediate gutter layer. PDMS has quite good affinity for both materials, and besides having the same effect as Chitosan, PDMS also covers surface defects. For all the fibres coated with PVAm, the PSf support was first placed in water to increase the PSf fibres affinity to water as much as possible [11].

2.6 Composite membranes

The composite membranes are asymmetric membranes, which consist of a porous support layer and a thin dense top layer made of different polymeric materials [5]. Integrally skinned membranes are another type of asymmetric membrane. These membranes are usually made by using the phase-inversion technique, and consist of a porous support layer and a thin dense top layer made of same polymeric materials [44]. Chung, T.-S., et al [44] points out that composite membranes have several advantages compared to integrally skinned membranes. Integrally skinned asymmetric membranes will not be cost effective when expensive materials are used. In a composite membrane the expensive material may be limited only to the top

layer, and cheaper materials may be used for the support. Highly selective but brittle polymers must be used for integrally skinned membranes, and these are hard to form, and for composite membranes can each of the components be optimized individually, making it easier to produce defect-free membranes. The factors influencing the coating layer properties of the composite membrane are discussed earlier in chapter 2.2.

The effect of coating with PVAm on poly(phenylene oxide) (PPO) and PSf was investigated by Sandru, M., et al [36]. For the PVAm/PSf composite membrane the selective layer was 0.7-1.5 μm . It obtained a CO_2/N_2 selectivity between 100 and 230 and CO_2 permeance from 0.006 to 0.022 $\text{m}^3(\text{STP})/(\text{m}^2\text{bar h})$. For the PVAm/PPO membrane, a selectivity between 20 and 500 and a permeance between 0.11 to 2.3 $\text{m}^3(\text{STP})/(\text{m}^2\text{bar h})$ was obtained. This shows that also the type of support membrane is influencing the overall separation properties of the composite membrane. It was also shown that the CO_2 permeance before coating was similar to the CO_2 permeance after coating with PVAm for both types of support during humid testing conditions. This confirms that the main resistance to mass transport for this kind of system resides in the thick support and not in the selective top layer. The CO_2/N_2 selectivity of the composite membrane increases when coated with PVAm because CO_2 is transported by facilitated transport as the water swollen PVAm form a bicarbonate complex with CO_2 , and CO_2 is transported through the membrane as a bicarbonate complex in addition to solution diffusion mechanism. The N_2 does not form complexes with PVAm and is transported purely by solution diffusion mechanism. This leads to an increase in CO_2/N_2 selectivity when coating with PVAm [10, 36].

An advantage of composite membranes is that it is easy to form a defect free selective layer relative to the integrally skinned membranes. Still, a completely defect free, thin selective layer may be hard to achieve because the support may not be defect free. Shieh, J.-J., et al [42] and Henis, J.M.S., and Tripodi, M.K [9] suggests that the composite membrane should be coated on top of the selective layer with a highly permeable material. The idea is that this highly permeable material will seal the remaining surface defects and protect the selective layer without having a noticeable impact on the flux through the membrane. By coating with a protecting layer, Henis, J.M.S., and Tripodi, M.K [9] also point out that a less flawless support may be accepted than for conventional composite membranes which do not have a protective coating layer. The experiment by Henis, J.M.S., and Tripodi, M.K [9] was performed on a PSf support membrane coated with silicone rubber, but they suggest that the relative behaviour will be the same on any other combination as long as the porosity is the same and the coating layer on top of the selective layer is highly permeable. Hwang, H.Y., et al. [45] reports that their PSf fibres coated with PDMS obtained selectivity much higher than the PDMS intrinsic selectivity. The selectivity of the membrane was similar to the intrinsic selectivity of PSf. This implies that the gas separation occurs on the PSf layer and PDMS coating layer only cover defects on the membrane surface, so it can maintain its selectivity [45]. An advantage with this method is that there are not required ultrathin coatings which are hard to apply and which often are difficult to deal with when applied to a glassy polymer. The ultrathin coating is avoided as the permeability of the silicone rubber coating material is close to the intrinsic permeability of the support membrane, and thus can a thicker coating layer be applied without influencing the permeance as the main resistance for mass transfer will be in the thick support. Chung, T.-S., et al. [44] and Heni, J.M.S., and Tripodi, M.K [9] have reported good results with PDMS as a highly permeable sealing layer.

PDMS can be used as a highly permeable intermediate sealing gutter layer to cover defects in the porous support, or as a highly permeable protective and sealing layer to cover defects and

to protect the intermediate selective layer. The selective layer could for instance be PVAm. Sandru, M., et al. [46] reports that composite PVAm membranes have similar CO₂/N₂ selectivity as other FSC membranes. This requires two coating steps, one for PDMS and one for PVAm, and this is a time consuming process.

Two different composite membranes were made in the Specialization project [11]. There were performed coatings of a PSf support with both PDMS and PVAm as the top layer with the other coating layer as the intermediate layer. The composite fibre with PVAm as the intermediate layer showed the best selectivity and permeance with different pressure. It had a selectivity from 94-64 and a permeance from 0.08-0.06 m³(STP)/(m²bar h) when the pressure was changed from 1.2-8 bar. The fibre with PDMS as the intermediate layer had a selectivity of 82-41 and a permeance on 0.06-0.04 m³(STP)/(m²bar h) [11]. This shows that the composite membrane with PVAm as intermediate layer and PDMS as the top layer has the best mechanical resistance to changes in pressure. This could be due to the fact that the PDMS layer is protecting the PVAm selective layer from external effects when PDMS is coated on top. For the fibre first coated with PDMS the selectivity at 8 bar was lower than for the same fibre only coated with PDMS. After the permeation test, the membrane was checked for leakage, but no leakage was found. It was expected that the selectivity would be higher for all pressures for this membrane, and this could indicate that one of the fibres has collapsed due to the high pressure applied. The difference in permeance for the two composite membranes can result from that the fibre that had PVAm as the intermediate layer only had one PDMS layer, while the other composite membrane had two layers of PDMS. Another reason for a higher permeance for the fibre coated first with PVAm and then with PDMS one time, is that PDMS as a slightly hydrophobic polymer will not attach so good to the hydrophilic PVAm surface, which it would have done to the PSf surface. This might give a thinner PDMS layer, resulting in higher permeance [11].

2.7 Blend membranes

Instead of coating the support membrane with the selective component, the selective component can be introduced to the dope solution. This can have the advantage of forming a membrane with both high permeance and high CO₂/N₂ selectivity in one step. The time-consuming coating procedure, as for composite membranes, is avoided when preparing blend membranes. In Helberg [12] a blend membrane was made by adding 0.2% of the selective material PVAm in the dope solution. This blend was tested in the Specialization project and a new blend membrane with 1 % PVAm was made and tested [11]. The influence of relative humidity on the blend membranes were tested with changing the relative humidity of the feed gas from 40 to 100%. When the humidity was increased the selectivity increased from 43 to 56 for 0.2% PVAm/PSf blend as shown in figure 2.7.1 a. This proves that by increasing the relative humidity of the feed gas from 40 to 100%, the presence of a very small amount of PVAm contributes to a higher selectivity. PVAm is a polymer which selectively transports CO₂ in a humid atmosphere. The water in the polymer from the humid gas feed increases the CO₂ diffusivity, by facilitating the reaction between amino groups and CO₂. No effect of humidity is expected for a pure PSf hollow fibre, as PSf is relatively hydrophobic and does not interact with water. The highest selectivity obtained for this membrane was 78 with a permeance of 0.06 m³(STP)/m² bar h. The preparation of the 1% PVAm/PSf blend membrane was not successful in the specialization project, and it was believed that the selective component was removed from the dope solution before the membrane was prepared. Figure 2.7.1b shows no increase in CO₂/N₂ selectivity as the humidity increases for the blend

membrane supposedly containing 1% PVAm, indicating that there were no selective component in the membrane [11].

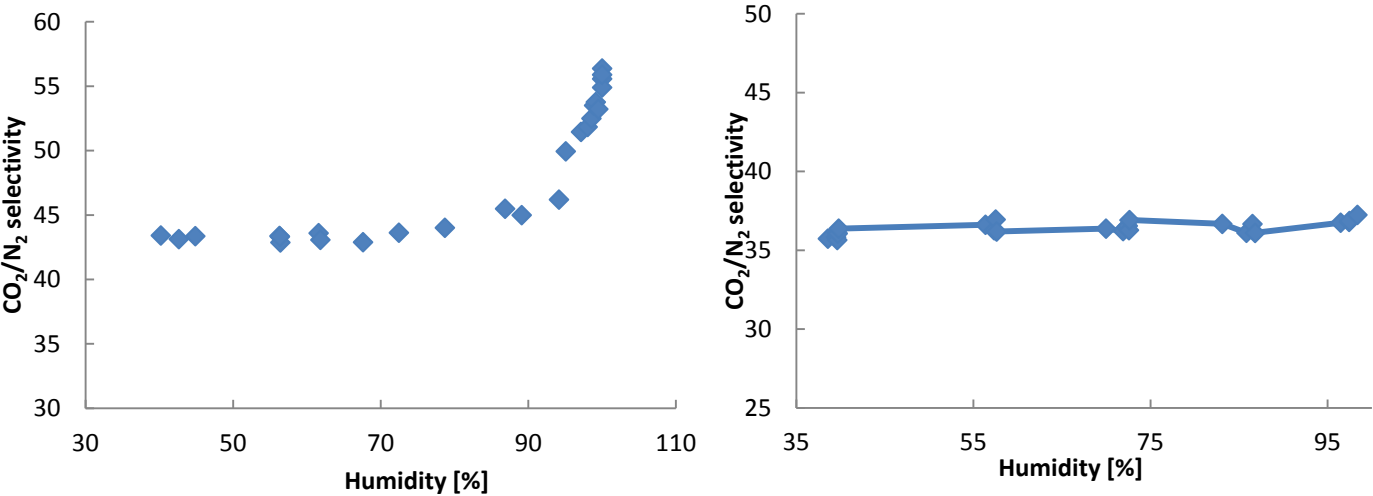


Figure 2.7.1: (a) The influence of relative feed humidity on selectivity for 0.2% PVAm/PSf blend coated two times with 5% PDMS. (b) Selectivity of 1% PVAm/PSf blend fibre coated two times with 5% PDMS plotted against the relative humidity of the feed [11].

Chapter 3: Theory

3.1 Membrane definition

A membrane can be considered a selective barrier or interface between two phases, where phase one is the feed and phase two is the permeate. Separation between different components is possible because the membrane has the ability to transport one component from the feed more readily than the other components. Separation occurs because of difference in physical or chemical properties between the membrane material and the components in the permeate [5].

3.2 Membrane classification

Membranes can be divided into two groups, natural and synthetic. Synthetic membranes consist of organic membranes which are polymeric or liquid and inorganic membranes which are ceramic or metal. Solid synthetic membranes can further be divided by difference in morphology and structure into symmetric or asymmetric membranes [5].

Symmetrical membranes are homogeneous. These membranes are completely uniform in structure and composition. Asymmetric membranes consist of a support membrane with a very thin dense top layer. The dense skin layer and porous support may consist either of the same or different materials. The asymmetrical membranes main types are integrally skinned membranes and composite membranes [5].

3.2.1 Composite membranes

Composite membranes consist of a porous support membrane which is coated with a thin dense top layer. The dense top layer and the porous support layer consist of different polymers, which make it possible to optimize each layer independently. Another advantage with composite membranes is the high chemical and thermal stability. The function of the support membrane is to provide mechanical strength, while the top layer function is to selectively transport molecules through the membrane. The rate limiting step for the composite membrane is mostly transport through the dense top layer [5].

Single layer composite membrane

In a single layer composite membrane the selective layer is coated on a symmetric porous support membrane. In figure 3.2.1.1 a schematic drawing of a single layer composite membrane is shown.

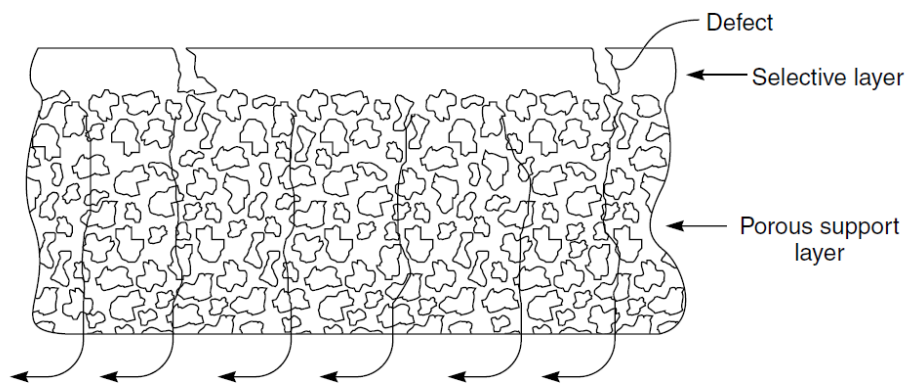


Figure 3.2.1.1: Single layer composite membrane [16]

Multilayer composite membrane

The selective layer should be as thin as possible, but still defect free. Defects from gas bubbles, dust particles and surface defects at the support can be hard to eliminate [16]. A solution to this is the addition of a highly permeable, non-selective intermediate layer, called a gutter layer, to the support membrane and the thin dense layer. This is a multi layer composite membrane. The gutter layer polymer could for example be PDMS [5]. PDMS is a sticky and highly permeable polymer, which seal surface defects. There are two types of multilayer composite membranes, one where the gutter layer is between the support membrane and the selective layer, and one with the selective layer between the support membrane and the gutter layer. In the last case, the gutter layer will protect the selective layer in addition to sealing surface defects. Figure 3.2.1.2 shows a multilayer composite membrane.

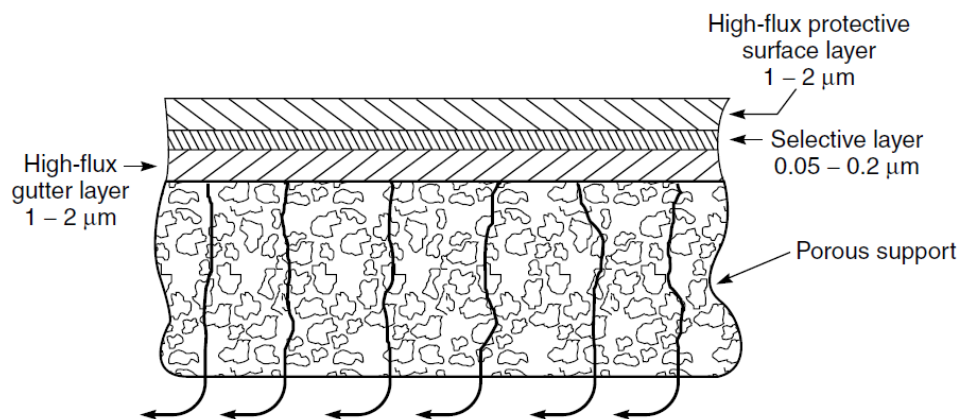


Figure 3.2.1.2: Multilayer composite membrane [16]

3.2.2 Polymer blend membranes

In a polymer blend membrane, two different polymers are mixed with each other on a molecular level, but few polymers are actually miscible. If mixing between two components causes a decrease in free enthalpy, the components are miscible. The entropy of mixing is very small for polymers, and the ability to mix is dominated by the heat of mixing alone. To ensure that two polymers are miscible, the enthalpy change has to be negative. The blend is homogenous if two polymers are miscible on a molecular level, while in a heterogeneous blend one polymer is dispersed in the other. The properties of a heterogeneous blend and homogenous blend are different. In a homogenous blend the properties of individual polymers disappear, and the properties of the blend lie between the properties of the two polymers. In a heterogeneous blend the properties of both polymers are conserved [5].

The starting point for making a polymer blend is a polymer solution containing a common solvent, or different but mutually miscible solvents for the two polymers. To form a blend, other polymers or additives are introduced to the dope solution. The introduction of another polymer can improve the membrane morphology and give better separation properties.

3.2.3 Carrier membranes

A carrier membrane is a membrane with a carrier inside. The carrier is generally a functional group or a material which has the ability to react specifically with only one of the components and the flux of that component can be improved. A carrier can be either mobile or fixed. If the carrier is mobile, the carrier is dissolved in a liquid. For a fixed carrier, the carrier is bound chemically or physically to a solid polymer [5].

3.2.4 Membrane of polysulfone

Polysulfone (PSf) is a polymer with very good chemical and thermal stability as the high glass transition temperature of 190°C indicates [5]. The glass transition temperature is the temperature where the state of the polymer is changed, from rubbery to glassy. The glass transition temperature may also be described as the temperature where the free volume between the polymer chains is large enough for the chains to rotate freely when a glassy polymer is heated, or the temperature when the free volume becomes so small that the polymer chains no longer can move when a rubbery polymer is cooled down [47]. Glassy polymers have high selectivity but low permeability, while rubbery polymers have low selectivity and high permeability. Polysulfone is often used as porous support material for composite membranes [5]. In figure 3.2.4.1 the chemical structure of polysulfone is shown.

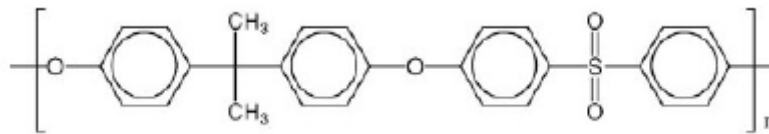


Figure 3.2.4.1: The chemical structure of polysulfone [5]

3.3 Gas transport in membranes

3.3.1 Driving force

A driving force is needed in order for the components in the feed to be transported through the membrane. The driving force may be due to a chemical potential difference or an electrical potential difference, which are a result of difference in either pressure supplied to the system, partial pressure, concentration, temperature or electrical potential gradients. The relationship between the flux and the driving force is shown in equation 3.3.1.1 [5].

$$J = -A \frac{dX}{dx} [5] \quad (3.3.1.1)$$

Where J is the flux, A is called the phenomenological coefficient and dX/dx is the driving force. X is the gradient and x is a coordinate perpendicular to the transport barrier [5].

3.3.2 Transport in porous membranes

The pores in a porous membrane are often small, and the diffusion of gases may depend on the diameter of the pores. The mean free path λ is the average distance a gas molecule travels before it collides with another gas molecule, see equation 3.3.2.1 [48].

$$\lambda = \frac{3,2\mu}{P} \sqrt{\frac{RT}{2\pi M}} [48] \quad (3.3.2.1)$$

Where λ is the mean free path [m], μ is viscosity [Pa·s], P is pressure [Pa], T is temperature [K], M is molecular weight [kg/kmol] and R is the universal gas constant $8.3143 \cdot 10^3$ [N·m/kmol·K]. The transport mechanisms which can occur in a porous membrane are Knudsen diffusion, molecular diffusion, which is viscous or convective flow, molecular sieving and surface selective flow. The last two mechanisms depend on the structure of the membrane. Figure 3.3.2.1 shows the different mechanisms.

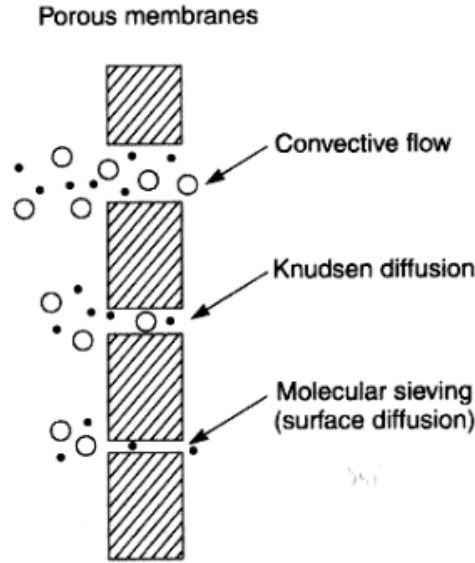


Figure 3.3.2.1: Different mechanisms in a porous membrane [16]

Knudsen diffusion

In Knudsen diffusion the gas molecules collide more often with the pore wall than with other gas molecules because the mean free path is large compared to the diameter of the membrane pores [48]. The pore sizes where Knudsen diffusion normally occurs is between 10 Å and 500 Å [49]. The Knudsen diffusion is independent of the pressure and can be calculated from equation 3.3.2.2 [48].

$$D_{KA} = \frac{2}{3} \bar{r} \bar{v}_A \quad [48] \quad (3.3.2.2)$$

Where D_{KA} is the diffusivity for Knudsen diffusion [m^2/s], \bar{r} is the average pore radius [m], \bar{v}_A is the average velocity for component A [m/s]. When the kinetic gas theory is used to evaluate \bar{v}_A the final equation for D_{KA} is equal to equation 3.3.2.3.

$$D_{KA} = 97,0 \bar{r} \left(\frac{T}{M_A} \right)^{1/2} \quad [48] \quad (3.3.2.3)$$

M_A is the molecular weight of A [kg/kmol] and T is the temperature [K]. Equation 3.3.2.3 shows that the transport of gases depends on the square root of the molecular weight. This makes the separation between the different molecules inversely proportional to the ratio of the square roots of the molecular weights of the gases [5], see equation 3.3.2.4.

$$\alpha_{A/B} = \sqrt{\frac{M_B}{M_A}} \quad (3.3.2.4)$$

Equation 3.3.2.4 shows that low separation is normally obtained for Knudsen diffusion, since a good separation requires a large difference in molecular weight between the molecules in the mixture.

The flux through the Knudsen regime is expressed in equation 3.3.2.5.

$$J = \frac{4r\epsilon}{3} \left(\frac{2RT}{\pi M_{m,g}} \right)^{1/2} \left(\frac{p_0 - p_l}{lRT} \right) \quad [16] \quad (3.3.2.5)$$

Where J is the flux [$\text{kmol A/s}\cdot\text{m}^2$], r is the pore radius [m], ε is the porosity of the membrane, M_{mg} is the molecular weight of the gas [kg/kmol], l is the length [m], T is the temperature [K], R is the ideal gas constant [$\text{N}\cdot\text{m/kmol}\cdot\text{K}$], p_0 and p_l are the absolute pressures of the gas at the beginning and the end of the membrane [Pa] [16].

Viscous flow

For pore sizes larger than $10\mu\text{m}$ viscous flow occurs. In viscous flow the gas molecules collide exclusively with each other and no separation is obtained between the different gaseous components [5]. The flux for viscous flow is shown in 3.3.2.6.

$$J = \frac{r^2 \varepsilon [p_0 - p_l] [p_0 - p_l]}{8\eta lRT} [16] \quad (3.3.2.6)$$

Where J is the flux [$\text{kmol A/s}\cdot\text{m}^2$], r is the pore radius [m], ε is the porosity of the membrane, η is the viscosity of the gas [$\text{Pa}\cdot\text{s}$], l is the length [m], T is the temperature [K], R is the ideal gas constant [$\text{N}\cdot\text{m/kmol}\cdot\text{K}$], p_0 and p_l are the absolute pressures of the gas at the beginning and the end of the membrane [Pa] [16].

Molecular sieving

For pore sizes in the range 5 to 20 Å, separation between different gaseous components are obtained by molecular sieving. The separation is obtained because the small molecules will go through the membrane while the larger molecules are retained. The transport mechanisms through these membranes are complex and include both diffusion in the gas phase and surface diffusion [16].

Surface selective flow/surface diffusion

In surface selective flow the separation between the different gas components takes place because of an interaction between the molecules and the pore wall of the membrane. This occurs in membranes with pore diameters smaller than 10 Å. This pore size gives a surface area of the pore walls about $100\text{ m}^2/\text{cm}^3$ and significant amounts of gas then adsorb onto the pore walls [16]. The molecules with the largest diameter have the highest solubility, and these molecules will react with the pore wall more readily [5]. The larger molecules then pass through the membrane, while the smallest components are retained. Surface diffusion often occurs simultaneously with Knudsen diffusion, but it is the dominant mechanism in a certain pore size regions [49].

3.3.3 Transport through dense membranes

Molecules with sizes within the same order of magnitude cannot be separated by a porous membrane. Instead, a dense membrane should be used. In dense membranes, pores are present on a molecular level so transport through such a membrane is possible. The molecular pores can be described in terms of free volume [5]. The free volume is created by oscillations caused by thermal vibrations in the molecules. These oscillations increase with temperature, which causes the free volume to increase as well [47]. Figure 3.3.3.1 shows a schematic drawing of transport through a dense membrane.

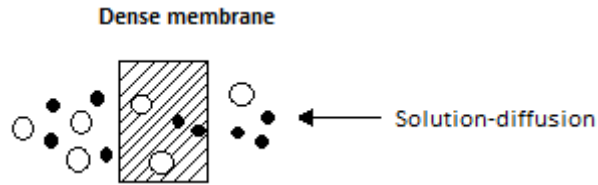


Figure 3.3.3.1: Transport through a dense membrane [16]

Transport by the solution-diffusion mechanism

Solution-diffusion is a mechanism that occurs in all dense membranes. The solute gas will dissolve in the dense membrane, and then diffuse through the membrane [48].

To describe the overall transport rate of molecules through a membrane, the parameter permeability is introduced. In a mixture of gases, the permeability of each gas is often reduced due to interactions between the gas molecules. Permeability is a function of solubility, S , and diffusivity, D_{AB} , as shown in equation 3.3.3.1 [48].

$$P = S \cdot D_{AB} \quad [48] \quad (3.3.3.1)$$

The thermodynamic parameter solubility, describes how well an amount of penetrant is sorbed by a membrane at equilibrium. Gases have a very low solubility in elastomer polymers, and the solubility can therefore be described by Henry's law, see equation 3.3.3.2. For organic vapours and liquids Henry's law cannot be used for describing solubility, as these fluids cannot be considered ideal [5].

$$C_i = S \cdot p_i \quad [48] \quad (3.3.3.2)$$

Where C_i [$\text{m}^3(\text{STP})/\text{m}^3$] and p_i [bar] are the concentration and partial pressure of species i , and S is the solubility of species i in the solid [$\text{m}^3(\text{STP})/\text{m}^3\text{bar}$]. Solubility for a gas can be determined by measuring how easily the gas condensates. Large molecules condensate faster than smaller ones and this makes solubility increase with increased molecule size [5].

The solubility and the permeability are independent of concentration in ideal systems. The dual sorption theory is introduced to describe the solubility of a gas in glassy polymers. The theory is that a sorption following Henry's law and a Langmuir type sorption is happening simultaneously. When added they give the total sorption [5].

The kinetic parameter diffusivity, describes how fast a penetrant is transported through the membrane. When molecule size increases, the diffusivity decreases [5]. The solubility and diffusion coefficient are both dependent of the polymer and penetrant [50]. Fick's law is the simplest way to describe transport of gases through a dense membrane, see equation 3.3.3.3 [5].

$$J = -D \frac{dc}{dx} \quad [5] \quad (3.3.3.3)$$

Where J is the flux of a component through a plane perpendicular to the direction of diffusion [$\text{kmol A}/\text{m}^2 \cdot \text{s}$], which is proportional to the concentration gradient dc/dx . D is the diffusion coefficient [m^2/s] [5]. Equation 3.3.3.4 is obtained by integrating over the cross section of the membrane.

$$J = \frac{D_A}{l} (c_{A,0} - c_{A,l}) \quad [5] \quad (3.3.3.4)$$

Where l is the thickness of the membrane [m], $c_{A,0}$ is the penetrant concentration of the feed side and $c_{A,l}$ is the penetrant concentration on the permeate side [kmol/m³] [5]. By introducing Henry's law, see equation 3.3.3.2 the concentration is related to the partial pressure, and equation 3.3.3.4 can be rewritten to equation 3.3.3.5.

$$J = \frac{P}{l}(p_1 - p_2) \quad [5] \quad (3.3.3.5)$$

Where P is the permeability [m³(STP)m/m²barh], p_1 is the partial pressure on the feed side and p_2 is the partial pressure on the permeate side [bar]. The driving force for solution-diffusion is the difference in partial pressure [5].

3.3.4 Transport through a composite membrane

In composite membranes the gas molecules will diffuse from the high-pressure to the low-pressure side when used for gas separation. The permeation through a composite membrane is a combination of the mechanisms in the porous and the dense layers and possibly facilitated transport, but the dense top layer is in most cases the rate limiting step.

3.3.5 Facilitated transport

Facilitated transport is a reversible complexation process in combination with a diffusion process. It occurs when a component and a carrier form a complex, which diffuse through the membrane. These combined processes result in a flux that no longer is proportional to the driving forces. This leads to high fluxes even for low concentrations in the feed. The facilitated transport could be either uncoupled or coupled. In uncoupled transport it is only one component that reacts with the carrier. This component is transported through the membrane with both solute-carrier complex diffusion and ordinary diffusion. The other components are only transported with ordinary diffusion. In coupled transport a second component also react with the carrier. This leads to the possibility of moving one of the components against the concentration gradient for that component from low to high concentration [5]. Figure 3.3.5.1 shows schematic drawings of transport in a membrane without carrier and transport with carrier both uncoupled and coupled transport mechanisms.

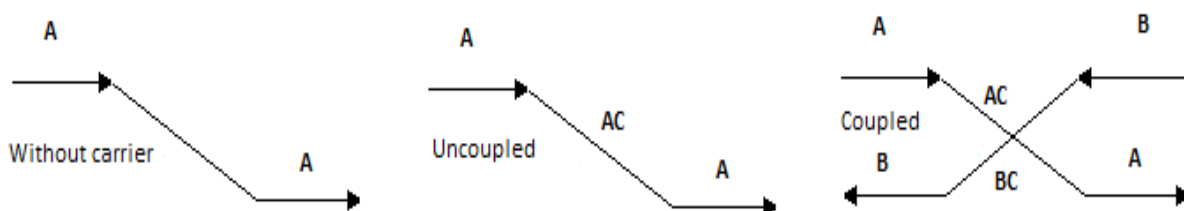


Figure 3.3.5.1: Transport without and with carrier and uncoupled and coupled transport [5]

The transport rate for a component through a membrane is the sum of the permeation caused by solution-diffusion and facilitated transport mechanisms. Permeation in the form of solution-diffusion occurs for all the components present at the feed side. Facilitated transport only happens for components that react with the carriers and form complexes. A component which reacts with the carrier can be transported across the membrane in either a non-complexed or a complexed form. The total flux for the component will be as shown in equation 3.3.5.1 [5].

$$J_A = \frac{D_A}{l}(c_{A,0} - c_{A,l}) + \frac{D_{AC}}{l}(c_{AC,0} - c_{AC,l}) \quad [5] \quad (3.3.5.1)$$

Where J_A is the flux [$\text{kmol}/\text{m}^2\cdot\text{s}$] D_{AC} is the diffusion coefficient for the complex [m^2/s], l is the membrane thickness [m] and $c_{AC,0}$ and $c_{AC,l}$ are the concentration of the carrier-solute complex at the two interfaces [kmol/m^3] [5]. For the other components, which do not react with the carrier the total flux will be as the flux for solution-diffusion, shown in equation 3.3.3.4.

Fixed site carrier membranes for CO_2 capture

Fixed site carrier membranes can be used for CO_2 capture, with amine groups bound to the polymer backbone as possible carriers. The polymer polyvinyl amine (PVAm) can be coated on a support membrane to achieve better selectivity, because CO_2 facilitated transport is created by the PVAm selective layer. In figure 3.3.5.2 a schematic drawing of the transport mechanism for PVAm fixed site carrier membrane is shown [10].

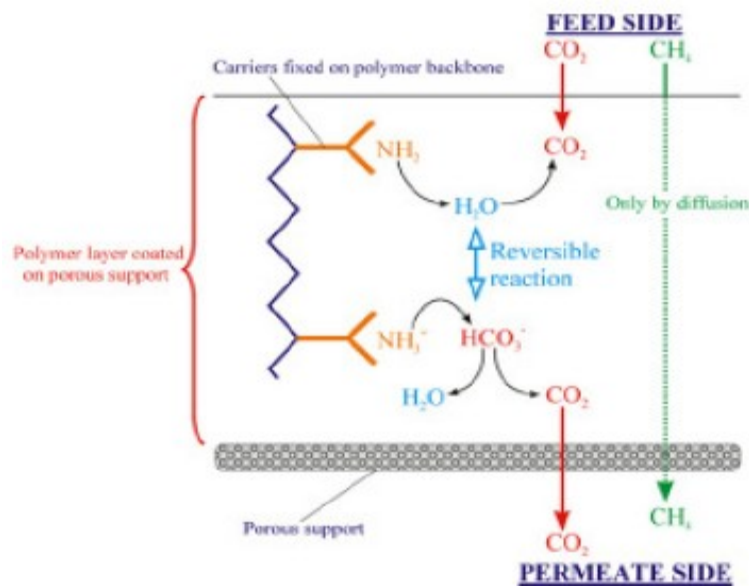
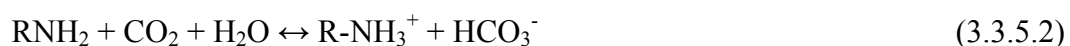


Figure 3.3.5.2: Facilitated transport for a PVAm membrane [10]

From the figure 3.3.5.2, it can be seen that CO_2 reacts with the primary amine PVAm and water to form bicarbonate, HCO_3^- , see equation 3.3.5.2. CO_2 is transported through the membrane in this form. A humid gas stream gives a better selectivity for a fixed site carrier membrane containing amino groups, because water in the membrane is acting as a mobile medium for transport of CO_2 and keeps the amino groups active. The CO_2 molecules are transported both by facilitated transport and solution-diffusion. The other components, such as N_2 and CH_4 , do not react with the carrier and are only transported by solution-diffusion [10].



3.4 Membrane terminology

3.4.1 Process parameters

The feed stream is the flow of either gas or liquid which enters the membrane module and divides into two streams, permeate and retentate. The permeate is the part of the feed which passes through the membrane, while the retentate is the part of the feed that is rejected by the membrane, thus passing straight through the module. In figure 3.4.1.1 a schematic drawing of

the membrane module with the position of streams is shown. Both the permeate stream and the retentate stream can be the product [5].

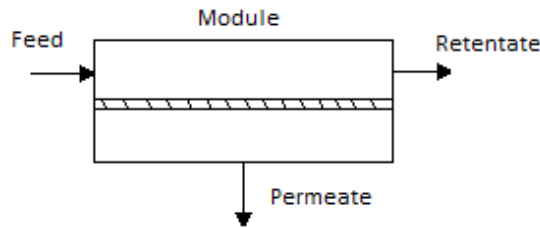


Figure 3.4.1.1: Schematic drawing of membrane module with flow descriptions [5].

3.4.2 Flux

The flux is the permeation rate. It is defined as the volumetric flow going through the membrane per unit area and time. The flux is given in equation 3.4.2.1 [5].

$$J_i = \frac{q_p \cdot x_{pi}}{A} [5] \quad (3.4.2.1)$$

Where J_i is the flux for component i [m/s], q_p is the permeate flow rate [m³/s], x_{pi} is the mole fraction in the permeate for component i and A is the membrane area [m²].

3.4.3 Membrane selectivity

The membrane selectivity is a measure of the membrane's ability to separate the permeating species relative to each other. The membrane selectivity is given as the permeability ratio for two species i and j in a mixture when they are permeating through a membrane, see equation 3.4.3.1 [15]. Membrane selectivity is also known as ideal selectivity [50].

$$\alpha_{i/j} = \frac{P_i}{P_j} = \left(\frac{D_i}{D_j} \right) \cdot \left(\frac{S_i}{S_j} \right) [15] \quad (3.4.3.1)$$

Where P is the permeability [m³(STP)m/m²barh], D is the diffusivity [m²/h] and S the solubility [m³(STP)/m³bar] for the species i and j [15].

3.4.4 Process selectivity

The process selectivity of a membrane gives an expression of the membrane's ability to separate two components in relation to each other, see equation 3.4.4.1 [5].

$$\alpha_{A/B} = \frac{y_A/y_B}{x_A/x_B} [5] \quad (3.4.4.1)$$

Where $\alpha_{A/B}$ is the selectivity, y_A and y_B are the mole fractions of species A and B in the permeate, and x_A and x_B are the mole fractions of species A and B in the feed. The selectivity is chosen so it becomes larger than one, which means that $\alpha_{A/B}$ is chosen if A is easiest transported through the membrane and $\alpha_{B/A}$ if B is easiest transported through the membrane. If the selectivity is equal to one, both components are transported at the same rate through the membrane, and the membrane does not favour transport of either of the components and no separation occurs [5].

3.4.5 Permeance

The permeance is given in equation 3.4.5.1

$$P_M = \frac{D_{AB} \cdot S}{L} = \frac{P}{L} \quad [48] \quad (3.4.5.1)$$

Where P_M is the permeance [$\text{m}^3(\text{STP})\text{m}/\text{m}^2\text{barh}$], D_{AB} is the diffusivity [m^2/h], S the solubility [$\text{m}^3(\text{STP})/\text{m}^3\text{bar}$] and L the membrane thickness [m] [48]. The permeance takes the thickness of the membrane into account, which makes it easier to compare membranes with different thicknesses.

3.4.6 Permeate purity

The permeate purity is defined as the mole fraction of desired component in the permeate stream [51]. The permeate purity can be calculated as shown in equation 3.4.6.1.

$$y_{ip,j} = \frac{F_{ip,j}}{\sum F_{kp,j}} \quad [51] \quad (3.4.6.1)$$

Where $y_{ip,j}$ is the permeate purity with respect to component i , $F_{ip,j}$ [mol/s] is molar flow of component i in the permeate, $\sum F_{kp,j}$ [mol/s] is the sum of all components at the permeate side [51].

3.4.7 Hydrophilic and hydrophobic

Hydrophilic materials have high affinity to water, while hydrophobic materials are highly repellent to water. The degree of hydrophilic or hydrophobic character can be measured from the contact angle between a droplet of water and the material [5]. A surface is considered hydrophilic when the contact angle between water and the surface is between 0° - 90° , and the surface is considered hydrophobic when the contact angle is 90° - 180° [15].

3.4.8 Complete mixing model

In the complete mixing model the concentrations at the feed and permeate side are constant at any point. The feed concentration is also equal to the retentate concentrations. Complete mixing can be found in systems that have low recovery. Recovery is defined as the fraction of the feed that has permeated through the membrane, see equation 3.4.8.1. Recovery is also known under the name stage cut [5].

$$S = \frac{q_p}{q_f} \quad [5] \quad (3.4.8.1)$$

Where q_f and q_p are the molar flows in feed and retentate [mol/s] By combining the flux Equation with Fick's law and the equation for solution-diffusion, the equation for the flux of a gas i through a membrane assuming perfect mixing is obtained, see equation 3.4.7.2.

$$J_i = \frac{P_i}{l} \Delta p_i = \frac{P_i}{l} (x_{r,i} p_h - x_{p,i} p_l) \quad [5] \quad (3.4.8.2)$$

Where P_i is the permeability coefficient of component i [$\text{m}^3(\text{STP})\text{m}/\text{m}^2\text{barh}$], l is membrane thickness [m], p_h is partial pressure of component i at the feed side [bar], p_l is partial pressure of component i at the permeate side [bar], and $x_{r,i}$ and $x_{p,i}$ are the constant mole fractions of component i in the feed and permeate [5].

3.5 Membrane formation

3.5.1 Ternary system

A ternary system consists of a solvent, a non-solvent and a polymer [5]. In figure 3.5.1.1 is a ternary phase diagram shown.

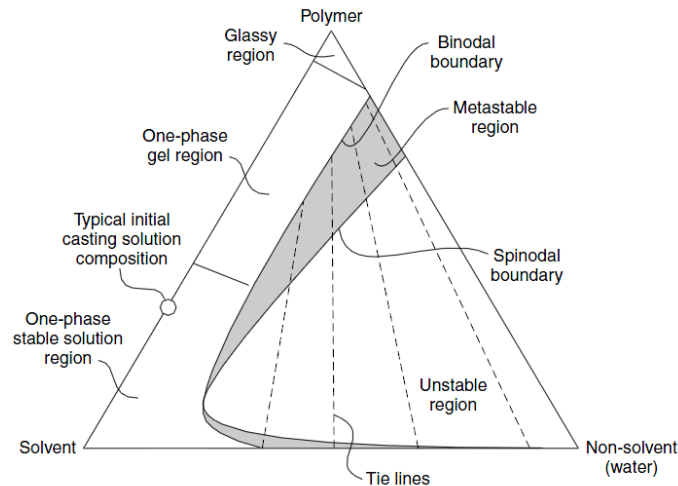


Figure 3.5.1.1: Schematic drawing of a ternary system [16]

The corners of the triangle represent the pure components, such as solvent, non-solvent and polymer, while the points within the triangle represent mixtures of the three components. The diagram consists of two principal regions, a one-phase region and a two-phase region. In the one-phase region all the components are miscible, while in the two-phase region the system separates into a solid and a liquid phase. The solid phase is polymer-rich and liquid phase is polymer-poor. These two phases are separated by the binodal boundary [16].

The casting solution concentration is located on the polymer-solvent line. When precipitation occurs, the solution loses solvent and gains non-solvent. The final casting solution concentration lies on the polymer/non-solvent line. This means that the casting solution moves from a concentration in the one-phase region to a concentration in the two-phase region [16].

During the precipitation process, the casting solution moves from the one-phase area to the two-phase area by crossing the binodal boundary. This brings the casting solution into a metastable two-phase area. In this region the polymer solution composition is thermodynamically unstable, but will not normally precipitate unless the nucleation is well established. When more solvent leave and more non-solvent enters the casting solution, the solution enters another region of the phase diagram. Here in this region the single-phases are not thermodynamically stable and the casting solution spontaneously separate into two phases. Between the metastable and unstable region the boundary is referred to as the spinodal boundary [16].

3.5.2 Mechanism of membrane formation

The membrane is made by precipitating one liquid polymer solution into two separate phases. The liquid-liquid demixing process can result in two different types of membrane

morphology, instantaneous liquid-liquid demixing and delayed onset of liquid-liquid demixing. In instantaneous demixing the membrane is formed immediately when it is immersed in the coagulation bath. With delayed demixing, it takes some time before the membrane is formed [5].

For liquid-liquid demixing the composition path gives the concentration in the film at a specific moment in time of $t < 1$ second. This path illustrates the composition, both as a function of time and as a range between the film and the interface. The composition path represents both the composition of element in the solution as a function of time and the composition range between interface and film. In figure 3.5.2.1 a schematic drawing of the composition path of a cast film immediately after immersion for instantaneous demixing and delayed onset of liquid-liquid demixing is given. Point t in figure 3.5.2.1 gives the concentration in the topside of the film, while b gives the bottom concentration of the film. The diffusion process start at the film/bath interface, therefore are changes in composition first noticed in the upper part of the film. For instantaneous demixing the film beneath the top layer t has crossed the binodal, which means that liquid-liquid demixing start immediately after immersion. For delayed demixing all the compositions directly beneath the top layer still lie in the one phase region, this means they are still miscible. This means that no demixing occurs immediately after immersion, but after a long time eventually the composition beneath the top layer will cross the binodal and liquid-liquid demixing will occur [5].

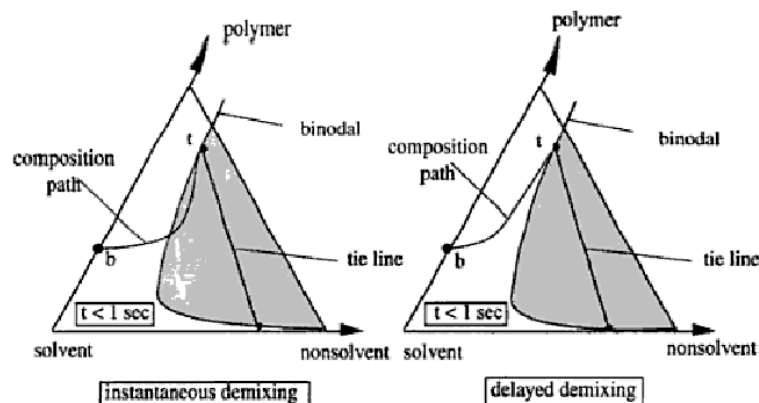


Figure 3.5.2.1: Ternary diagram for instantaneous demixing and delayed demixing [5]

When instantaneous liquid-liquid demixing between the solvent and the non-solvent occurs, a membrane with a relative porous top layer is formed and favours the forming of porous membranes. For delayed demixing the demixing mechanism results in membranes with relative dense morphology. In both cases the thickness of the top layer is dependent on the membrane forming parameters [5].

3.5.3 Formation of macrovoids

A macrovoid is an open space in the membrane material, which often can be formed in the porous sub layer of asymmetrical membranes. The presence of macrovoids is not favourable, because the macrovoids will lead to weak areas in the membrane. It is very important to avoid macrovoid formation when high pressure is applied, as in gas separation. This is because the macrovoids affect the overall membrane strength, which makes the membrane less pressure resistant. Macrovoids can also result in unwanted transport as Knudsen diffusion. From examination of many membranes it looks like macrovoids appear as a consequence of the

liquid-liquid demixing process. This indicates that the mechanism that favours the formation of porous membranes can also favour the formation of macrovoids [5].

3.6 Preparation techniques for hollow fibres

Both flat membranes and hollow fibre membrane can have similar performances, but the procedures for their preparation are different. This is because hollow fibres are self-supporting, and this makes the fibre dimensions very important. In addition, demixing takes place both from the bore side and from the shell side in hollow fibre preparation, while in preparation of flat membranes demixing occurs only from one side. There are three different methods for making hollow fibre membranes, wet spinning (dry-wet spinning), melt spinning and dry spinning. Dry-wet spinning is the most common method of preparation [5].

In a dry-wet spinning process, a viscous polymer solution is used. It contains a polymer, solvent and in some cases additives which can be a second polymer or a non-solvent. The polymer solution is pumped through a spinneret. The solution is filtered before it enters the spinneret. The bore solution is pumped through the inner tube of the spinneret. After a short residence time in the air, the fibres enter the coagulation bath where precipitation occurs. The distance between the spinneret and the coagulation bath is called the air gap. The solvent diffuses into the coagulation bath and the non-solvent from the coagulation bath will diffuse into the fibre. After a given period of time the exchange of solvent and non-solvent has reached a certain level of thermodynamically instability and demixing will occur [5]. After the coagulation bath, the fibres enter a second water bath called the flushing bath. The fibres are drawn by the speed-controlled wheel in the end of the flushing bath before the fibres enter the storage tank. Figure 3.5.1 shows a schematic drawing of the dry-wet spinning process.

In preparation of hollow fibres the spinning parameters and the membrane forming parameters affects the membrane morphology.

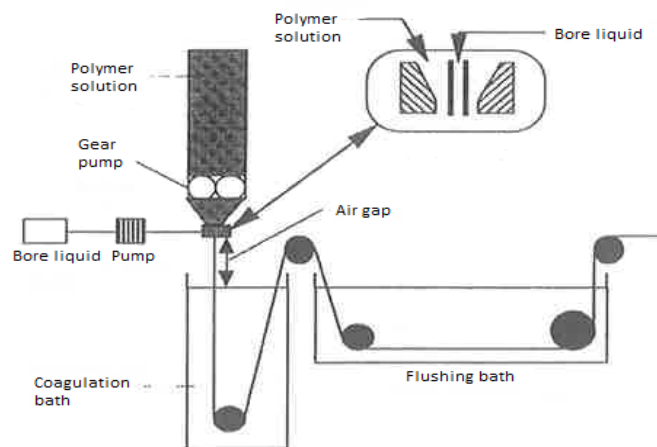


Figure 3.5.1: Schematic drawing of a dry-wet process [5]

3.6.1 Membrane forming parameters

Polymer concentration

Increasing the initial polymer concentration leads to higher concentration at the interface. This leads to a reduction of the porosity and flux. Hollow fibre spinning normally requires a higher concentration in the dope solution than flat membranes. This is because it is important for hollow fibres to be able to withstand the applied pressure of the process without collapsing.

The use of a more concentrated solution increases the thickness of the hollow fibre skin layer [16].

Solvent/non-solvent system

The best suitable solvent for the polymer is an aprotic solvent which is miscible with water. The solvent should also be non-volatile to create a porous structure. NMP has these specifications and is a good solvent for PSf. Water is most commonly used as the non-solvent in the coagulation medium. Water is the best choice from an environmental and economical point of view [5, 16]. Multiple solvents may be suitable for the chosen polymer, but the solvent and non-solvent should be completely miscible. A high miscibility is synonymous with a high mutual affinity. Water and NMP have high mutual affinity [5]. When high mutual affinity exists, a porous membrane is obtained, because higher miscibility between the solvent and the non-solvent decrease the likelihood of delayed demixing [5].

Addition of a non-solvent to the polymer solution

Addition of a non-solvent to the polymer solution has a considerable effect on the membrane structure. The ternary diagram gives the maximum amount of non-solvent that can be added to the polymer solution. The compositions must be in the one-phase region where all the components are completely miscible with each other. When a non-solvent is added to a solution it increases the composition path, shifts to the binodal and eventually crosses it. A polymer solution which has delayed demixing can shift to instantaneous demixing by the addition of a non-solvent to the polymer solution. This gives a membrane with a more porous and more open structure. It is normal to add another non-solvent than the one used as the coagulation medium [5].

Composition of the bore fluid and the coagulation bath

If the bore solution is water and the coagulation bath consist of some solvent, precipitation will happen first and most rapidly on the inside surface of the fibre. If the bore solution contains some solvent and the coagulation bath is water, outside precipitation occurs. Precipitation can in many cases happen at both the inside and outside surface. A dense anisotropic skin will be formed on the side where the precipitation occurs first and most rapidly. It is important to have the ability to manipulate the position of the dense layer, because the dense layer normally should face the feed flow [16]. This is shown in figure 3.6.1.1.

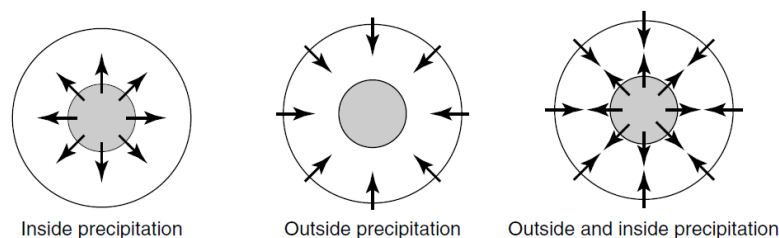


Figure 3.6.1.1: Forming of dense skin layer on the inside, the outside or on both sides of the hollow fibre [16]

3.6.2 Spinning parameters

Extrusion rate of the polymer solution and the bore fluid rate

Slow precipitation produces dense, more isotropic membranes, because of greater molecular orientation and chain package. Rapid precipitation gives porous, anisotropic membranes. The injection rate of bore fluid into the fibres is the decisive factor for the fibre wall thickness [16].

Air gap

When an evaporation step is introduced before immersion in the coagulation bath, it is possible to prepare defect-free asymmetric membranes [5]. Both solvent evaporation and intake of water can occur in the air gap. These phenomena may affect the fibre structure by generating a phase separation of the dope solution. The inner surface is dominated by the interaction of the solvent with the bore liquid, and water vapour in the air gap will not affect this surface. Increase in the air gap distance leads to decrease in the permeance. A too large air gap can create defects, because of gravity and elongational stresses [52].

Coagulation bath temperature

The temperature of the coagulation bath which is used to precipitate the polymer solution is an important parameter. In commercial membrane plants this temperature is controlled. Generally at low temperature of the coagulation bath, the precipitation produces more retentive membranes with a low flux [16].

3.7 Membrane coating

Coating is a technique where a thin dense top layer is supported on a porous support. The selectivity, permeation rate, and chemical and thermal stability can be improved by optimising each layer independently. There are numerous techniques for coating of polymer membranes, here only the most common technique is presented [5].

3.7.1 Dip-coating

Dip-coating is the most common coating technique for hollow fibres, but it can also be used on flat sheet membranes. This technique is very simple to perform. The membrane is immersed in the coating solution containing the coating polymer at low concentration. When the membrane is removed from the coating solution, a thin layer of the solution is attached to the membrane's surface. Eventually the membrane is placed in an oven for the solvent to evaporate [5]. For controlling the coating layer thickness, the membrane can be lead through a slot at the liquid surface after the membrane is removed from the coating solution. This is less favourable for very thin layers and solutions with low viscosity [39]. Figure 3.7.1.1 shows a schematic drawing of dip-coating.

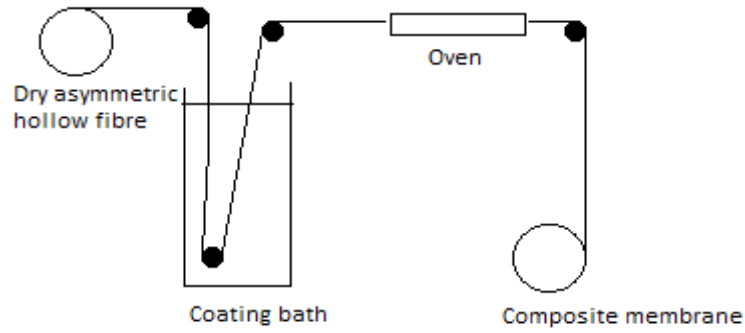


Figure 3.7.1.1: Schematic drawing of dip-coating [39]

The equilibrium thickness of the coated layer is reached after a given period of withdrawal time of the fibre from the solution, when the gravity and drag forces are balanced. Equation 3.7.1.1 shows how the equilibrium thickness can be calculated [5].

$$h_{\infty} = \frac{2}{3} \sqrt{\frac{\eta v}{\rho g}} \quad [5] \quad (3.7.1.1)$$

h_{∞} is the equilibrium thickness [m], v is the coating velocity [m/s], η is the viscosity [Pa·s], ρ is the density of the solution [kg/m³] and g is the gravity [m/s²]. The equilibrium thickness can also be calculated from equation 3.7.1.2.

$$h_{\infty} = \frac{0,94(\eta U)^{2/3}}{\gamma_{lv}^{1/6} (\rho g)^{1/2}} \quad [39] \quad (3.7.1.2)$$

h_{∞} is the equilibrium thickness [m], U is the withdrawal speed of the membrane [m/s], η is the viscosity [Pa·s], ρ is the density [kg/m³], g is the gravity [m/s²] and γ_{lv} is the liquid-vapour surface tension [N/m]. From the equation can it be seen that the duration the membrane is immersed in the coating solution does not affect the thickness layer. An increase in withdrawal speed and viscosity of the solution will lead to an increase in the thickness of the layer, while an increase in the density and liquid-vapour surface tension will lead to a decrease in the layer thickness [39]. After the solvent is evaporated, a thin polymer film is formed at the surface of the membrane with a thickness proportional to volume fraction of polymer in the solution [5].

To achieve a thin and defect-free layer with dip-coating, it is preferable that the polymer is in the rubbery state. If the polymer is glassy, the glass transition temperature may be reached and passed during the evaporation process. This can lead to defects and consequently in leakages. If the support membrane is porous, pore penetration can occur during dip-coating. This is because of capillary forces in the support membrane. Pore penetration will reduce mass transfer through the membrane and also cause non-uniform coating thickness. The most common method to avoid or reduce pore penetration is to pre-fill the pores. This prevents the coating solution to penetrate. A water solution can be used as coating solution to prevent pore penetration if the support membrane is hydrophobic [5].

The inside of a hollow fibre can be coated instead of the surface. In this method, the coating solution is introduced into the inside of the hollow fibre and removed afterwards. The hollow fibres have to be cut in a certain length when this method is used, so the coating solution gets to the inside of the fibre. In this method, it is more difficult to reveal defects in the coating layer, because it is not possible to observe the coating process on the inside of the fibre [39].

Chapter 4: Experimental

The experimental part of the master thesis consisted of examining composite hollow fibre and blend membranes for CO₂ capture from flue gas. The membranes were produced using porous PSf as a support membrane coated with PDMS and PVAm. The PSf support was attempted optimized by altering the spinning conditions and the three different hollow fibres that seemed best suited with respect to SEM pictures were examined further and coated with PVAm and PDMS. The selectivity and permeability was also tested for a PVAm/PSf blend membrane by introduction of 1% PVAm in the spinning dope. The membrane's structure and geometry were examined with SEM. The risk assessment for the experiment is shown in Appendix A.

4.1 Materials and chemicals

The PSf used for preparation of hollow fibres was supplied by UDEL (P-3500). As a solvent, 1-Methyl-2-pyrrolidone (NMP) from Merck was used. The co-solvent for the PVAm/PSf blend membranes Tetrahydrofuran (THF) was supplied by Merck. The PSf fibres non solvent Glycerol was provided by Merck. Protonated and purified high molecular weight PVAm used in PVAm/PSf blend membranes and for coating of PSf FSC composite membranes was supplied from BASF. The PDMS solution was made of a silicone elastomer base and a silicon elastomer curing agent both supplied from Dow Chemicals (Sylgard 184), as a solvent n-Hexane from Merck was used. Ethylene glycol provided by Fluka was used as a solvent for PVAm. Tap water was used as the coagulation medium. Araldite 2012 glue was used in preparation of the modules. For mixed gas permeation, a gas cylinder containing 10% CO₂ and 90% N₂ from Yara was used. Helium gas from Yara was used as sweep gas.

4.2 Spinning of PVAm/PSf blend membrane

The fibres were spun in two spinning sessions for this master thesis. The spinning sessions are referred to as spinning 1 and spinning 2. Spinning 1 is spinning of 1% PVAm/PSf blend membrane, while spinning 2 is to optimize PSf fibres as support membranes.

4.2.1 Dope preparation

Spinning 1

The PSf polymer pellets were dried in an oven at 120 °C for 18 hours to remove moisture. After the drying process, PSf was dissolved in NMP by continuously stirring for 71 hours before addition of THF. The solution was stirred another 4 hours, before the PVAm solution was added in small portions to the solution while continuously stirring in 2 hours. This was done to avoid precipitation to occur. Then the dope solution was stirred in 71 hours. The PVAm solution was made by dissolving PVAm in ethylene glycol. The PVAm solution was stirred for 75 hours. The dope composition is shown in table 4.2.1.1.

Table 4.2.1.1: Concentration of the dope compositions for spinning 1

Dope component	Concentration [wt%]
PSf	32
NMP	43
THF	15
PVAm	1
Ethylene glycol	9

Spinning 2

The PSf polymer pellets were dried in an oven at 120 °C for 18 hours. Then PSf was dissolved in NMP by continuously stirring for 26 hours before addition of glycerol. The temperature in the dope formulation tank was 45 °C. Glycerol was added in small portions to the solution while continuously stirring in 2 hours. Then the solution was stirred in 2 hours. The dope composition is shown in table 4.2.1.2.

Table 4.2.1.2: Concentration of the dope compositions for spinning 2

Dope component	Concentration [wt%]
PSf	32
NMP	58
Glycerol	10

4.2.2 Spinning

Spinning 1 was done at the old spinning rig and the spinning 2 was done at the new spinning rig at NTNU by Dr. Marius Sandru and Petra-Kristine Johannessen during March 2012.

The blend dope solution was left for settling to remove air bubbles over night. Dope solution in spinning 2 was pumped from the dope formulation tank through a filter to the dope storage tank and left for settling to remove air bubbles. The dope storage tank had a temperature of 45 °C. Both the dope solutions were then pumped through a spinneret and passed through an air gap region before entering the precipitation bath. The air gap region had a fixed length. After precipitation, the fibres passed through a flushing bath and were stored in a container bath of water. The spinning mechanism is described in detail in chapter 3.6. After the spinning process the fibres were washed in a water bath for 72 hours at 15°C. After the washing process the fibres were air dried. The fibres used for gas permeation were dried in a vacuum oven at 120°C for 90 hours.

Table 4.2.2.1 and table 4.2.2.2 shows the different spinning parameters that were used during spinning 1 and spinning 2 respectively.

Table 4.2.2.1: Spinning parameters for spinning 1

Dope flow rate [ml/min]	1, 0.5
Bore fluid [wt% NMP, wt% water]	80/20
Bore flow rate [ml/min]	0.65, 0,32
Spinneret dimension [mm]	ID*= 0.5 OD*= 1.2
Spinneret temperature [°C]	25
Length of air gap [cm]	28
Non-solvent/coagulant	Water
Spinning temperature [°C]	25
Take-up speed/ Spin rate [m/min]	8

*ID= inner diameter OD= outer diameter

Table 4.2.2.2: Spinning parameters for spinning 2

Dope flow rate [ml/min]	2, 1
Bore fluid [wt% NMP, wt% water]	80/20, 50/50
Bore flow rate [ml/min]	1.3, 0.65
Spinneret dimension [mm]	ID*= 0.5 OD*= 1.4
Spinneret temperature [°C]	25
Length of air gap [cm]	50, 61
Non-solvent/coagulant	Water
Spinning temperature [°C]	25
Take-up speed/ Spin rate [m/min]	7, 10, 14, 16, 18, 20

*ID= inner diameter OD= outer diameter

4.3 Making of the composite membranes

4.3.1 Preparation of PDMS and PVAm coating solution

The PDMS-solution was made by dissolving silicone elastomer curing agent and silicone elastomer base in n-hexane. The solution was stirred for 30 minutes. Table 4.3.1.1 shows the composition of the PDMS coating solution.

Table 4.3.1.1: Composition of the PDMS coating solution

Component	PDMS [wt%]		Hexane[wt%]
	Silicone elastomer base	Silicone elastomer curing agent	
Concentration	4.55	0.46	95

The PVAm coating solution was made by dissolving PVAm in water during stirring over night. Table 4.3.1.2 shows the composition of the PVAm coating solution.

Table 4.3.1.2: Composition of PVAm coating solution

Component	Water [wt%]	PVAm [wt%]
Concentration	97	3

4.3.2 Coating of hollow fibres

The fibres spun in spinning 1 and 2 were coated with 5% PDMS two times to cover possible surface defect. A 29% PSf hollow fibre from Helberg's specialization project [29] was also coated two times with 5% PDMS and compared with the 32% PSf hollow fibre. This was done to investigate if the lower PSf concentration could improve the CO₂ permeance of the membrane. All the fibres were coated using the dip coating method, see figure 4.3.2.1. In the master thesis, the focus was on coating with PDMS and PVAm because of promising results from the specialization project. Coating using other polymers was not performed because of lack of time.

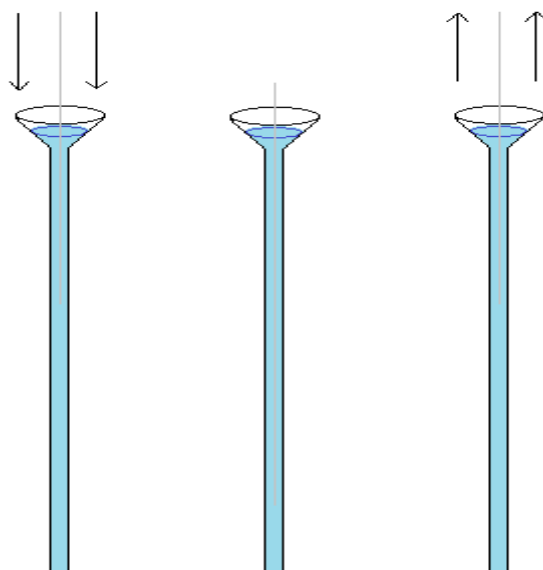


Figure 4.3.2.1: Dip-coating procedure

The hollow fibres were manually immersed in a PDMS hexane solution for 1 minute. The fibres were lifted out at a constant speed. This was done manually and it is therefore not granted that the speed was constant. Before the fibres entered the coating solution, one end of the fibres was fixed in a metal clip. The other end was clenched, so that liquid would not enter into the fibres. After coating, the fibres were air dried at ambient temperature for at least 48 hours. All the different fibres were coated both one and two times with the PDMS-solution. For the fibres coated two times, the fibres were turned upside down before the next coating.

There were done coatings of the three fibres from spinning 2 that seemed best with respect to the obtained spinning conditions and SEM pictures. These fibres were both coated with PDMS and PVAm. The PDMS layer was the top layer and the PVAm layer was the intermediate layer. Table 4.3.2.1 gives an overview of the different coating sequences for each spinning sessions.

Table 4.3.2.1: Different coating sequences for each fibre type

Fibres	2x PDMS	3x PVAm and 1x PDMS
PVAm/PSf blends	X	
PSf HF from spinning 2	X	
PSf HF from spinning 2		X
29% PSf fibres	X	

Before the fibres entered the PVAm-solution, one end of the fibres was fixed in a metal clip. The other end was clenched, so that liquid would not enter into the fibres. The fibres were washed with distilled water for 20 hours, before entering the coating solution. The hollow fibres were manually immersed in a PVAm aqueous solution for 1 minute. The fibres were lifted out with a constant speed. The fibres were immersed in the PVAm aqueous solution three times. Between each coating the fibers were turned upside down. After each immersion the fibres were immediately placed in a preheated oven at 45°C without ventilation for 75 minutes. This was done to reduce the effect of air flow on the coating layers. The day after the coating procedure, the fibres were heat treated at 105°C for 1 hour.

4.4 Characterization methods

4.4.1 Scanning electron microscopy (SEM)

The morphology of the fibres spun in this project and the coated fibres used for gas permeation were investigated in Hitachi S-3500N LV Scanning Electron Microscope. The blend fibres spun in this project were investigated by SEM pictures to determine pore size, the number of macrovoids, surface and geometry. The cross-section of the blend fibres was studied and the wall-thicknesses of the fibres were measured from the SEM pictures. The fibres cross sectional areas were calculated from the inner and outer diameter measured from the pictures. For the coated fibres, the SEM pictures were used to measure the thickness of the coating layer.

Fibres that were analyzed by SEM pictures were fixed onto a round metal chip, after a piece of the fibres were broken under liquid nitrogen. Carbon tape was used to fix the fibre pieces to the metal chip. The samples were coated with gold from a sputter coater, Edwards Sputter Coater S150B. This was done to make the sample conductive as this prevents electrical charging of the surface [5]. The samples were ultimately investigated in SEM.

4.4.2 Differential scanning calorimetry (DSC)

This method is used to measure first-order and second-order transition. First-order transition corresponds to crystallisation and melting, and second-order transition corresponds to the glass transition temperature [5]. The transitions involve energy changes or heat capacity changes that can be measured by the DSC. DSC is a thermoanalytical method which measures the difference between the heat required to increase temperature in a sample and in a reference as a function of temperature [53]. The idea is that a different amount of heat will have to flow to the sample than to the reference to maintain equal temperatures when the sample undergoes physical transformations. Whether the sample needs more or less heat than the reference is determined by the process, if it is exothermic or endothermic [15]. The temperature was increased from -20°C to 400°C for the 1% PVAm/PSf hollow fibre and polymer solution. The heating and cooling rates were 10°C/min. The cycle was repeated three times for the sample.

4.5 Gas permeation test

The membranes tested for gas permeation were tested on the permeation rig at Memfo, NTNU.

4.5.1 Module making

Membrane modules of stainless steel were used for gas permeation tests. Each module consisted of 3-4 fibres with a length of 30, 32 or 34 cm. For gluing the ends of the fibres inside the module the glue Araldite 2012 was used. A small circle of paper was placed under the glue to make sure that the glue stayed in place, see figure 4.5.1.1.

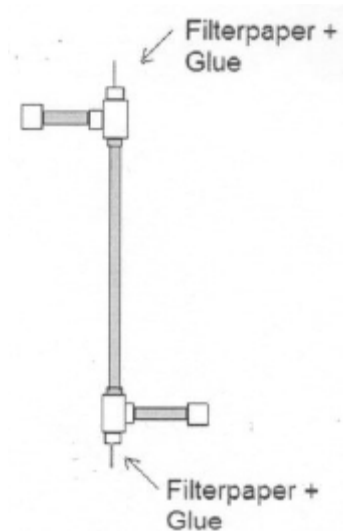


Figure 4.5.1.1: Module with hollow fibres

4.5.2 Testing of membrane with mixed gas permeation

The fibres were tested by mixed gas permeation of 10% CO₂ and 90% N₂ premixed gas. Helium was used as sweep gas, which is applied so the permeating species will be transported out of the bore side. This is done to make sure that the concentration gradient is maintained. The feed flows on the outside of the fibres and the sweep on the inside is sent counter-currently relative to each other. The gas molecules that are transported through the membrane, enters the inside of the fibres and are transported with the sweep out of the fibres. Gas permeation experiments with mixed gas were performed in a laboratory set up as shown in figure 4.5.2.1. Pressure, temperature, relative humidity of the gases and gas flow rates were measured during the experiments.

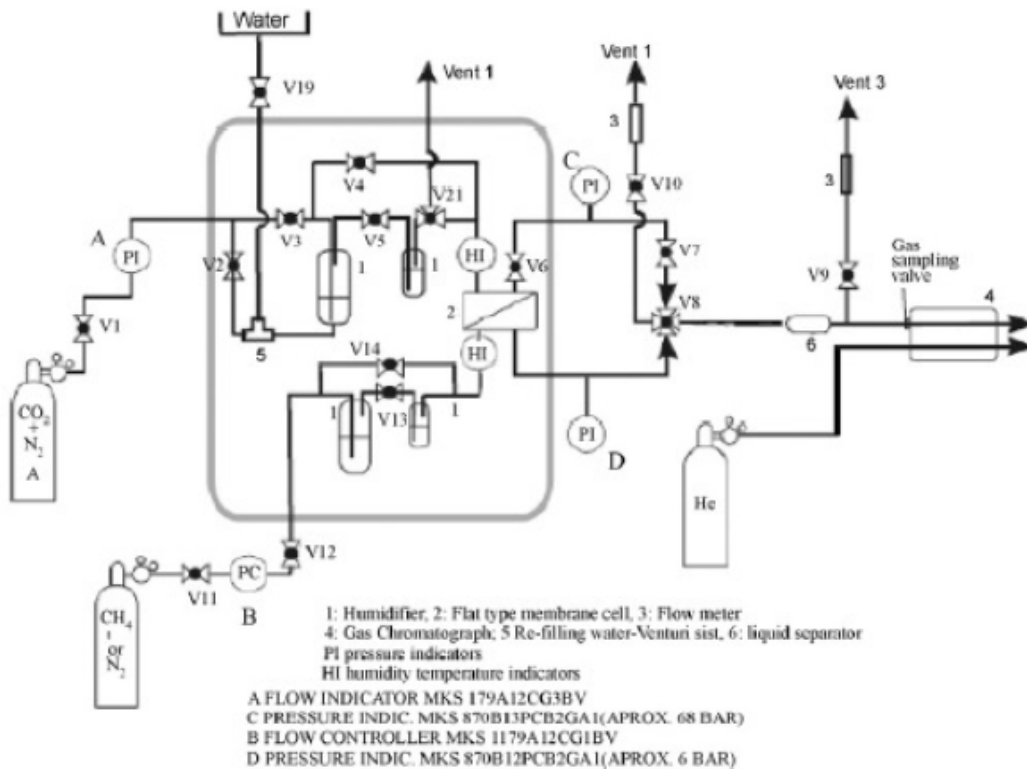


Figure 4.5.2.1: Gas permeation set up [15]

The experiments performed for the chosen fibre membranes from spinning 2 that were coated with PVAm in addition to PDMS were tested at 25°C and 100% humidity for feed and sweep gas. The feed pressure and sweep flow were varied, using feed pressure of 1.2, 3, 5 and 8 bar and tested for sweep around 5, 11, 30, 45 ml/s. Sweep flow rate had small deviations depending on which module was tested. The 1% PVAm/PSf blend membranes from spinning 1 were tested on a temperature of 25°C, feed pressure of 1.2, 3, 5, 8 bar, sweep around 5, 11, 30, 47 ml/s and feed humidity ranging from 40% to 100%. In table 4.5.2.1 the parameter that is varied for the different fibres are shown. The fibres from spinning 2 and the 29% PSf fibre coated two times with PDMS were tested at 1.2 bar, a temperature of 25°C, a sweep flow rate of around 11 ml/min and at 100% humidity for the feed flow. Only wet sweep gas was tested for all the experiments. The total permeate flow rate, J_i was measured with a soap bubble meter. The measurements were done at steady state condition. The composition of the permeate flow was analyzed by a micro gas chromatograph Agilent 3000 every 10 minutes.

Table 4.5.2.1: Varied parameter for the different tested fibres

Parameter	Pressure	Sweep	Humidity
1% PVAm/PSf blend	X	X	X
The PVAm and PDMS coated fibres from spinning 2	X	X	

The gas permeance was measured to quantify the membrane's ability to transport and separate CO₂ from N₂. The permeance of CO₂ and N₂ were found by use of the complete mixing model, see equation 4.5.2.1. The complete mixing model can be used when the permeate stream is much smaller than the retentate stream. When this is the case, the flow rate of the retentate can be assumed the same as for the feed.

$$P_M = \frac{P}{l} = \frac{J_i}{A(p_f x_{fi} - p_p x_{pi})} \quad (4.5.2.1)$$

Where P_M is the permeance [$\text{m}^3(\text{STP})/\text{m}^2 \text{ bar}$], P is the permeability [$\text{m}^3(\text{STP})\text{m}/\text{m}^2\text{bar}$], x mole fraction, l the membrane thickness [m] and p is pressure [bar] [5]. The selectivity was calculated from equation 4.5.2.2.

$$\alpha_{i/j} = \frac{P_{Mi}}{P_{Mj}} \quad (4.5.2.2)$$

Chapter 5: Results and discussion

The main goal of this master thesis was to investigate composite hollow fibre membranes and blend membranes for CO₂ capture from a mixture of 10% CO₂ and 90% N₂. The composite membrane consists of a PSf support coated with PDMS and PVAm. The PSf support in the composite hollow fibre membranes was optimized by altering the spinning conditions to achieve a composite membrane with better separation properties. The PVAm/PSf blend membranes were produced by introduction of PVAm directly in the spinning dope together with the polysulfone (PSf). The different membranes were investigated and compared with respect to structure, geometry, permeance and selectivity. All SEM pictures are given in Appendix B.

5.1 Optimizing the PSf support

One of the main goals in the master thesis was to optimize the PSf support for the FSC PVAm/PSf composite membrane, as the support membrane will influence the performance of a composite membrane in a negative or a positive way, depending on the support characteristics. The limiting step in order to achieve a successful FSC composite membrane is the support itself [15]. The desired characteristics of the hollow fibre support are a structure with controlled pore size, a high CO₂ permeance, as few macrovoids and surface defects as possible. The effect of changing the polymer concentrations, air gap, take-up speed and dope flow rate was investigated. The purpose of this investigation was to make PSf hollow fibres with the wanted characteristics. The fibres that seemed best suited with respect to SEM pictures, the spinning conditions and gas permeation test were chosen as the support membrane for the FSC PVAm/PSf composite membranes (PVAm added by coating and not as a blend in the spinning dope solution). Before the new dope solution was made, the best support from the specialization project containing 32% PSf was compared with a support containing 29% PSf, this is shown in chapter 5.1.1. This comparison was performed to assess if the PSf concentration in the dope solution should be decreased in order to increase the CO₂ permeance. Table 5.1.1 shows the preparation conditions of the fibres prepared and tested. The gas permeation results are investigated in chapter 5.1.2-5.1.5. All the fibres were tested by mixed gas permeation, where the feed stream consists of 90% N₂ and 10% CO₂. The gas permeation test was performed at a temperature of 25°C, pressure 1.2 bar, sweep flow rate between 10 and 11 ml/min and with 100% relative humidity for both the sweep and feed streams.

Table 5.1.1: Different spinning conditions for the investigated fibres in this chapter

Fibres	O	J	W	B
Dope flow rate [ml/min]	1	2	2	1
Bore fluid [wt% NMP, wt% water]	80/20	80/20	80/20	80/20
Bore flow rate [ml/min]	0.65	1.3	1.3	0.65
Spinneret temperature [°C]	25	25	25	25
Length of air gap [cm]	50	61	61	61
Non-solvent/coagulant	water	water	water	water
Spinning temperature [°C]	25	25	25	25
Take-up speed/ Spin rate [m/min]	10	20	18	16

5.1.1 Influence of polymer concentration

Before the new polymer dope solution for the spinning of PSf supports was made, a PSf hollow fibre containing 29% PSf, spun by Helberg, was coated two times with 5% PDMS and tested in a gas permeation rig. This dope solution consisted of 29% PSf and 71 % NMP. The results were compared with the best PSf support tested during the specialization project coated two times with 5% PDMS, made from a dope solution containing 32% PSf, 58% NMP and 10% glycerol. This was done in order to determine if the PSf concentration in the spinning dope solution should be lowered to increase the permeance. A lower polymer concentration in the spinning dope, should result in a more porous membrane yielding higher permeance [23, 24]. The SEM pictures and spinning conditions are given in figure 5.1.1.1.

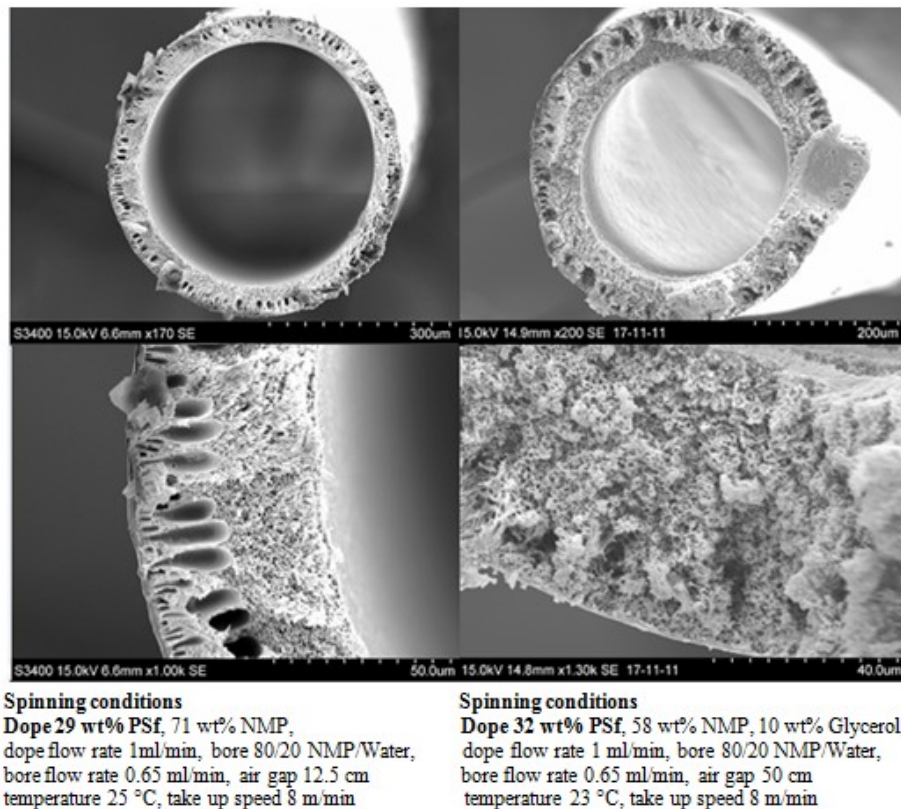


Figure 5.1.1.1: SEM pictures of cross section and wall morphology. The left pictures are the 29% PSf hollow fibre and the right pictures are the 32% PSf hollow fibre.

The permeance and CO₂/N₂ selectivity for the two different fibres is given in table 5.1.1.1

Table 5.1.1.1: Separation properties for a 29% PSf fibre and 32% PSf fibre coated two times with 5% PDMS

Membrane	CO ₂ permeance [m ³ (STP)/m ² bar h]	N ₂ permeance [m ³ (STP)/m ² bar h]	CO ₂ /N ₂ selectivity
29 %	0.01	0.001	13
32 %	0.11	0.002	61

From table 5.1.1.1, it can be seen that the fibre containing 32% PSf has a much higher selectivity and CO₂ permeance than the fibre containing 29% PSf. It was expected from literature that the permeance for the 29% PSf fibre should be higher, but the 32% PSf spinning dope solution contained 10% of the non-solvent glycerol. The non-solvent causes instantaneous demixing, which gives membranes with high permeance [24, 25]. In order to

achieve the wanted permeate gas flow for the 29% PSf fibre, the sweep flow rate had to be increased to higher values than usual testing sweep flow. An increase in permeance with increasing sweep flow rate indicates that the fibre is not very permeable and requires bigger driving forces to permeate the feed gas. This can indicate that the 29% PSf fibre experienced considerable amounts of back diffusion, as the driving forces had to be high to be able to dominate the separation process relative to the increased resistance to mass transfer that the back diffusion induces. From the SEM pictures shown in figure 5.1.1.1, it can be seen that the fibre with 29% PSf has a substructure containing many macrovoids, and such structure makes the membrane more vulnerable to back diffusion. This could be an explanation for the low permeance obtained for the 29% PSf fibre. For fibers having lower polymer concentration in the spinning dope, the coagulation medium (water) can easily penetrate into the chain space of polymer solution and form macrovoids by diffusional and convective movement [20]. Macrovoids lowers the selectivity of the membrane, and this also makes the fibre more susceptible for back diffusion, which causes a loss of permeance. An increase in air gap reduces the formation of macrovoids [20]. The 29% PSf hollow fibre membrane has a lower air gap, which also may be an explanation for the high amount of macrovoids. The influence of the air gap on the membrane properties will be discussed further in 5.1.2. Even though the air gap was lower and a non-solvent was absent for the 29% PSf hollow fibre, the separation properties were unsatisfactory, and a dope solution containing 32% PSf was chosen for further fibre spinning.

5.1.2 The influence of air gap

The maximum air gap used for the PSf fibre production and testing in the specialization project was 28 cm due to limitations in the “old” spinning machine. For the hollow fibres spun during the master thesis, the air gap was increased from 28 cm to 50 and 61 cm. According to literature an increase in air gap will suppress the formation of macrovoids [20]. This occurs because the air gap gives the solvent more time to diffuse out of the hollow fibre and the elongational stress makes the polymer chains align more tightly. This reduces the possibility for the coagulant to penetrate into the fibre when the fibre enters the coagulation bath, and the formation of macrovoids is reduced. From figure 5.1.2.1 is it apparent that fibre B, with the highest air gap, has a porous structure without macrovoids. The fibre O, with the lowest air gap, also has a porous structure, but contain some small holes. Another explanation is proposed by Tsai, H.A., et al [28], which states that during residence in the air gap, the macrovoids occurs, disappears, reappears and reappears depending on the length of the air gap. It was suggested that when hollow fibres enter the air gap, the formation of a transient gel will occur, which inhibits the phase separation of the dope and thus suppress the formation of macrovoids. At higher air gap lengths, the gel is no longer present, and macrovoids are formed until the critical air gap length where the phase separation is complete and no more macrovoids are present. This critical air gap length is proposed to be 60 cm for a PSf hollow fibre having 26% PSf in the spinning dope, and the critical air gap length is reduced with increasing humidity in the air [28]. From figure 5.1.2.1 it can be seen that the fibre with an air gap of 50 cm has holes, while for the fibre with an air gap of 61 cm the macrovoids have disappeared. Fibre B has a higher take-up speed, which also will suppress the formation of macrovoids according to Peng, N., et al [20]. The influence of take-up speed will be discussed further in chapter 5.1.3. Figure 5.1.2.1 shows that a higher air gap distance leads to a slightly smaller wall thickness of the hollow fibers compared to the other. This can be explained by a higher elongational stress due to the higher air gap, which again results in faster solidification.

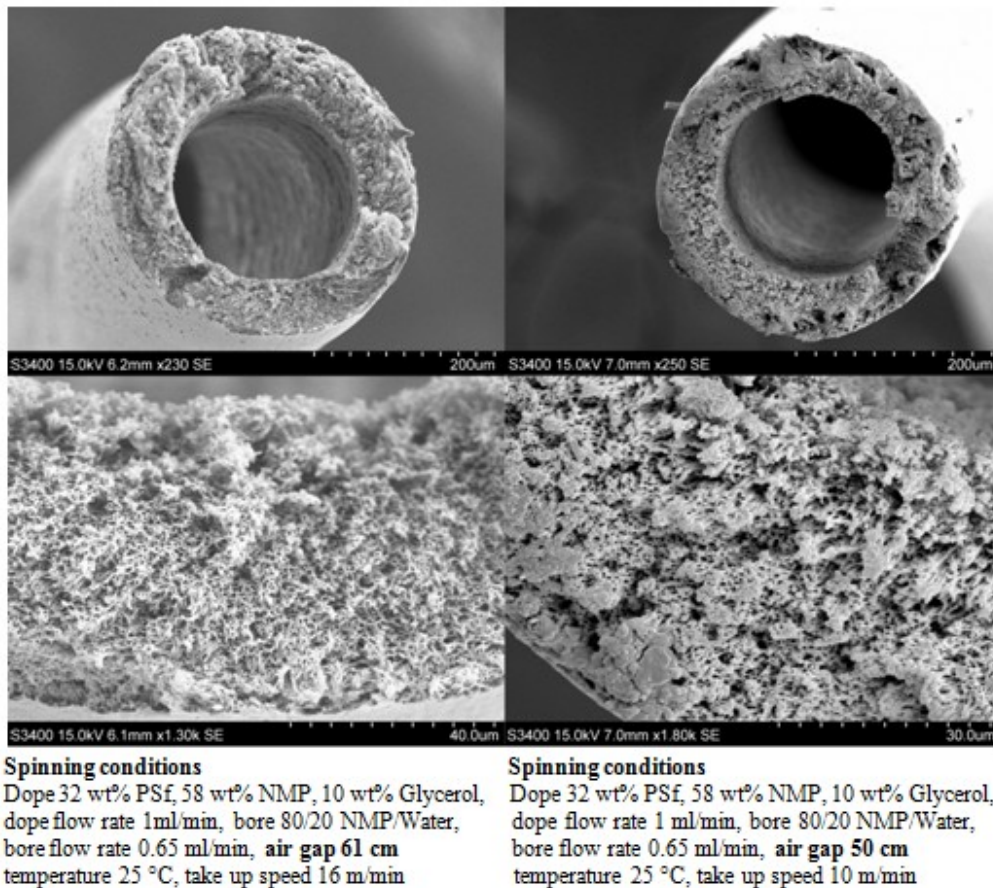


Figure 5.1.2.1: SEM pictures of fibres with air gap of 61(B) and 50 cm (O)

The results from the gas permeation tests for fibre B and fibre O, are shown in Table 5.1.2.1. Both fibres are coated two times with 5% PDMS.

Table 5.1.2.1: Separation properties of PSf hollow fibres at 1.2 bar with different air gap lengths.

Membrane	Air gap [cm]	CO ₂ permeance [m ³ (STP)/m ² bar h]	N ₂ permeance [m ³ (STP)/m ² bar h]	CO ₂ /N ₂ selectivity
B	61	0.22	0.01	17
O	50	0.08	0.02	4

From Table 5.1.2.1 it can be seen that the fibre with the highest air gap, B, is the fibre with best separation properties. The permeance is high, but the CO₂/N₂ selectivity is quite low at 17. The low CO₂/N₂ selectivity for this fibre could be a consequence of surface defects caused by too high elongational stress applied. This will be further discussed in chapter 5.1.5.

5.1.3 The influence of take-up speed

Peng, N., et al [20] reported a minimum take-up speed of 50 m/min in order to produce macrovoid free hollow fibres. Therefore the take-up speed was increased in the new spinning rig from the maximal take-up speed of 8 m/min in the old one. A maximal take-up speed of 20 m/min was used, and further increase was not achievable as the fibres broke above this speed. This might be due to too high elongational stress. The increase of take-up speed gives higher elongational stress as the hollow fibre is stretched at a higher rate by the take-up unit. This is favourable for the morphology of the fibre, as increased elongational rates cause higher degree of chain packing and might prevent external coagulants (water) from entering the

internal structure, as described in chapter 2.3.2. SEM pictures of the hollow fibres W and J, with a take-up speed of 18 m/min and 20 m/min respectively, are shown in figure 5.1.3.1.

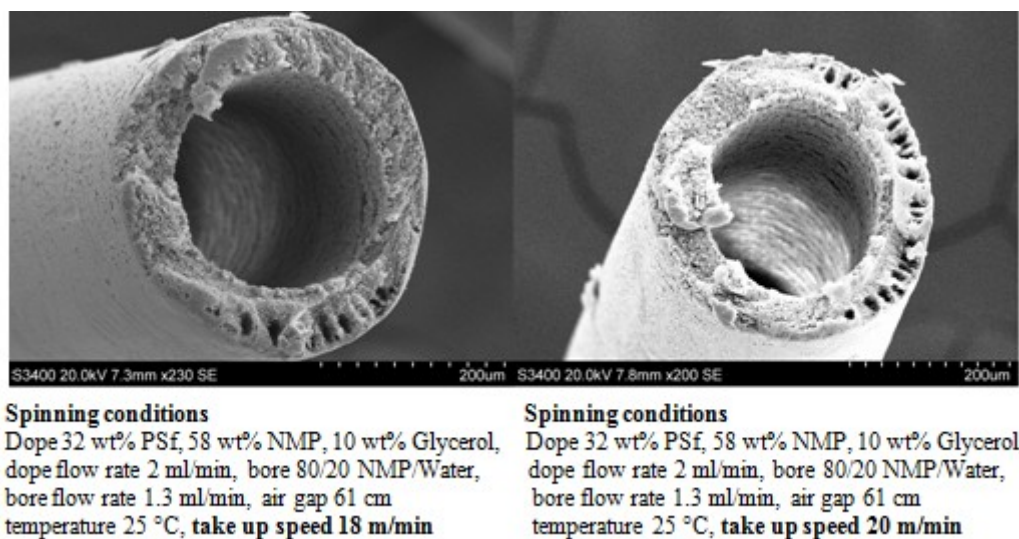


Figure 5.1.3.1: SEM pictures of PSf fibres with a take-up speed of 18 m/min (W) and 20 m/min (J)

From figure 5.1.3.1, it can be seen that the structure of both the fibres contains macrovoids. These are in both cases localized on one side of the cross section, and this might be related to uneven take-up speed on each side of the fibre. It could appear during the spinning procedure as one of the wheels in the take-up unit seemed slower than the rest, so the speed might have been different on different sides of the fibres. The different morphology of the fibres can be caused by the fact that different demixing has occurred in different regions of the hollow fibres. In the region with macrovoids instantaneous demixing may have happened, while in the region without macrovoids delayed demixing may have occurred. Membranes without macrovoids are formed when delayed demixing occurs [18]. As the macrovoids are localized on one side of the fibres, is it possible that the production of these defects is related to the take-up wheel during spinning. The fibres are collected and are in contact with each other and the take-up wheel, which may have scratched the fibres causing defects. Another reason may be that the minimum take-up speed of 50 m/min to produce membranes without macrovoids reported by Peng, N., et al [20] was not reached. The results from the gas permeation tests for fibre J and fibre W, is shown in Table 5.1.3.1. Both fibres are coated two times with 5% PDMS.

Table 5.1.3.1: Separation properties of PSf hollow fibres at 1.2 bar with different take-up speed

Membrane	Take-up speed [m/min]	CO ₂ permeance [m ³ (STP)/m ² bar h]	N ₂ permeance [m ³ (STP)/m ² bar h]	CO ₂ /N ₂ selectivity
J	20	0.23	0.02	13
W	18	0.23	0.02	12

From table 5.1.3.1 it can be seen that both fibres have relatively high permeance and low selectivity. The reason for this could be the presence of macrovoids. Also, the elongational stress experienced from the spinning procedure may have caused surface defects as well. This is further discussed in chapter 5.1.5. The permeance and selectivity are quite the same for the two fibres, the reason for this can be that the spinning conditions were similar and the difference in take-up speed was only 2 m/min.

5.1.4 The influence of dope and bore flow rate

The best PSf hollow fibre support membrane from the specialization project was made using a dope flow rate of 1 ml/min, and this was the desired flow rate for the continuation of these experiments. It was very difficult to obtain a stable spinning without breaking the fibres with a 1 ml/min dope flow rate, high air gap and high take-up speed. Therefore, some of the fibres were spun with a dope flow rate of 2 ml/min. In these situations, the bore flow rate was increased accordingly, in order to have a constant dope flow rate/bore flow rate ratio of 0.65. This ratio is an important parameter for the value of the inner diameter of the fibre, and as this is constant, similar inner diameters were expected. An increase in the dope flow rate is reported in literature to increase the outer diameter [27]. Figure 5.1.4.1 shows SEM pictures of the cross section of a hollow fibre with a dope flow rate of 1 ml/min, B, and a hollow fibre with a dope flow rate of 2 ml/min, O. Both fibres have a dope flow rate/bore flow rate ratio of 0.65.

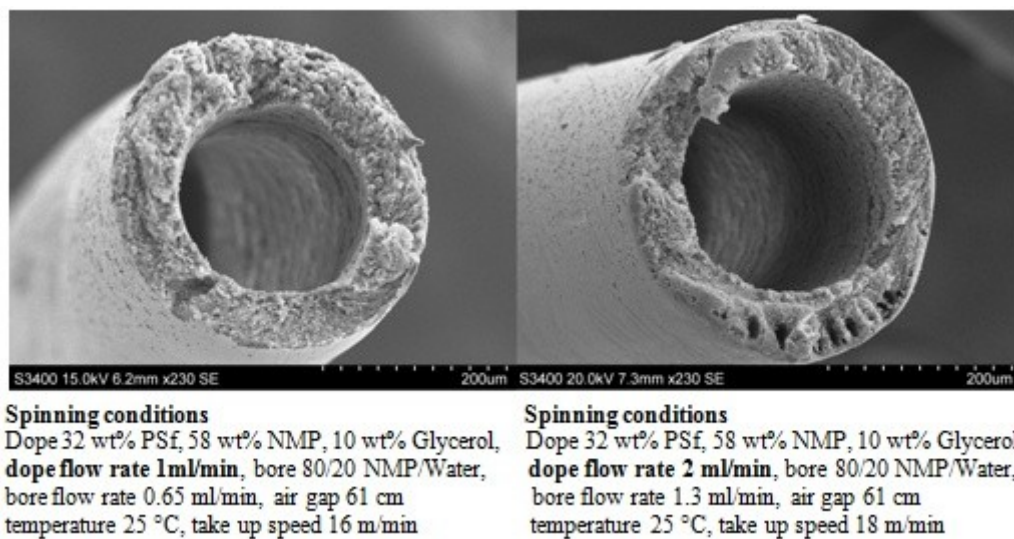


Figure 5.1.4.1: SEM pictures of fibres with a dope flow rate of **1 ml/min** (B) and **2 ml/min** (W)

From figure 5.1.4.1 it can be seen that the outer diameter of the fibre with highest dope flow has increased compared to the fibre with lower dope flow and the wall thickness has slightly increased as well, this is according to other results in literature [27]. The wall thickness and outer diameter for the fibres are given in table 5.1.4.1. From figure 5.1.4.1 it can also be seen that the fibre with a dope flow rate of 1 ml/min has a macrovoid free structure, while the fibre with a dope flow rate of 2 ml/min has a structure containing some macrovoids locating in a specific region. An explanation can be that when the dope rate is decreased the elongational stress increase. This is because when the dope flow rate is decreased less amount of the dope solution goes through the spinneret, leading to a thinner fibre, which makes it easier for the solvent to diffuse out of the fibre.

Table 5.1.4.1: Outer diameter and wall thickness as a function of dope flow rate

Membrane	Dope flow rate [ml/min]	Outer diameter [μm]	Wall thickness [μm]
B	1	315	62.5
W	2	386	68.6

The results from the gas permeation tests for fibre B and fibre W, is shown in Table 5.1.4.2. Both fibres are coated two times with 5% PDMS.

Table 5.1.4.2: Separation properties of PSf hollow fibres at 1.2 bar with different dope flow rates

Membrane	Dope flow rate [ml/min]	CO ₂ permeance [m ³ (STP)/m ² bar h]	N ₂ permeance [m ³ (STP)/m ² bar h]	CO ₂ /N ₂ selectivity
B	1	0.22	0.01	17
W	2	0.23	0.02	12

From table 5.1.4.1 it can be seen that both fibres has quite high permeance and low selectivity. The reason for this could be the presence of macrovoids in fibre W. Also, the elongational stress experienced from the spinning procedure may have caused surface defects as well. This is further discussed in chapter 5.1.5.

5.1.5 Summary of effects of spinning conditions

From the results presented in the previous chapters it can be seen that the fibres spun with a dope flow rate of 1 ml/min contains no macrovoids or very small holes, while the fibres with a dope flow rate of 2 ml/min has some fingerlike macrovoids in the structure. This indicates that the choice of dope flow rate is the most important parameter in order to produce hollow fibre membranes without macrovoids, compared to air gap and take-up speed. As discussed in chapter 5.1.4, the low dope flow rate makes the fibre thinner, and solvent can diffuse out of the internal structure more rapidly than in a thicker membrane. This prevents solvent from being captured in holes in the membrane structure, which suppresses the ability to form macrovoids.

The fibre O was by far the fibre with lowest permeance compared to the other ones as shown in table 5.1.2.1 in chapter 5.1.2. O is the fibre with lowest air gap and take-up speed, see table 5.1.1. This may indicate that air gap and take-up speed is important regarding the permeance of the fibres, and it might seem as the permeance increases with increasing air gap and take-up speed. This can be related to the fact that increasing the air gap and take-up speed gives a more porous and open structure in the hollow fibre membranes [20].

In figure 5.1.5.1, SEM pictures of the outer surface of the PSf hollow fibres B, J, O and W are shown.

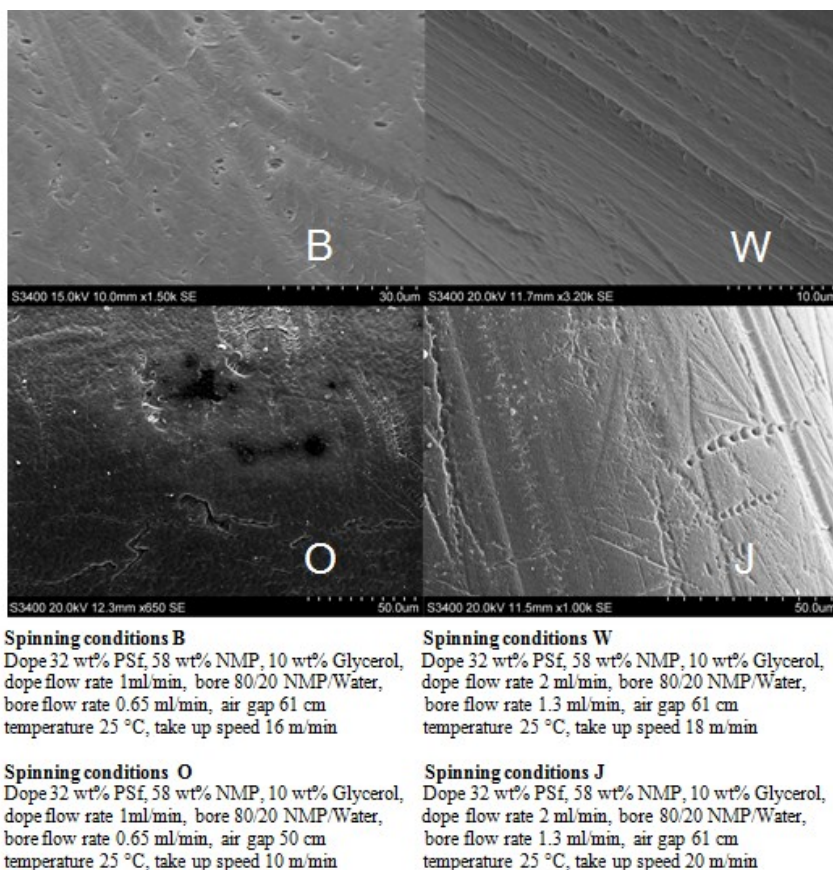


Figure 5.1.5.1: SEM pictures of the outer surface of the different PSf hollow fibres

From figure 5.1.5.1 it is apparent that all the fibres contain many defects, scratches and holes on the surface. This might be a reason for the low CO_2/N_2 selectivity exhibited by these fibres. The explanation for this might be that the fibres are spun with perhaps too high air gap and high take-up speed simultaneously. These factors increase the elongational stress. This may have caused the elongational stress to become too high, so the top layer has been stretched causing holes in the surface. The hollow fibre B has in addition to high air gap and high take-up speed, low dope flow rate, which further increases the elongational stress. From the figure 5.1.5.1 it can be seen that B is the fibre with biggest holes and defects. From the figure, it can also be seen that the surfaces have longitudinal scratches following the spinning direction. These lines may have been caused by stretching during spinning, or they may also have been scratched during this procedure, or when collected on the take-up wheel. There is also a possibility that the markings have been formed after the spinning, but as the fibres only have been washed in a water bath and dried is this more unlikely.

As the CO_2/N_2 selectivity is substantially lower than the intrinsic CO_2/N_2 selectivity for PSf of 38 [23], this indicates that other transport mechanisms than solution diffusion, as viscous flow and Knudsen diffusion, which yields a much lower CO_2/N_2 selectivity plays an important role for the separation properties. The CO_2/N_2 selectivity for Knudsen diffusion is 0.79 and for viscous flow it is 0.84, see chapter 3.3.2. It is possible that a combination of these three transport mechanisms has been present, and the reason for the appearance of Knudsen diffusion and viscous flow may be explained by the large amount of surface defects exhibited by the hollow fibres as shown in figure 5.1.5.1.

The desired characteristics of the PSf hollow fibres were not entirely obtained. The spinning yielded PSf hollow fibres with good permeance and a structure without macrovoids, but the

surface contained holes and defects, so the obtained CO₂/N₂ selectivity of the fibres was very low. The surface defects are probably a consequence of too much elongational stress caused by a combination of high take-up speed and air gap, so for later hollow fibre spinnings, only one of these parameters should be increased to such high values.

5.2 Composite membranes

Three of the fibres investigated in chapter 5.1 were selected as PSf supports for PVAm/PSf FSC composite membranes. The main requirements for the support are high CO₂ permeance and few macrovoids. For the purpose of making a composite membrane, the hollow fibres B, J and O were chosen as the support. B and J exhibited high permeance and B also had a macrovoid free structure. O does not have that high permeance, but a macrovoid free structure. All the fibres have some surface defects and holes as mentioned previously. The PSf fibres were coated two times with 5% PDMS during the investigation of the PSf support. When the composite membranes were prepared, the fibres were coated with both PDMS and PVAm, in order to eliminate the significance of the surface defects. PVAm is a material that selectively transports CO₂ [10, 15]. The PSf fibres were first coated three times with 3% PVAm and then one time with 5% PDMS by dip coating, giving the coating layers on the outside of the hollow fibres. As the PVAm used for coating is hydrophilic and the coating solution is PVAm solved in water, it is difficult for the PVAm to attach to the slightly hydrophobic PSf. Therefore, the coating has to be performed three times in order to make sure that the entire PSf surface is covered with a thin, uniform layer of PVAm. The hydrophilic PVAm layer will take-up water and swell the coating layer, thus making the CO₂ able to react with the amino groups, and then be transported by facilitated transport [10, 15]. In figure 5.2.1 the SEM pictures of the coating layer thickness for the different PSf supports are shown. The coating layer was found to be between 1-1.5 µm. It can also be seen that the PDMS coating has slipped over the porous PSf cross section, and it was impossible to distinguish the PDMS coating layer from the PVAm.

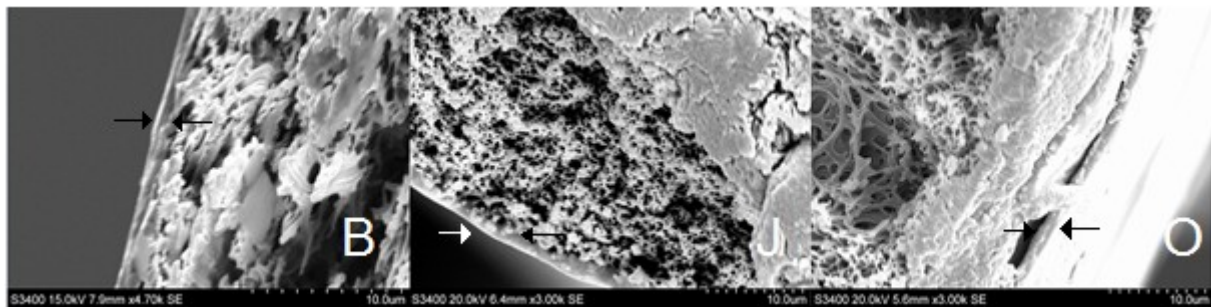


Figure 5.2.1: SEM pictures showing coating thickness for the B, J and O type PSf hollow fibre coated three times with PVAm and one times with PDMS

5.2.1 Gas permeation test for the different PVAm/PSf FSC composite membranes

The mixed gas permeation experiments were performed using a feed consisting of 10% CO₂ and 90% N₂. The gas permeation was performed from the shell side of the membranes, leading to an outside-in operation. The gas permeation test was executed at a temperature of 25°C and with 100% relative humidity for both sweep and gas feed streams.

Influence of feed pressure

The composite membranes were tested at 1.2, 3, 5 and 8 bar feed pressure. The composite membrane that had J as support (air gap 61 cm, take-up speed 18 m/min, dope flow rate 2 ml/min), collapsed when the pressure was increased from 1.2 bar, and was not tested for pressure influence. The sweep flow rate was constant at 11 ml/min. In table 5.2.1.1 the CO₂ and N₂ permeance for the FSC composite membranes is given.

Table 5.2.1.1: Permeance for the FSC composite membranes with B and O as support

Pressure [bar]	B CO₂ permeance [m³(STP)/m² bar h]	B N₂ permeance [m³(STP)/m² bar h]	O CO₂ permeance [m³(STP)/m² bar h]	O N₂ permeance [m³(STP)/m² bar h]
1.2	0.08	0.0016	0.08	0.004
3	0.08	0.0014	0.06	0.005
5	0.07	0.0021	0.07	0.006
8	0.07	0.0034	0.07	0.011

The composite membrane with fibre B as a support experienced a big decrease in permeance after coating with 3% PVAm three times and 5% PDMS one time relative to the support fibre coated two times with 5% PDMS discussed in chapter 5.1. Table 5.2.1.1 shows a permeance of 0.08 m³(STP)/(m² bar h) for the composite membrane with fibre B as the support and for the composite membrane with fibre O at 1.2 bar. This is a big decrease from 0.22 m³(STP)/(m² bar h) for the composite membrane with fibre B as the support, and no decrease for the composite membrane with fibre O as the support. All the support fibres spun had surface defects and holes prior to coating. It is possible that the thicker coating layer for the composite membranes has sealed these defects more thoroughly, preventing non-selective viscous flow and Knudsen diffusion which gives high permeance and non-selective transport. As support fibre B had more surface defects than support fibre O, as shown in figure 5.1.5.1, this fibre experienced a larger decrease in permeance after coating three times with 3% PVAm and one time with 5% PDMS. It is also possible that PVAm has penetrated into the support fibres and blocked the internal pores, leading to further decrease in CO₂ permeance. Support fibre B, with a lot of surface defects and holes will be more vulnerable than support fibre O as PVAm can penetrate more easily. Another possible explanation is that the humid sweep gas can have lead to condensation inside of the bore of the hollow fibres. The bore side could have been partially blocked with water which has lead to a less effective separation area, which gives a lower CO₂ permeance.

In figure 5.2.1.1 the CO₂/N₂ selectivity for the FSC composite membranes is given. The lines between data points are added only to show trends in the result.

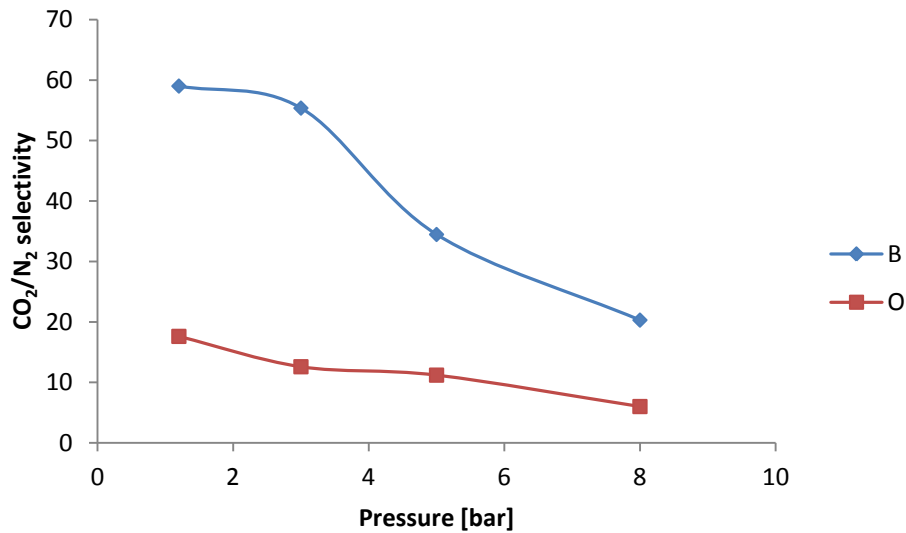


Figure 5.2.1.1: Selectivity of FSC composite membranes with B and O as the support as a function of pressure

Figure 5.2.1.1 shows that the selectivity is low for the PVAm/PSf composite membrane with fibre B as the support, and very low for the PVAm/PSf composite membrane with fibre O as the support. Support fibre O had some macrovoids in the structure, and this could be the reason for the low selectivity. Support fibre B had a porous, macrovoid free structure, see figure 5.1.2.1, but a considerable amount of surface defects as shown in figure 5.1.5.1. The selectivity is expected to decrease as the pressure increases due to saturation of the fixed carrier sites supplied by the PVAm [15]. This happens as the amount of CO₂ in the feed increases while the amount of carrier sites stays the same. This gives a situation where there are fewer carrier sites available for facilitated transport relative to the amount of CO₂, and the carriers are saturated. More CO₂ molecules will have to permeate by solution-diffusion or other transport mechanisms and this leads to a reduction in permeance. Usually the N₂ molecules are transported by solution diffusion mechanism, so the permeance of N₂ will not be affected as the pressure increases. This leads to reduction in CO₂/N₂ selectivity. In this case, the N₂ permeance increases with increasing pressure, and this indicates that the increased pressure opens the previously sealed surface defects and holes. As these surface defects reopens, the transport by viscous flow and Knudsen diffusion increases relative to the transport by the solution diffusion transport mechanism for N₂. The fact that both CO₂ permeance and selectivity decreases with increased feed pressure, verify that the facilitated transport mechanism is present [36]. In table 5.2.1.2 the CO₂ purity, the CO₂ concentration in the permeate, for the FSC composite membranes is given.

Table 5.2.1.2: The CO₂ purity for the FSC composite membranes with B and O as support with different pressure

Pressure [bar]	CO ₂ purity for composite B [%]	CO ₂ purity for composite O [%]
1.2	83	60
3	82	52
5	75	49
8	64	35

From table 5.2.1.2 it can be seen that the PVAm/PSf composite membrane with fibre B as the support has a highest purity of 83, while the PVAm/PSf composite membrane with fibre O as the support has a highest purity of 60. This difference is directly related to the selectivity shown in figure 5.2.1.1, and the low purity is a consequence of the bad separation properties.

Support fibre O has a structure with some holes in the structure, and more N_2 will be transported, leading to lower permeate CO_2 purity than for the PVAm/PSf composite membrane with fibre B as the support. As reported by Hussain, A., and Hägg, M.-B [51], for the membrane separation process to be competitive with amine absorption, the CO_2 purity has to be above 90%. For many applications where CO_2 is captured, it is not necessary with a purity above 90%, and in these processes could the membranes with purities around 80% be a viable option. Usually a two-stage membrane is used in order to obtain a CO_2 purity above 90%. In figure 5.2.1.2 and 5.2.1.3 the SEM pictures of the surface of the coated and uncoated hollow fibres B and O.

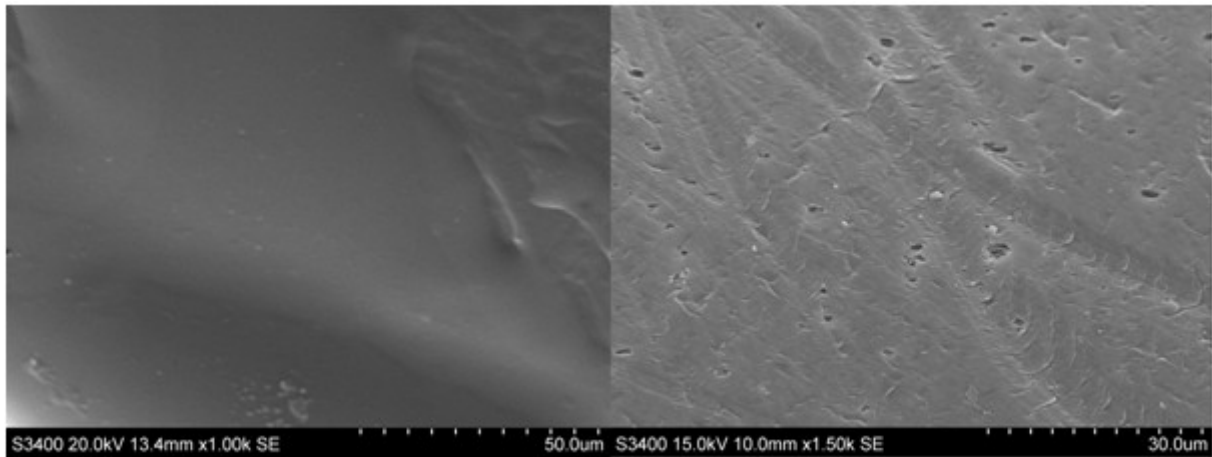


Figure 5.2.1.2: Left: PSf hollow fibre B coated three times with 3% PVAm and one time with 5% PDMS
Right: Uncoated PSf hollow fibre B

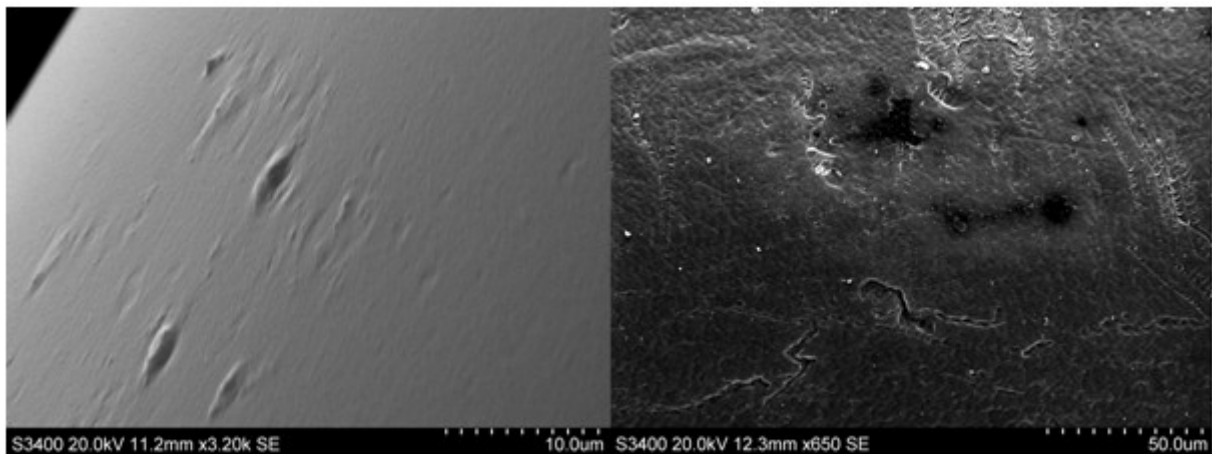


Figure 5.2.1.3: Left: PSf hollow fibre O coated three times with 3% PVAm and one time with 5% PDMS
Right: Uncoated PSf hollow fibre O

Figure 5.2.1.2 and figure 5.2.1.3 shows that the coating has had a large effect in covering the holes and defects on the hollow fibre surface. As the SEM pictures only show a small part of the total surface, is it possible that there still are uncovered defects causing the low selectivity. Even though the coating improves the surface, there are defects in the surface that are too large for the PVAm coating layers to cover. This is the reason for the low CO_2/N_2 selectivity.

Influence of sweep flow rate

During sweep flow testing, the pressure was kept constant at 1.2 bar. In figures 5.2.1.4-5-2.1.6 CO₂ and N₂ permeances for the PVAm/PSf FSC composite membranes with B, J and O as the support are given in a logarithmic scale and plotted against sweep flow rate. The lines are added only to see trends in the result.

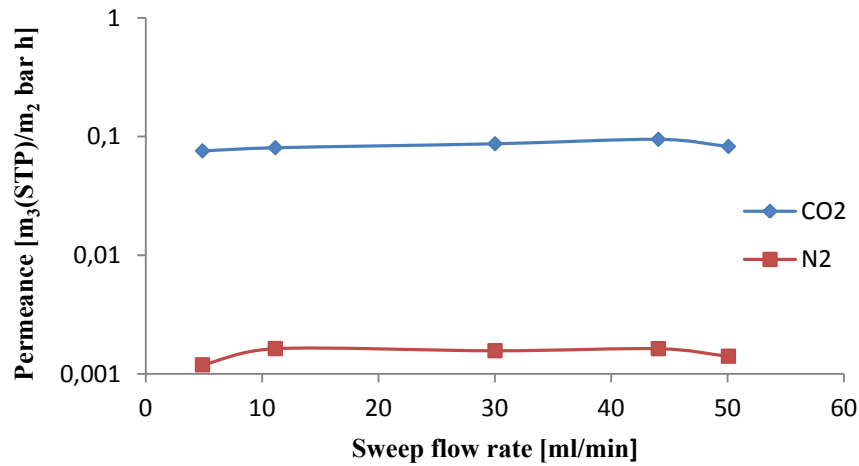


Figure 5.2.1.4: CO₂ and N₂ permeance for the PVAm/PSf composite membrane **with B as support** as a function of the sweep flow rate

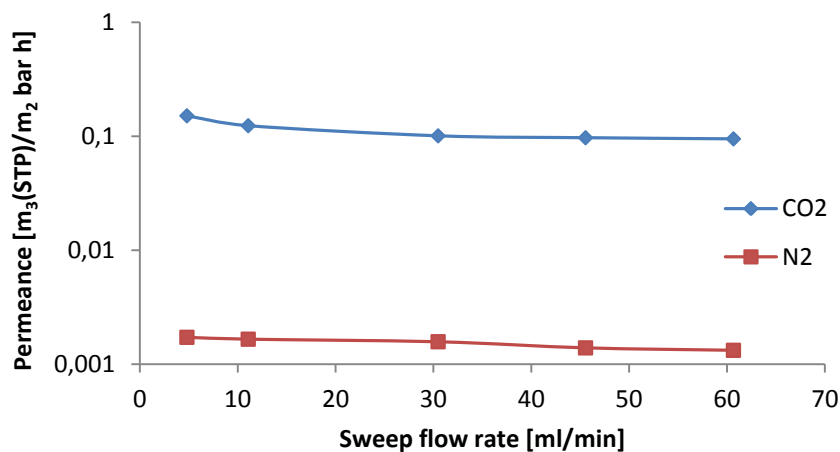


Figure 5.2.1.5: CO₂ and N₂ permeance for the PVAm/PSf composite membrane **with J as support** as a function of the sweep flow rate

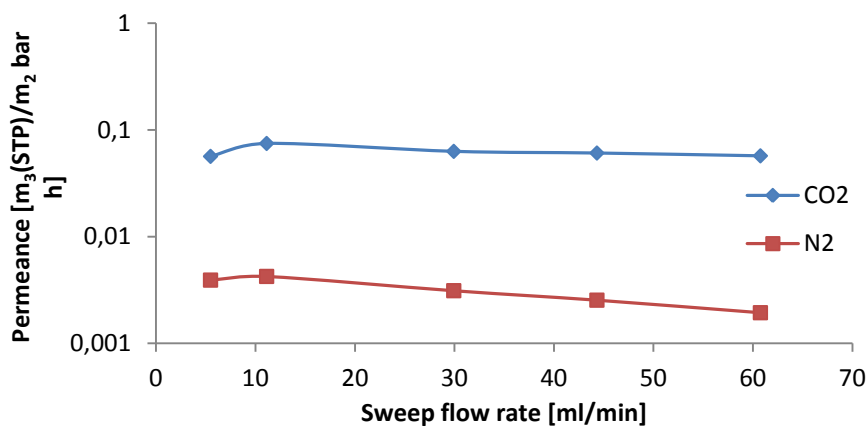


Figure 5.2.1.6: CO₂ and N₂ permeance for the PVAm/PSf composite membrane **with O as support** as a function of the sweep flow rate

From the figures 5.2.1.4-5.2.1.6 it can be seen that the PVAm/PSf composite membrane with fibre J as the support obtains the highest CO₂ permeance. The highest obtained value was 0.15 m³(STP)/(m² bar h) at a sweep flow rate of 5 ml/min. The permeance for the PVAm/PSf composite membrane with fibre B as the support is quite constant with increasing sweep flow rate, while for the PVAm/PSf composite membranes with fibre J and O as the support, the permeance is slightly decreasing with increased sweep flow rate. A possible explanation is that the sweep gas will permeate into the feed-retentate stream at higher rates when the sweep flow rate is higher. This back diffusion will prevent some of the transport from the feed side through the membrane. The retentate flow may act as a “sweep” for the sweep gas, and this gives a driving force for back diffusion. This effect becomes an extra resistance to the most permeable gas [15]. The low permeance for the PVAm/PSf composite membranes coated three times with 3% PVAm and one time with 5% PDMS compared to the permeance for the PSf supports coated only two times with 5% PDMS, might be due to a thicker dense top layer, penetration of PVAm into the pores of the support or blockage by humid sweep gas. This was discussed under influence of pressure earlier in this chapter.

The CO₂/N₂ selectivity for the PVAm/PSf FSC composite membranes with B, J and O as the support plotted against different sweep flow rates is given in figure 5.2.1.7-5.2.1.9. The lines are added to point out trends in the result.

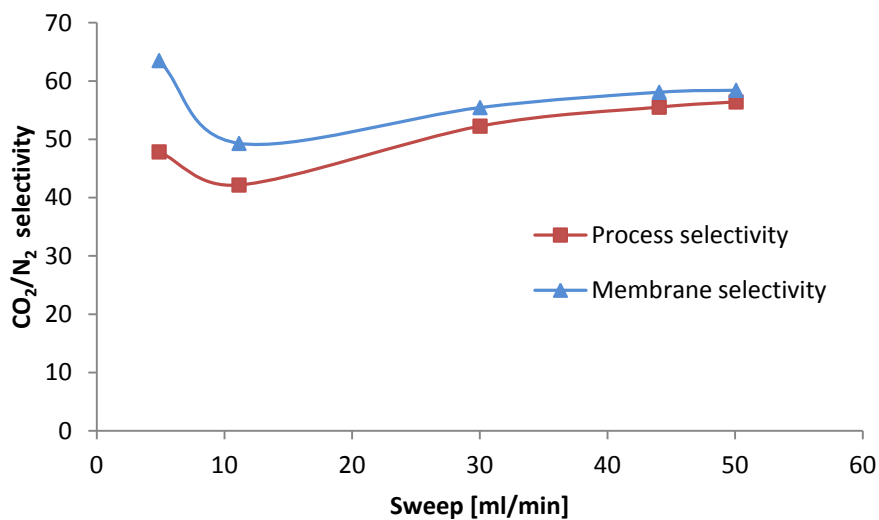


Figure 5.2.1.7: Process and membrane CO₂/N₂ selectivity for the PVAm/PSf composite membrane with B as support as a function of the sweep flow rate

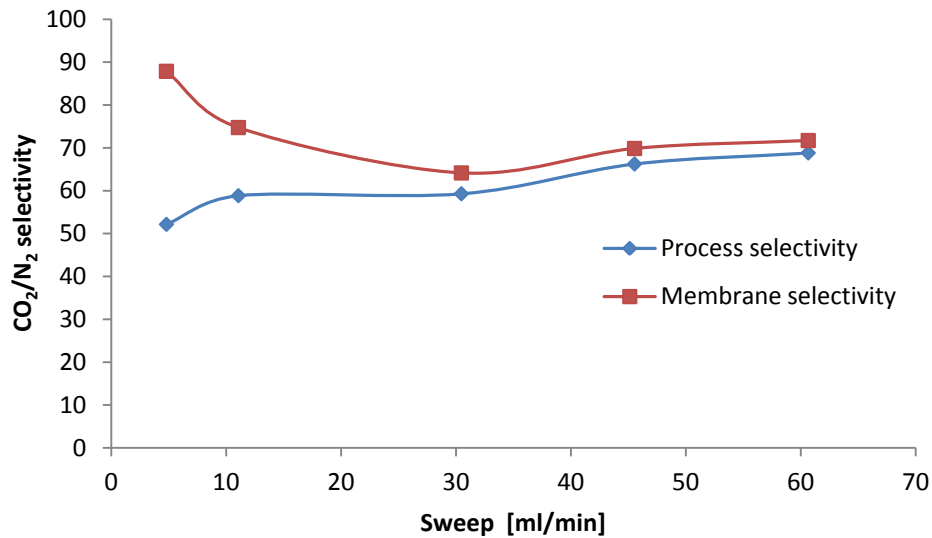


Figure 5.2.1.8: Process and membrane CO_2/N_2 selectivity for the PVAm/PSf composite membrane with **J** as support as a function of the sweep flow rate

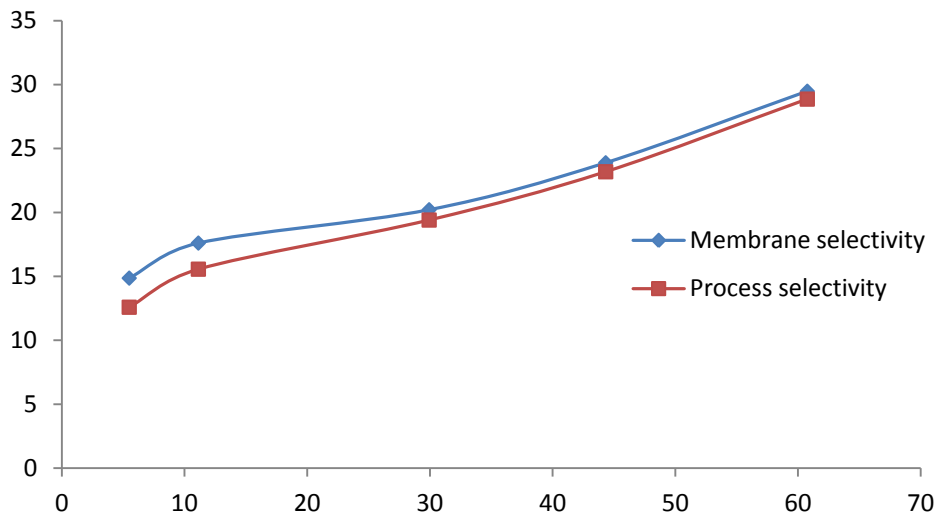


Figure 5.2.1.9: Process and membrane CO_2/N_2 selectivity for the PVAm/PSf composite membrane with **O** as support as function of the sweep flow rate

Figure 5.2.1.7-5.2.1.9 shows a general trend of increasing CO_2/N_2 selectivity as the sweep flow rate increases. This is due to increased driving forces for CO_2 transport as a higher sweep flow rate will carry the permeating CO_2 out of the membrane at a higher rate, reducing the partial pressure of CO_2 on the permeate side. This is the case for the PVAm/PSf hollow fibre composite membrane with fibre O as the support. The PVAm/PSf composite membranes with B and J as support, exhibits first a decrease in CO_2/N_2 selectivity at sweep flow rates of 4 ml/min for fibre B and 4 ml/min and 30 ml/min for fibre J. The selectivity increases at higher sweep flow rates. A reason for this might be that the surfaces of the hollow fibres have a lot of defects, and this causes a loss in CO_2/N_2 selectivity due to back diffusion which reduces the rate of the CO_2 that permeates. At higher sweep flow rates, the increase of driving forces becomes more important for the separation than the rate of back diffusion, and the CO_2/N_2 selectivity increases. As shown earlier in this chapter (figure 5.2.1.4-5.2.1.6), the permeance decreases when the sweep flow rate increases, and the increase in CO_2/N_2 selectivity happens because the CO_2 permeance is reduced less than the N_2 permeance. The process selectivity approaches the membrane selectivity when the sweep flow rate is increased. This is because

when the $P_{\text{feed}}/P_{\text{permeate}}$ ratio is large enough, the process selectivity value approaches the membrane selectivity. This indicates that when the pressure ratio is large enough, the overall selectivity is determined by the membrane itself and not the process conditions [16]. The PVAm/PSf hollow fibre composite membrane with fibre J as the support (figure 5.2.1.8) exhibits the highest CO_2/N_2 selectivity at all sweep flow rates, ranging from 90 to 70. This fibre had some macrovoids in the structure, but the surface with fewest defects. The PVAm/PSf hollow fibre composite membrane with fibre B as the support (figure 5.2.1.7) had a surface with a lot of defects, but a porous structure without macrovoids. The CO_2/N_2 selectivity ranged from 64 at a sweep flow rate of 5 ml/min to 58 at 50 ml/min, and is lower than the composite membrane with fibre J as the support. It might therefore seem that the amount of surface defects is more important for a high selectivity than the amount of internal macrovoids, as the composite membrane with B as the support have more surface defects than the composite membrane with fibre J as the support. The composite membrane with fibre O as the support has a considerable lower CO_2/N_2 selectivity than the two other composite membranes. The reason for this may be that the PSf fibre O has some small holes in the structure in addition to surface defects. In figure 5.2.1.10 the CO_2 purity for the PVAm/PSf FSC composite membranes with B, J and O as support is given. The lines are added to see trends in the result.

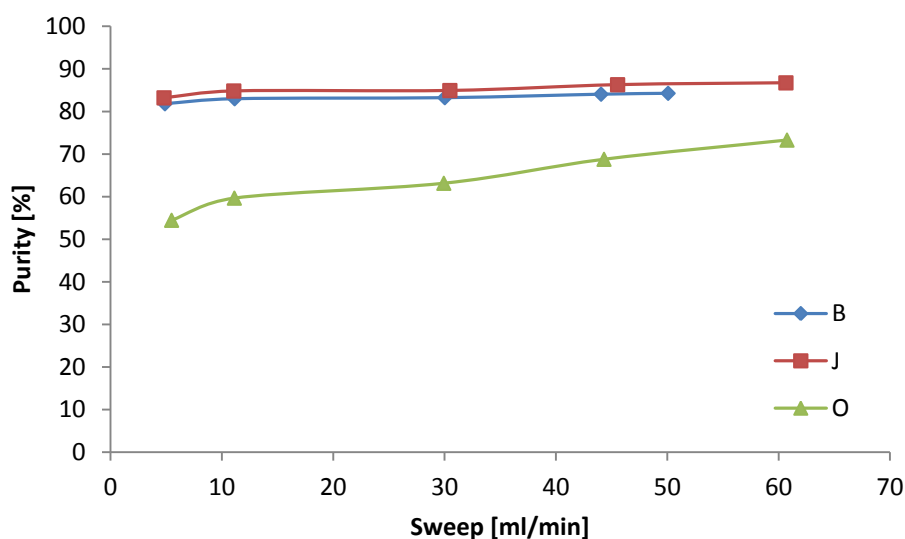


Figure 5.2.1.10: The CO_2 purity of PVAm/PSf FSC composite membranes with B, J and O as support as a function of the sweep flow rate

From figure 5.2.1.10 it can be seen that the composite membrane with O as support produces a permeate with very low CO_2 purity, and this is related to poor morphology and low selectivity. The two other composite membranes have much higher and similar CO_2 purity, even though the selectivity of the PVAm/PSf composite membrane with J as support is bigger than the selectivity of the PVAm/PSf composite with B as support. This is consistent with the results of Sandru, M., et al [36], which states that from a purity of 80% at $P_{\text{fCO}_2}/P_{\text{pCO}_2} \approx 3$ up to $P_{\text{fCO}_2}/P_{\text{pCO}_2} \approx 20$, the permeate purity increases fast with increasing driving forces. Above this interval, the purity increases at much slower rates, and the CO_2 purity becomes completely dependent on the membrane selectivity. None of the composite membranes have a CO_2 purity that is above 90%, which is the critical CO_2 purity in order to be competitive to amine absorption technology [51]. But the composite membrane with J as support is very close with a CO_2 purity of 87.

5.2.2 Comparison of the FSC composite membranes with the best obtained composite membrane made in the specialization project.

The PVAm/PSf FSC composite membranes that were best under pressure and sweep flow rate measurements were compared to the best composite membrane from the specialization project. This composite membrane from the specialization project consists of a PSf support (D) which was coated first three times with PVAm and then one time with PDMS, which is the same coating sequence. When compared for influence of pressure, the PVAm/PSf composite membrane with B as support is used, for sweep flow rate influence is the composite membrane with J as support used. Fibre D has the same dope composition, 10% glycerol, 58% NMP, 32% PSf. The spinning conditions for fibre B and J are repeated, while the spinning conditions for fibre D are given in table 5.2.2.1.

Table 5.2.2.1: Spinning conditions for PSf fibre B, J and D

Fibres	B	J	D
Dope flow rate [ml/min]	1	2	1
Bore fluid [wt% NMP, wt% water]	80/20	80/20	80/20
Bore flow rate [ml/min]	0.65	1.3	0.65
Spinneret temperature [°C]	25	25	23
Length of air gap [cm]	61	61	27.2
Non-solvent/coagulant	water	water	water
Spinning temperature [°C]	25	25	23
Take-up speed/ Spin rate [m/min]	16	20	8

Pressure comparison

In table 5.2.2.2 the comparison of the permeance for the composite membrane from the master thesis and specialization project is shown.

Table 5.2.2.2: Permeance for the PVAm/PSf FSC composite membranes with B and D as support

Pressure [bar]	B CO ₂ permeance [m ³ (STP)/m ² bar h]	B N ₂ permeance [m ³ (STP)/m ² bar h]	D CO ₂ permeance [m ³ (STP)/m ² bar h] [11]	D N ₂ permeance [m ³ (STP)/m ² bar h] [11]
1.2	0.080	0.0016	0.081	0.0009
3	0.077	0.0014	0.075	0.0008
5	0.072	0.0021	0.063	0.0008
8	0.069	0.0034	0.055	0.0010

The CO₂ permeance for the two composite membranes from the specialization project and the master thesis is almost identical, as can be seen from table 5.2.2.2. It can be seen that the permeance for the composite membrane with fibre D as the support also has a decrease in

CO₂ permeance as the pressure increases due to saturation of the carriers supplied by the PVAm, but the N₂ permeance is approximately constant as the pressure increases. This is expected because N₂ is not transported by facilitated transport. However, for the composite membrane with fibre B as the support, the N₂ permeance increases with increasing pressure, indicating that the previously sealed surface defects have been opened and non-selective flow by Knudsen diffusion or viscous flow is present. This result indicates that the quality of the PSf support hollow fibre is essential for the separation properties of a PVAm/PSf hollow fibre composite membrane. This supports the theory that the fibres spun during the master thesis experienced too high air gap, low dope flow rate and too high take-up speed, which may have caused too high elongational stress. The D fibre had much lower air gap and lower take-up speed, which gives a lower elongational stress. This may have given better morphology without surface defects.

In figure 5.2.2.1 the comparison of the CO₂/N₂ selectivity for the composite membrane from the master thesis and specialization project is shown.

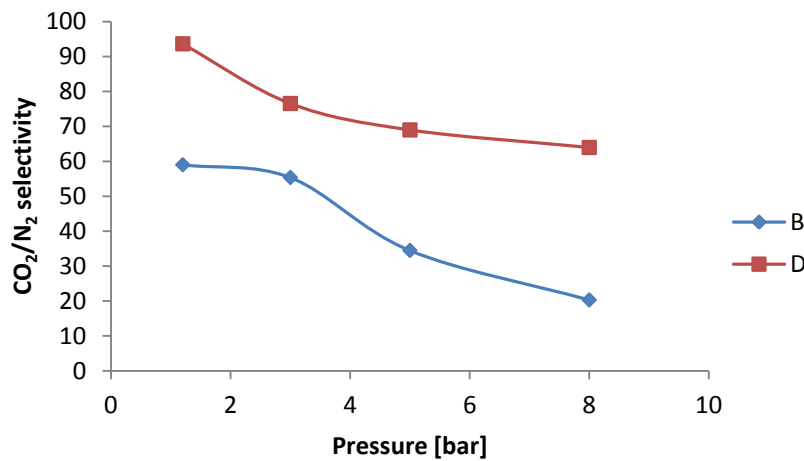


Figure 5.2.2.1: CO₂/N₂ selectivity for the PVAm/PSf FSC composite membranes with B and D as support as a function of pressure

The selectivity for the composite membrane from the specialization project is much higher than the selectivity of the composite membrane from the master thesis, see figure 5.2.2.1. This is because even though the CO₂ permeance for both composite membranes is similar, is the N₂ permeance much higher for the composite membrane with fibre B as support, which results in a much lower selectivity. The CO₂/N₂ selectivity decreases with increasing pressure due to saturation of the carrier sites provided from the PVAm, but for the composite membrane with B as the support, the decrease is more rapid and this is because the N₂ permeance increases with increased pressure for this membrane. In table 5.2.2.3 is the CO₂ purity for the two composite membranes given.

Table 5.2.2.3: The CO₂ purity for the FSC composite membranes with B and O as support

Pressure [bar]	CO ₂ purity for composite B [%]	CO ₂ purity for composite D [%]
1.2	83	87
3	82	86
5	75	85
8	64	84

The composite membrane with D as support gives a higher CO₂ purity in the permeate than the composite membrane with B as support, and the purity is also approximately constant at different pressures for the composite membrane with D as support. This difference in performance is because of the better morphology of the D support hollow fibre compared to the B support. The composite membrane with D as support is also below the purity of 90% [51].

Sweep flow rate comparison

The permeance of PVAm/PSf composite membrane with fibre D as support from the specialization project and the composite membrane with fibre J as the support from the Master thesis is shown in figure 5.2.2.2. This is not a mathematical relation, and the lines are added to see trends. The vertical axis is logarithmic.

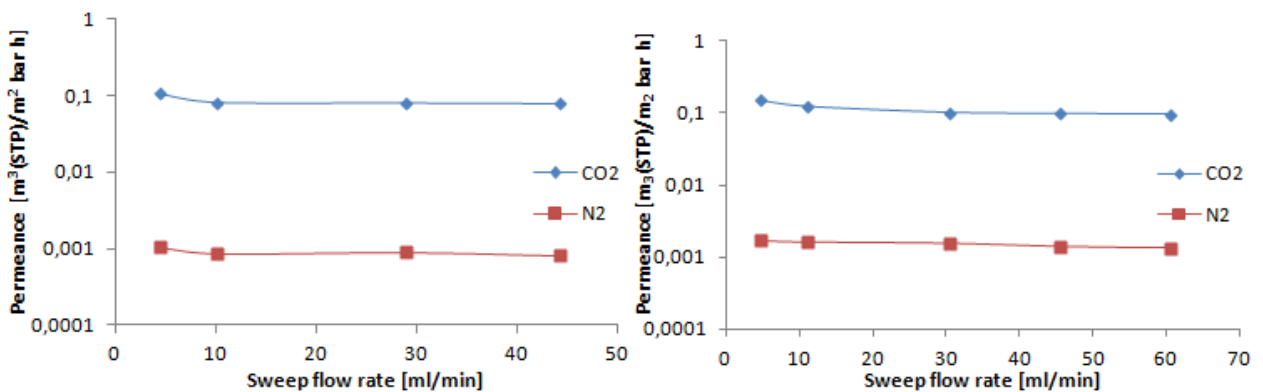


Figure 5.2.2.2: Permeance of CO₂ and N₂ against sweep flow rate for the PVAm/PSf composite membrane with D and J as support.

The CO₂ permeance for the two composite membranes is quite similar, but the one based on the new support, J, is slightly higher. For the N₂ permeance is the difference more profound, and also here is the composite membrane with fibre J as support the one with highest permeance. This is due to the higher amount of surface defects in this support. The CO₂/N₂ selectivity of PVAm/PSf composite membrane with fibre D as support from the specialization project and the composite membrane with fibre J as the support from the master thesis is shown in figure 5.2.2.3.

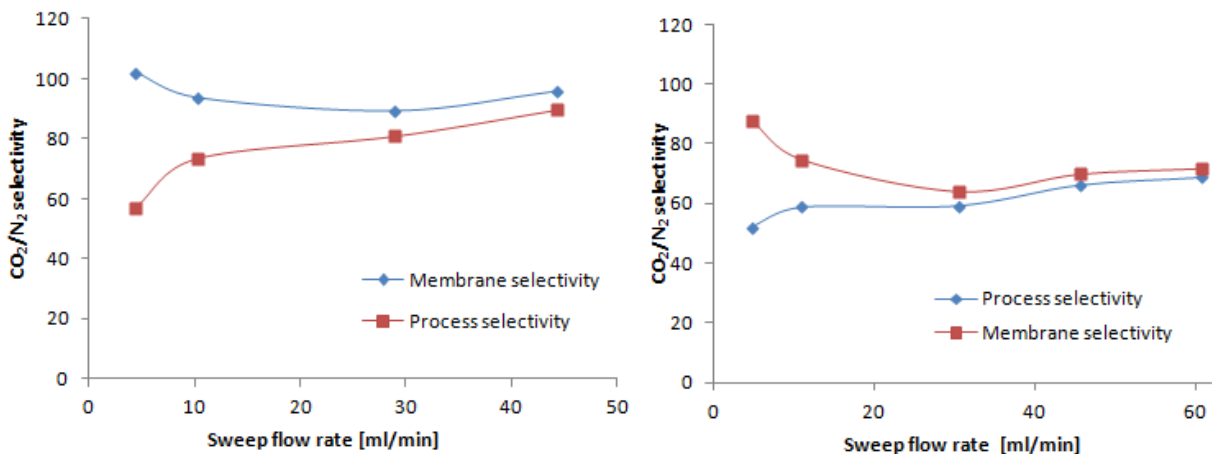


Figure 5.2.2.3: CO₂/N₂ selectivity against sweep flow rate for the PVAm/PSf composite membrane with D and J as support

The CO₂/N₂ selectivity is highest for the PVAm/PSf FSC composite membrane with the D fibre as the support. This is related to the surface defects discussed earlier. In figure 5.2.2.4 is the CO₂ purity for the two composite membranes given as function of the sweep flow rate.

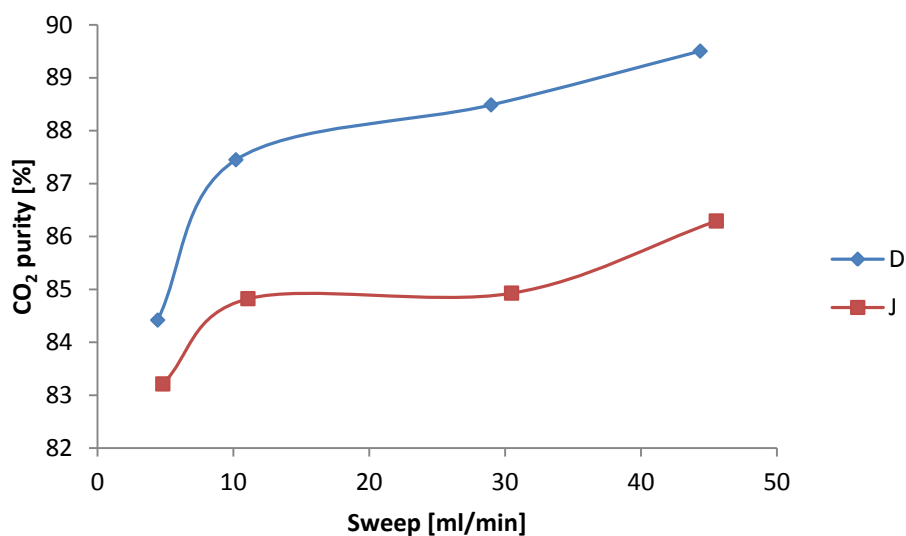


Figure 5.2.2.4: The CO₂ purity of the PVAm/PSf FSC composite membranes with D and J as the support as a function of the sweep flow rate

The purity is also highest for the composite membrane from the specialization project. At a sweep flow rate of 44 ml/min, the CO₂ purity for the composite membrane with D as support is 90% which is on target for the critical purity in order to be competitive with amine absorption [51].

The comparison of the PVAm/PSf FSC composite membrane from the master thesis and the PVAm/PSf FSC composite membrane from specialization project shows that the composite membrane from the previous project is best with respect to CO₂/N₂ selectivity and CO₂ purity when both the pressure and sweep flow rate are varied. The CO₂ permeance is slightly higher for the composite membrane from the master thesis or almost the same as for the other composite membrane, but the N₂ permeance is much higher for the composite membrane from the master thesis. This is probably caused by the surface defects of the PSf support spun in the master thesis.

5.3 The importance of the PSf support and the PVAm selective coating layer

In this chapter the purpose is to investigate whether the porous support itself or the PVAm coating layer is the most important step in order to successfully produce a PSf/PVAm FSC composite membrane with required permeance and CO₂/N₂ selectivity. Table 5.3.1 shows the comparison between the PSf support membrane only coated with non-selective PDMS and the PSf support coated with PVAm. The membrane considered is the membrane with PSf fibre J as support, and the results are based on a pressure of 1.2 bar, 25°C and humid sweep and feed gas.

Table 5.3.1: Comparison of the separation properties of a PSf hollow fibre, J, with and without a selective PVAm coating layer

Coating sequence	CO ₂ permeance [m ³ (STP)/m ² bar h]	N ₂ permeance [m ³ (STP)/m ² bar h]	CO ₂ /N ₂ selectivity
2 x 5% PDMS	0.23	0.02	13
3% PVAm 1% PDMS	0.12	0.0002	75

As mentioned earlier, the PSf support fibre J contained many surface defects and holes, and from table 5.3.1 it can be seen that the CO₂/N₂ selectivity for the support membrane both with and without a selective PVAm layer is relatively low. Sandru, M. et al [36] reported a CO₂/N₂ selectivity between 100 and 230 for PVAm/PSf composite membranes, and this can indicate that even though a selective coating layer is applied, does the support affect the selectivity.

Before coating with PVAm, the permeance of PSf hollow fibres was relatively high, but after coating with PVAm the permeance had decreased to half. This might be an indication that the selective coating layer prohibits permeation through the membrane, and could show that the rate limiting step for gas transport through a composite membrane is transport through the dense top layer [5]. The high amount of holes and surface defects on the PSf support hollow fibre could also be a large contributor to the high permeance recorded before coating with PVAm. When the PVAm was applied to the surface of the support, it is possible that PVAm penetrated into the support and plugged the pores, which also resulted in a thinner selective top layer. This effect could reduce both permeance and CO₂/N₂ selectivity and is reported by Kim, Li and Hägg [10]. If a support with high internal porosity and a dense skin layer without defects and holes was successfully made, it is possible that the PVAm coating layer would not affect permeance to such a large extent as no pore penetration would occur. This indicates that the PSf support itself has a large impact on the separation properties of a FSC composite membrane, and that an optimally produced support is essential in order to successfully make a FSC composite membrane.

5.4 Blend hollow fibre membranes

Helberg [12] introduced the use of PVAm directly in the spinning dope solution, and this work was continued first in the specialization project and now in the master thesis by increasing the PVAm concentration in the spinning dope from 0.2% to 1%. The wanted result was an increase in effect of PVAm polymer for the separation properties of the PVAm/PSf hollow fibres. By adding PVAm to the spinning dope solution, the goal was to make PVAm/PSf blend membrane with high CO₂/N₂ selectivity and high CO₂ permeance in one step.

5.4.1 Preparation of blend membranes

PVAm was successfully dissolved in ethylene glycol which is a weak non-solvent for PSf and has the role of increasing the porosity of the hollow fibre. When PVAm/ethylene glycol was mixed with the PSf/NMP dope solution, a homogenous mixture was obtained. Table 5.1.1.1 shows the concentration of the dope components and the spinning conditions from the spun blend fibres in the master thesis and the blend fibre spun in Helberg's master thesis [12]. The blend fibre spun during Helberg's master thesis was tested in the specialization project and will be compared to the blend fibres spun during this master thesis.

Table 5.4.1.1: Concentration of the dope components and the spinning condition for PVAm/PSf blend

Spinning condition	1% PVAm/PSf blend HF nr 1	1% PVAm/PSf blend HF nr 2	0.2% PVAm/PSf blend HF [12]
Dope composition [wt%]	32 PSF, 43 NMP, 15 THF, 1 PVAm, 9 Ethylene glycol	32 PSF, 43 NMP, 15 THF, 1 PVAm, 9 Ethylene glycol	32 PSF, 43 NMP, 15 THF, 0.2 PVAm, 9.8 ethylene glycol
Dope flow rate [ml/min]	1	0.5	0.5
Bore fluid [wt%]	80/20 NMP/water	80/20 NMP/water	80/20 NMP/water
Bore flow [ml/min]	0.65	0.32	0.32
Temperature [°C]	25	25	25
Air gap [cm]	28	28	28
Take-up speed [m/min]	8	8	8

During the attempt to make a 1% PVAm/PSf blend membrane in the specialization project, the wanted spinning conditions were not obtained. These conditions were not obtained, as some of the dope solution was retained by a blocked filter before entering the spinneret and the amount of filtered 1% PVAm/PSf blend solution was too small to reach the wanted spinning conditions. In the master thesis, the wanted conditions were reached as the air gap was increased while the bore fluid and the dope fluid rates were successfully reduced.

The DSC results for the spun 1% PVAm/PSf blend hollow fibres for three cycles are shown in figure 5.4.1.1 and 5.4.1.2. In figure 5.4.1.1 and 5.4.1.2 all the cycles for the fibres have glass transition temperatures (T_g) around the T_g for PSf. In figure 5.4.1.3 three cycles for dry polymer dope solution is shown. From the figure it can be seen that the polymer dope solution has a lower T_g for the first cycle compared to the T_g for PSf. For the second and third cycles, the T_g s were the same as the T_g for PSf. The deviations in the measured T_g s for the first cycles may appear because the dry polymer from the dope solution used for spinning still contained some solvent. This indicates that the hollow fibres were washed sufficiently and all of the solvent was removed.

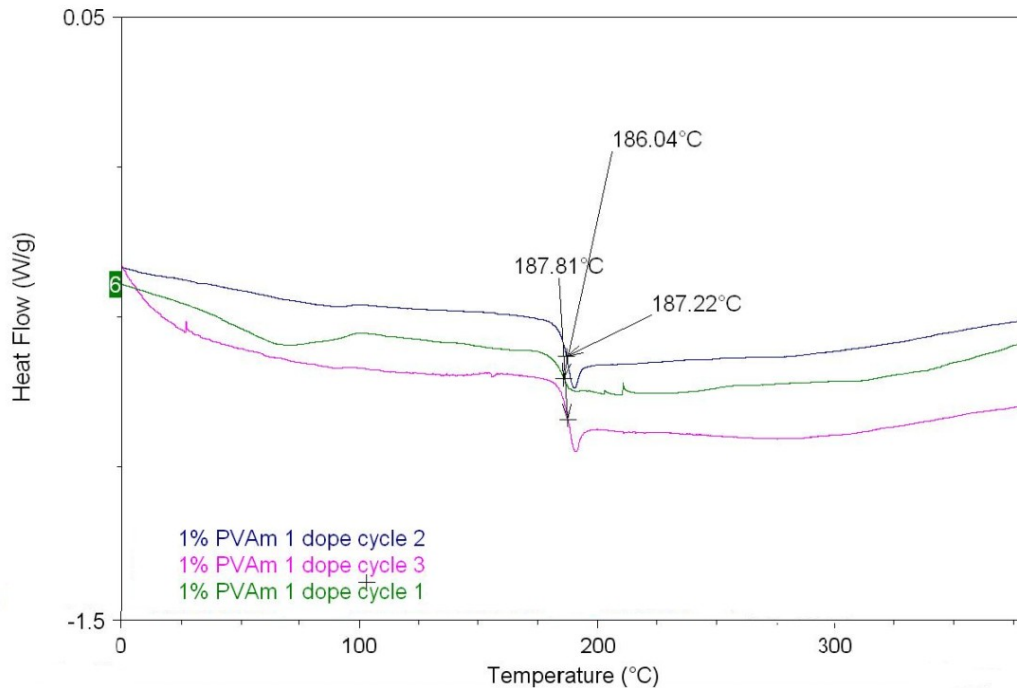


Figure 5.4.1.1: DSC measurements of hollow PVAm/PSf blend hollow fibre nr 1 for three cycles.

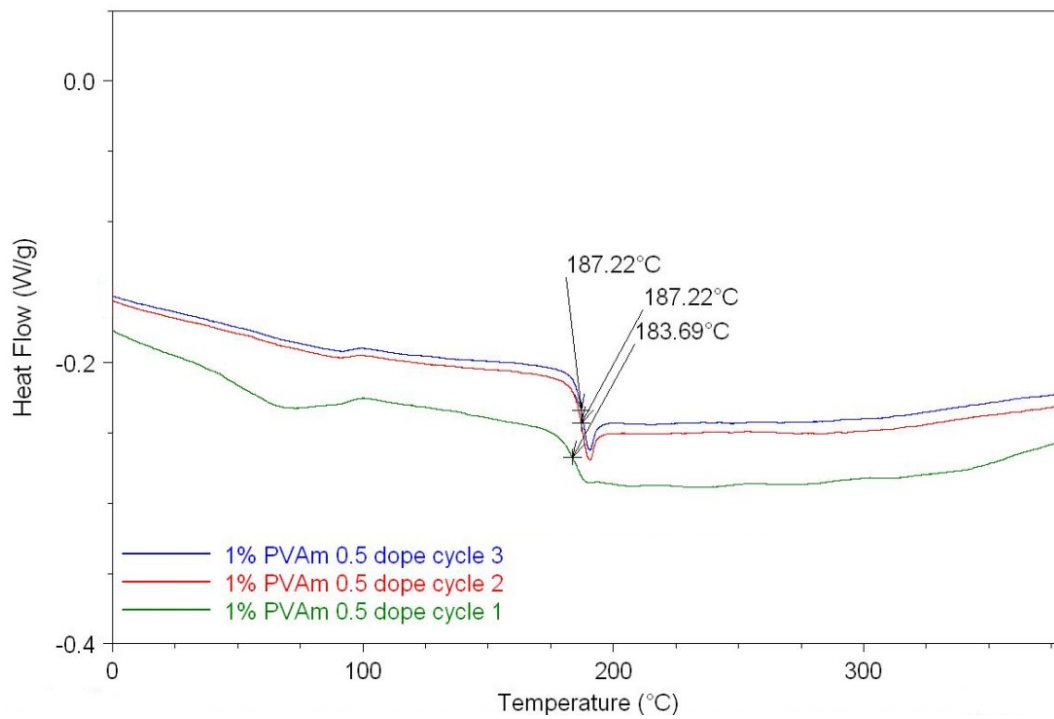


Figure 5.4.1.2: DSC measurements of PVAm/PSf blend hollow fibre nr 2 for three cycles.

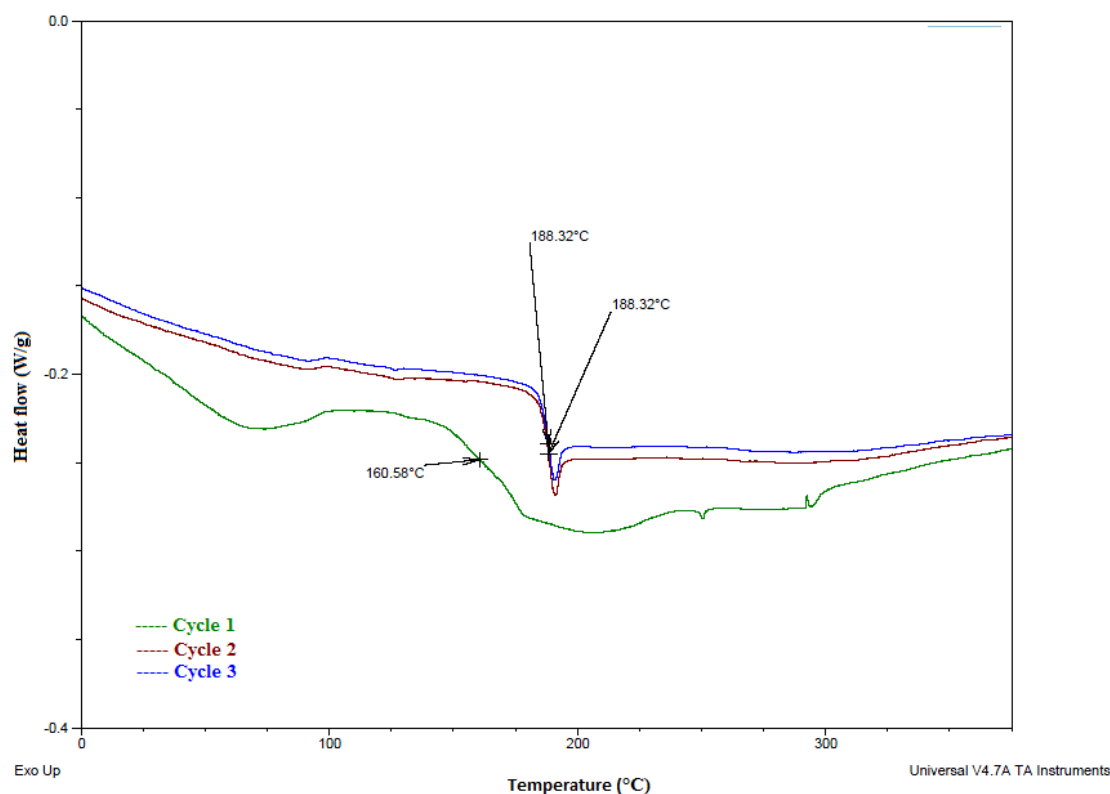


Figure 5.4.1.3: DSC measurements of dry PVAm/PSf polymer from dope solution for three cycles [11]

Cycle three for 1% PVAm/PSf hollow fibre in figure 5.4.1.1 and 5.4.1.2 is compared with DSC results for pure PSf in figure 5.4.1.4 and pure PVAm in figure 5.4.1.5. In both figures the results are compared with the 0.2% PVAm/PSf blend hollow fibre. From the figure 5.4.1.4 it can be seen that 0.2% PVAm/PSf blend curve is very similar to the pure PSf curve. It has the same T_g as PSf, but it also has a small decrease in heat flow where pure PVAm melts, as seen in figure 5.4.1.5. This indicates that 0.2% PVAm/PSf blend consists of both PSf and PVAm, but since PSf is the main component in the blend, the curve is most similar to the pure PSf curve.

For 1% PVAm/PSf curve it was expected a curve that was even more similar to the pure PVAm curve, since the amount spinning dope contains five times higher PVAm concentration compared to 0.2% PVAm/PSf blend. The figure 5.4.1.4 shows that the 1% PVAm/PSf curve is very similar to the pure PSf curve. In figure 5.4.1.5 is it shown that the 1% PVAm/PSf curve shows no similarity to the pure PVAm curve. Where 0.2% PVAm/PSf blend showed a decrease in heat flow where pure PVAm melts, is the 1% PVAm/PSf blend curve is quite constant. The curve shows a small change in curvature where PVAm melts. The reason for this result may be that PVAm and PSf has perhaps separated and become non homogenous, because the dope solution stood idle for four days after it was prepared as the spinning rig was not available. This might have caused regions with more PVAm and regions with less or without PVAm. In the specialization project it was believed that the PVAm had been removed during filtration of the blend due to filter fouling, but this cannot be the case in the master thesis as the components were filtrated before blending. Another explanation can be that PVAm has reacted with PSf when the blend stood still for several days before the spinning rig was available. The PVAm solution was heated to 40°C to enhance the dissolution before it was blended with the PSf dope solution. An increase in temperature would increase the reactivity and make it more probable that a reaction has occurred. When a reaction occurs and a homogeneous blend is formed, the properties of the blend will lie between the properties of

PSf and PVAm [5]. The amount of PSf in the blend is much higher than the amount of PVAm, and the T_g should therefore be close to the T_g of PSf. Also, the PVAm is much more crystalline and a clear glass transition temperature is not observed before melting temperature. This could explain why the DSC only gives indication of PSf in the blend. Another method that could be used to analyze the PVAm/PSf blend membranes is infrared (IR) spectroscopy. This was used in the specialization project, but it gave no clear results and was not used for the master thesis.

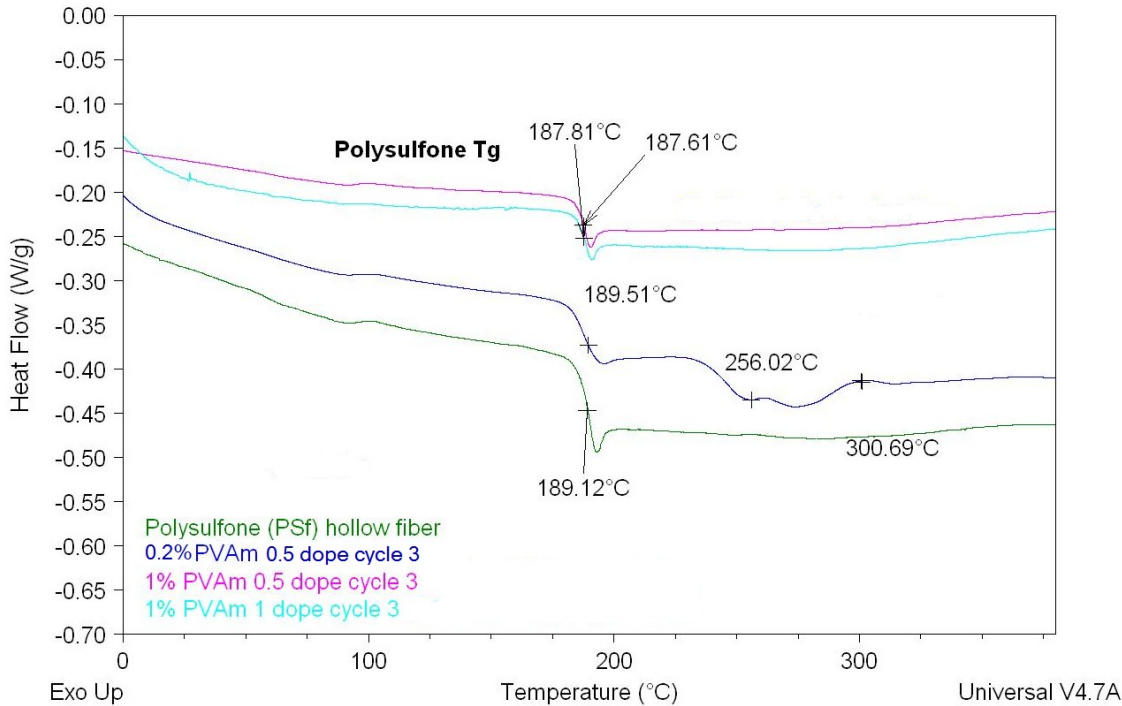


Figure 5.4.1.4: DSC measurements for pure PSf, 0.2% PVAm/PSF and 1% PVAm/PSf blends

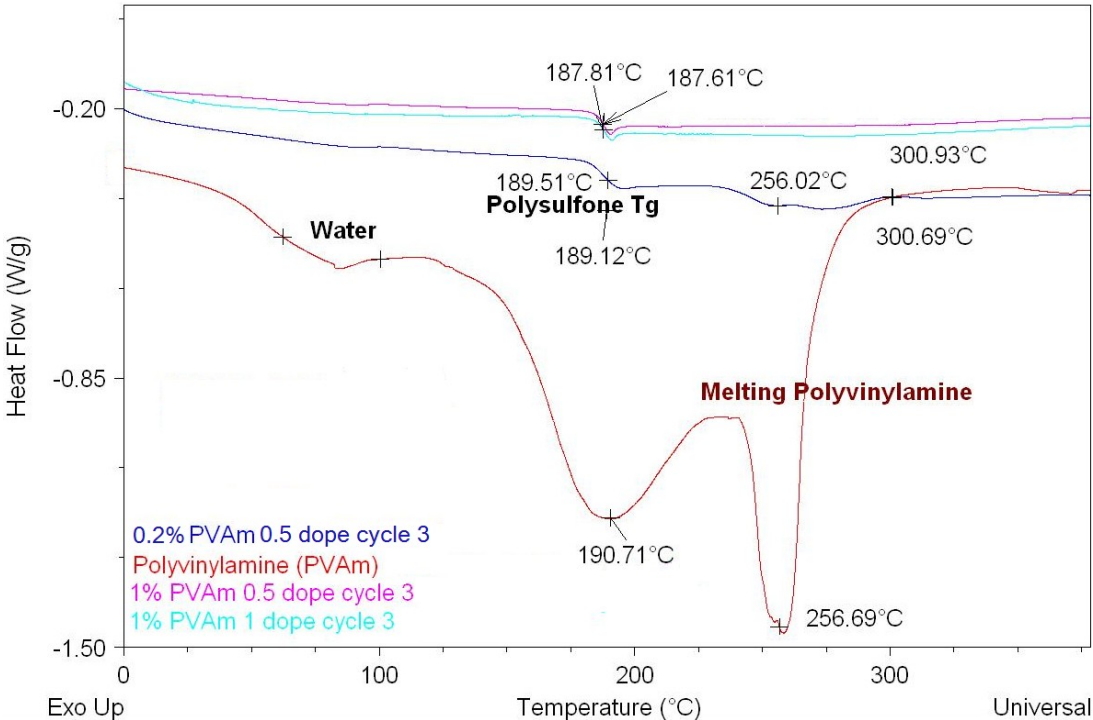


Figure 5.4.1.5: DSC measurements for pure PSf, 0.2% PVAm/PSF and 1% PVAm/PSf blends

The 1% PVAm/PSf blend hollow fibres spun in this master thesis was also investigated by use of SEM. This was done to investigate the fibres' morphology. The SEM pictures of the cross section and wall section for the 1% PVAm/PSf blends nr 1 and nr 2 are shown in figure 5.4.1.6 and 5.4.1.7 respectively.

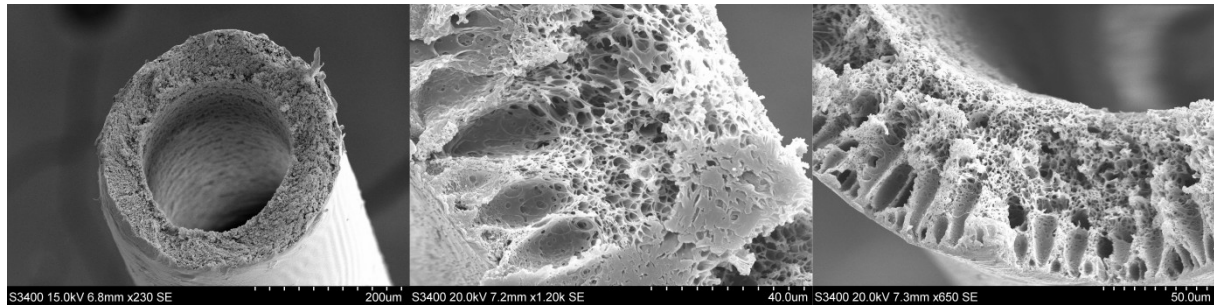


Figure 5.4.1.6: Cross section and wall cross section of 1% PVAm/PSf blend nr 1 spun in this project

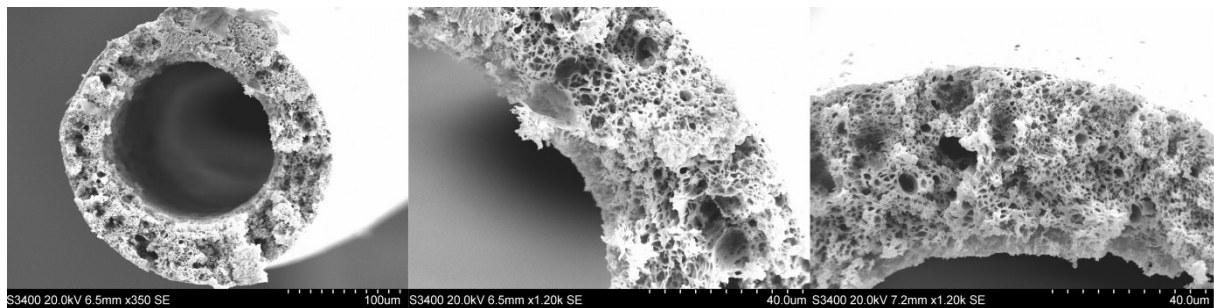


Figure 5.4.1.7: Cross section and wall cross section of 1% PVAm/PSf blend nr 2 spun in this project

The pictures taken using SEM of 1% PVAm/PSf blend hollow fibre shows a porous structure with some macrovoids. The wanted morphology is that the fibres are porous without macrovoids. From figure 5.4.1.6 and 5.4.1.7 it can be seen that 1% PVAm/PSf blend nr 1 has more and bigger macrovoids than 1% PVAm/PSf blend nr 2. The reason for this may be that nr 2 has a lower dope and bore flow rate of 0.5 ml/min compared to nr 1 which has 1 ml/min. The reason for this may be that lower dope flow rates gives higher elongational stress. This is because when the dope flow rate is decreased less amount of the dope solution goes through the spinneret, leading to a thinner fibre, which makes it easier for the solvent to diffuse out of the fibre. The macrovoids may be due to an air gap that was only 28 cm. Number of macrovoids per unit area decrease as the air gap increase, and the only way to make sure macrovoids are not formed, is to have a sufficient long air gap [20]. The take-up speed was 8 m/min which is below the critical value of 50 m/min for the formation of macrovoid free hollow fibre membranes reported by Peng, N., et al [20]. Figure 5.4.1.8 and 5.4.1.9 shows the surface of 1% PVAm/PSf blend hollow fibre for batches nr 1 and nr 2 respectively. From the pictures it can also be seen that the cross section and wall thickness of the 1% PVAm/PSf blend nr 2 is much thinner compared to 1% PVAm/PSf blend nr 1.

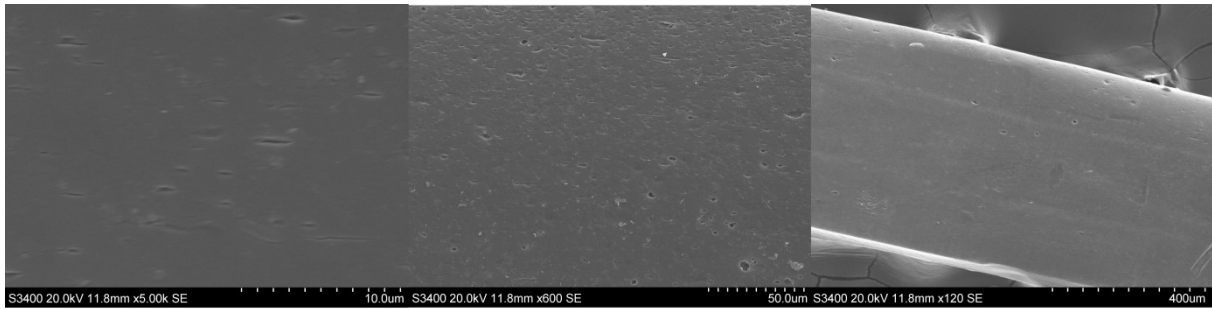


Figure 5.4.1.8: Surface of 1% PVAm/PSf blend nr 1 spun in this project

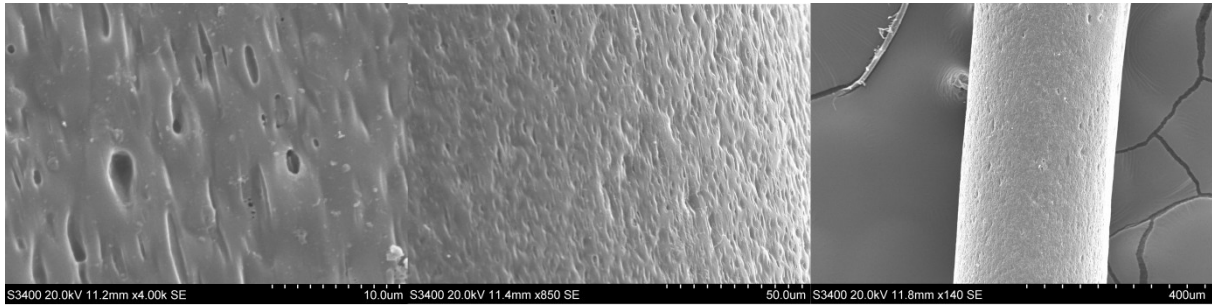


Figure 5.4.1.9: Surface of 1% PVAm/PSf blend nr 2 spun in this project

From the figures 5.4.1.8 and 5.4.1.9 it can be seen that the surface contains some defects for both the fibre types. But it is much fewer holes and defects than the spun PSf support fibres discussed earlier and the holes are smaller and oblong. This makes it much easier to seal the defects and holes with coating for the spun blend membranes. The reason for the better surface than the PSf supports spun in this master thesis could be that the spinning conditions were less severe as the take-up speed and air gap was much lower for the blend membranes. The 1% PVAm/PSf blend nr 2 has a slightly larger surface defects than 1% PVAm/PSf blend nr 1. In figure 5.4.1.10 the SEM pictures of the thickness of the coating layer for all the three blends, when they were coated two times with PDMS is shown. From the pictures it can be seen that the thickness of the coating layers are between 0.7 to 1 μm . When the SEM samples were prepared with liquid nitrogen, the PDMS coating layer had a tendency to slip and cover some of the cross section of the porous support. This made it difficult to take good SEM pictures of the coating layer thickness.

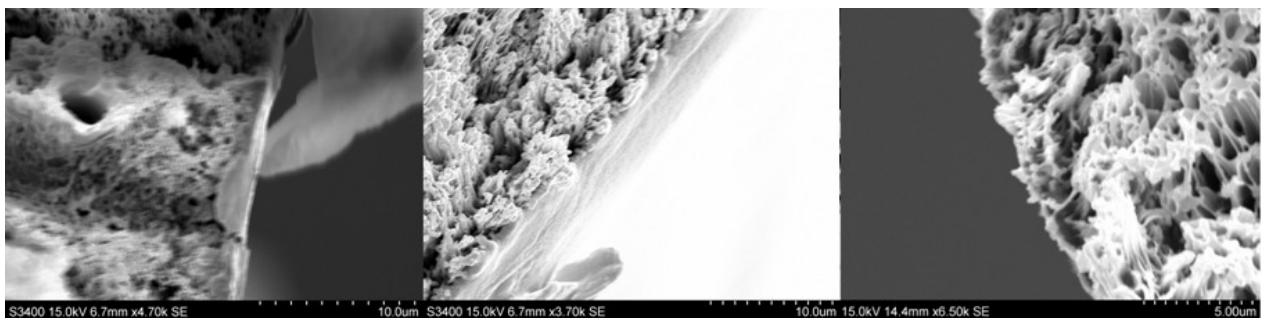


Figure 5.4.1.10: SEM pictures of the thickness of the coating layer when all the blend fibres were coated two times with 5% PDMS. The left pictures are 1% PVAm/PSf blend nr 1, the picture in the middle is the 1% PVAm/PSf blend nr 2 and the right picture is the 0.2% PVAm/PSf blend membrane

5.4.2 Gas permeation tests for both hollow fibre blends

The mixed gas permeation experiments were performed using a feed consisting of 10% CO₂ and 90% N₂ at 100% relative humidity for both the sweep and feed streams. The feed was fed from the shell side of the membranes, leading to an outside-in operation. The gas permeation test was executed at a temperature of 25°C. The 0.2% PVAm/PSf blend fibre membrane was tested during the specialization project and the results are presented here for comparison.

Influence of pressure

The blend membranes coated two times with 5% PDMS were tested at 1.2, 3, 5 and 8 bar. The sweep flow rate was constant between 8 and 11 ml/min. In table 5.4.2.1 the CO₂ permeance for the PVAm/PSf blend fibre membranes is given.

Table 5.4.2.1: CO₂ permeance of the different PVAm/PSf blend membranes for different pressure

Pressure [bar]	1% PVAm/PSf HF nr 1	1% PVAm/PSf HF nr 2	0.2% PVAm/PSf HF
	CO ₂ permeance [m ³ (STP)/m ² bar h]	CO ₂ permeance [m ³ (STP)/m ² bar h]	CO ₂ permeance [m ³ (STP)/m ² bar h]
1.2	0.096	0.046	0.066
3	0.088	0.042	0.057
5	0.075	0.051	0.051
8	0.072	0.049	0.046

From figure 5.4.2.1 can it be seen that the CO₂ permeance decreases with increased pressure for the 1% PVAm/PSf hollow fibre nr 1 and the 0.2% PVAm/PSf hollow fibre. This is as expected due to saturation of the carriers supplied by the PVAm. For all the blend membranes is the N₂ permeance approximately constant, except for 1% PVAm/PSf hollow fibre where the N₂ has increased from 0.0007 to 0.0012 m³(STP)/(m² bar h). The N₂ is transported by solution diffusion, and the N₂ permeance should not be affected by the increased pressure. The CO₂ permeance for the 1% PVAm/PSf hollow fibre nr 2 (dope flow 0.5 ml/min) increases for 5 and 8 bar, see table 5.4.2.1. One reason might be that some of the surface defects of the fibre have been opened with the increased pressure and the membrane become easier to penetrate through. This theory is supported by the facts that the N₂ permeance also increases from 0.0007 to 0.0012 m³(STP)/(m² bar h). The 1% PVAm/PSf hollow fibre nr 2 contained more surface defects compared to the 1% PVAm/PSf hollow fibre nr 1, and the CO₂ permeance first decreases for 3 bar before it increases for 5 and 8 bar. This indicates that facilitated transport was present and permeance decreased between 1 and 3 bar, because of saturation of the carriers. The CO₂ permeance increases when the pressure is increased further as surface defects are opened, which make it easier to pass through the fibre. The 1% PVAm/PSf hollow fibre nr 1 (dope flow 1 ml/min) has a much higher permeance compared to the other two blend membranes, see table 5.4.2.1. One explanation for the lower CO₂ permeance for the 1% PVAm/PSf hollow fibre nr 1 and the 0.2 % PVAm/PSf hollow fibre can be that the humid sweep gas may have lead to condensation inside the bore of the hollow fibres. The bore side could have been partially blocked with water which has lead to a less effective separation area, which gives a lower CO₂ permeance. The 1% PVAm/PSf hollow fibre nr 2 and the 0.2% PVAm/PSf hollow fibre are much thinner than the 1% PVAm/PSf hollow fibre nr 1 and could much easier be blocked. In figure 5.4.2.1 is the CO₂/N₂ selectivity given as a function of the pressure for the different blend membranes. The lines are added only to see trends in the result.

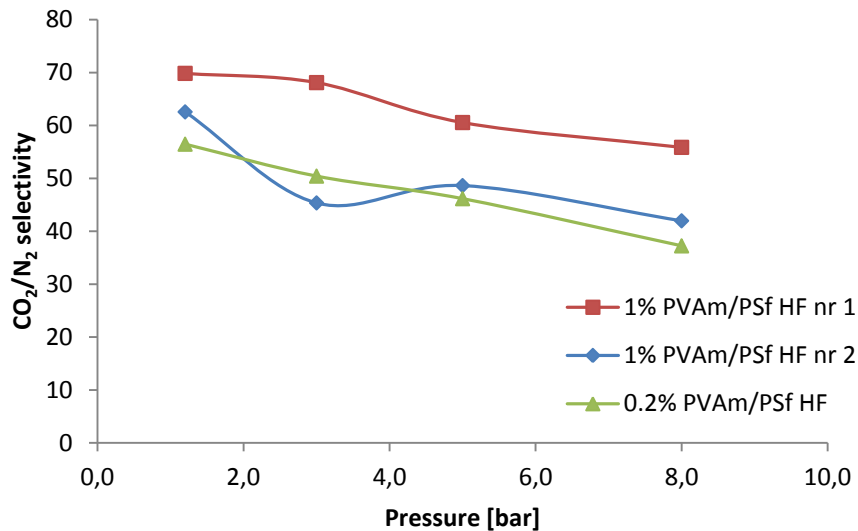


Figure 5.4.2.1: CO_2/N_2 selectivity for the different blend membranes as a function of pressure

From figure 5.4.2.1 it can be seen that the CO_2/N_2 selectivity decreases with increased pressure for all the fibres. This is expected in a situation with facilitated transport. Selectivity decreases as the pressure increases due to saturation of the fixed carrier sites supplied by the PVAm [15]. This happens as the amount of CO_2 in the feed increases while the amount of carrier sites stays the same. More CO_2 molecules will have to permeate by solution diffusion or other transport mechanisms and this leads to a reduction in permeance. The N_2 molecules are not transported by facilitated transport and the N_2 permeance is not affected as the pressure increases. This leads to a reduction in CO_2/N_2 selectivity. The selectivity for the 1% PVAm/PSf hollow fibre nr 1 and nr 2 is higher than for 0.2 % PVAm/PSf hollow fibre, except for at 3 bar for 1% PVAm/PSf hollow fibre nr 2 which could be due to an experimental error. This indicates the increased amount of PVAm has a positive effect on the separation properties of the PVAm/PSf hollow fibres. The lower selectivity for the 1% PVAm/PSf hollow fibre nr 2 compared with 1% PVAm/PSf hollow fibre nr 1, is probably because 1% PVAm/PSf hollow fibre nr 2 contains more surface defects that is opened when the pressure increase. The CO_2/N_2 selectivity decreases more rapidly for the 0.2 % PVAm/PSf hollow fibre compared to the 1% PVAm/PSf hollow fibres, except between 1.2 and 3 bar for 1% PVAm/PSf hollow fibre nr 2. This indicates that since 0.2% PVAm/PSf hollow fibre only contains 0.2% PVAm compared to 1% PVAm, it contains less fixed carrier and the carriers are saturated earlier. This also contributes to the conclusion that an increased amount of PVAm enhances the separation properties of the blend membrane. Since both the CO_2 permeance and selectivity decreases with increased feed pressure for the 1% PVAm/PSf hollow fibre nr 1 and the 0.2% PVAm/PSf hollow fibre, it is verified that the facilitated transport mechanism is present. For 1% PVAm/PSf hollow fibre nr 2 the selectivity decreases but the CO_2 permeance slightly increased. This is probably because of opened surface defects with increased feed pressure, and facilitated transport is most likely present for this membrane too. In table 5.4.2.2 the CO_2 purity for the blend membranes is given.

Table 5.4.2.2: CO₂ purity for the different blend membranes at different pressure

Pressure [bar]	CO ₂ purity for 1% PVAm/PSf blend HF nr1 [%]	CO ₂ purity for 1% PVAm/PSf blend HF nr2 [%]	CO ₂ purity for 0.2% PVAm/PSf blend HF [%]
1.2	84	85	82
3	84	80	81
5	83	81	80
8	83	79	77

All three fibres gives quite high and stable CO₂ purity in the permeate, see table 5.4.2.2, but all of them are lower than the critical purity of 90% [51]. The PVAm/PSf blend hollow fibre nr 1 gives the highest and most stable purity except for at 1.2 bar, where the PVAm/PSf blend hollow fibre nr 2 slightly has the highest value. This could be because the PVAm/PSf blend hollow fibre nr 1 has fewer surface defects and holes which reduces selectivity. Both the 1% PVAm/PSf blend membranes give a higher purity than the 0.2% PVAm/PSf blend hollow fibre. This is also an indication that adding more of the selective component PVAm to the blend gives better separation.

Influence of sweep flow rate

The blend membranes coated two times with 5% PDMS were tested at different sweep flow rates. The pressure was kept constant at 1.2 bar. In figure 5.4.2.2-5.4.2.4 the CO₂ and N₂ permeance for the PVAm/PSf blend fibre membranes are given on a logarithmic scale. The lines are added only to see trends in the result.

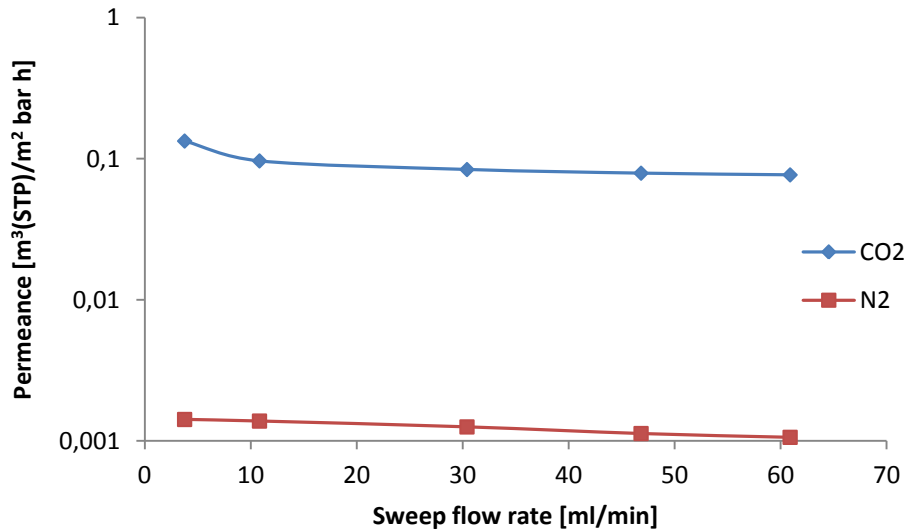


Figure 5.4.2.2: CO₂ and N₂ permeance for 1% PVAm/PSf blend hollow fibre nr 1 coated two times with 5% PDMS as a function of the sweep flow rate on a logarithmic scale

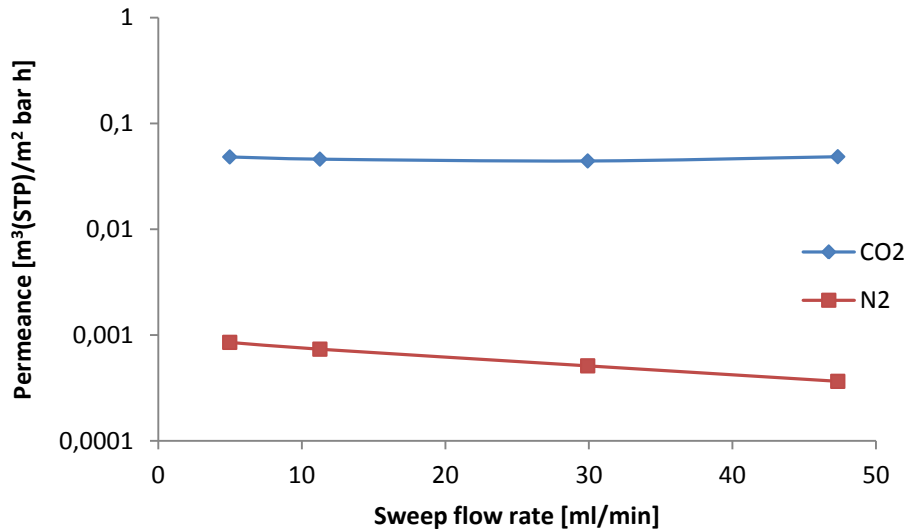


Figure 5.4.2.3: CO₂ and N₂ permeance for 1% PVAm/PSf blend hollow fibre nr 2 coated two times with 5% PDMS as a function of the sweep flow rate on a logarithmic scale

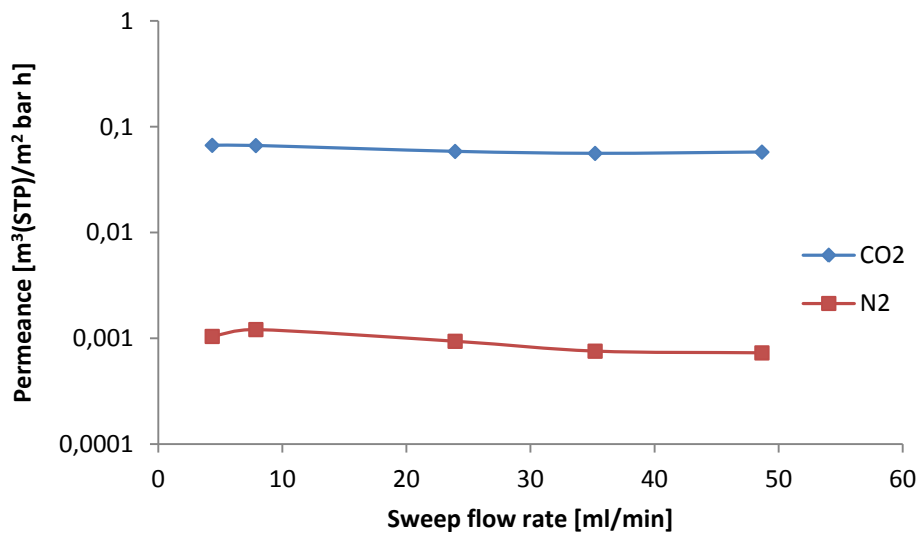


Figure 5.4.2.4: CO₂ and N₂ permeance for 0.2% PVAm/PSf blend hollow fibre coated two times with 5% PDMS as a function of the sweep flow rate on a logarithmic scale [11]

As can be seen from figures 5.4.2.2-5.4.2.4, the permeance of both CO₂ and N₂ decreases slightly when the sweep flow rate is increased. An explanation for this is that the sweep gas may penetrate the membrane in the opposite direction, causing an extra resistance for mass transfer for the permeating gas. The driving force for back diffusion occurs since the retentate may act as a “sweep” for the sweep gas [15]. The 1% PVAm/PSf blend membrane nr 2 and the 0.2% PVAm/PSf blend membrane have the lowest permeance, which is approximately constant at 0.05 m³(STP)/(m² bar h) for the 1% PVAm/PSf blend membrane nr 2 and ranging from 0.07 to 0.05 m³(STP)/(m² bar h) for the 0.2% PVAm/PSf blend membrane. This is much lower than the permeance for 1% PVAm/PSf blend membrane nr 1, which ranges from 0.1-0.07 m³(STP)/(m² bar h). The low permeance could be caused by condensation inside the bore of the hollow fibres, partially blocking it with water. As the bore flow rate was only 0.5 ml/min during spinning of these two fibres, they are much thinner than the 1% PVAm/PSf

blend membrane nr 1 with a bore flow rate of 1 ml/min, and are therefore more easily blocked by condensation. In figures 5.4.2.5-5.4.2.7 is the CO_2/N_2 selectivity for the blend membranes given. The lines are added only to see trends in the result.

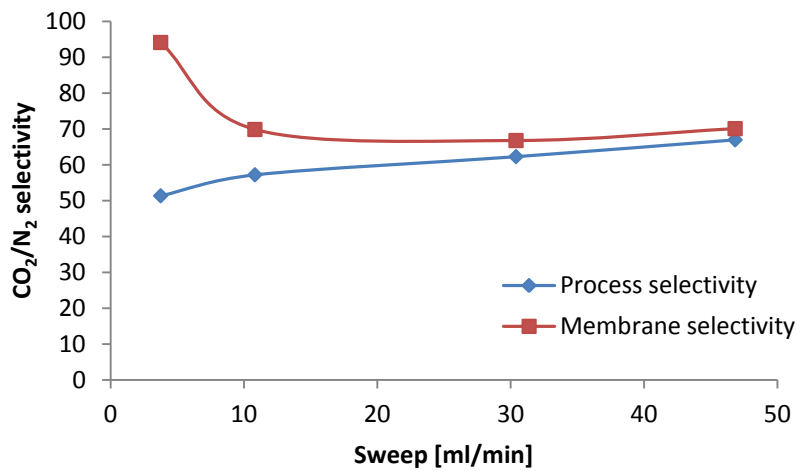


Figure 5.4.2.5: CO_2/N_2 selectivity for 1% PVAm/PSf blend hollow fibre nr 1 coated two times with 5% PDMS as a function of the sweep flow rate

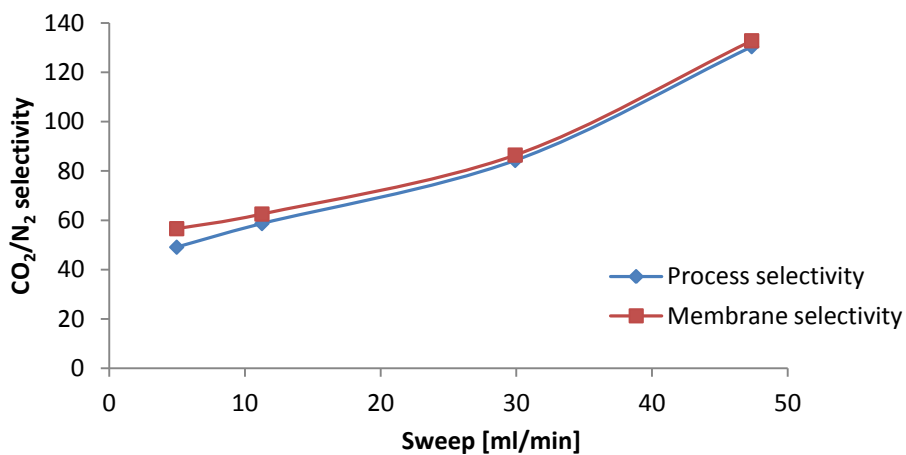


Figure 5.4.2.6: CO_2/N_2 selectivity for 1% PVAm/PSf blend hollow fibre nr 2 coated two times with 5% PDMS as a function of the sweep flow rate

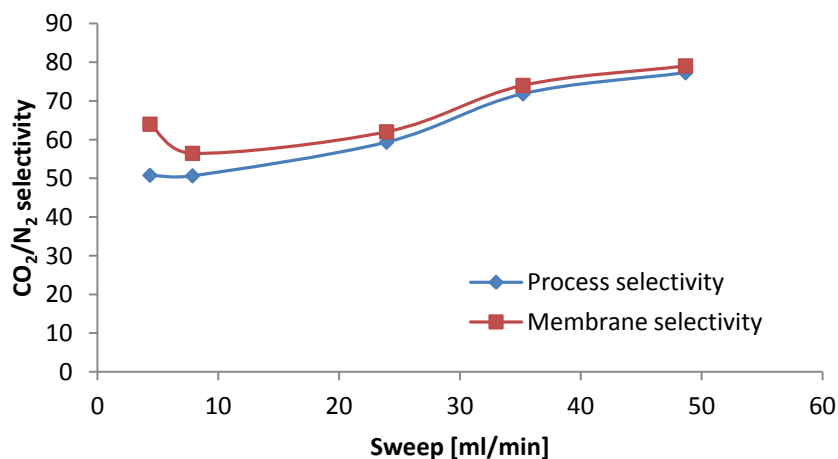


Figure 5.4.2.7: CO_2/N_2 selectivity for 1% PVAm/PSf blend hollow fibre nr 1 coated two times with 5% PDMS as a function of the sweep flow rate [11]

The general trend shown in figures 5.4.2.5-5.4.2.7 is an increase in selectivity with an increase in sweep flow rate (driving forces). Increasing the sweep flow rate also gives back diffusion which is an extra resistance to mass transfer. The permeance of N₂ decreased more than the CO₂ permeance because of back diffusion, and as a result does the selectivity increase as the sweep flow rate increases. The 1% PVAm/PSf blend hollow fibre nr 1 ranges from a selectivity of 94 to 70, 1% PVAm/PSf blend hollow fibre nr 2 ranges from a selectivity of 57 to 133, while the 0.2% PVAm/PSf blend hollow fibre ranges from 51 to 77. These results show that the 1% PVAm/PSf blend hollow fibre nr 1 shows lower selectivity than the 0.2% PVAm/PSf blend hollow fibre, except for sweep value of 4 ml/min. The 1% PVAm/PSf blend hollow fibre nr 2 is much better than both of them. This support the theory that the PVAm and the PSf had separated to a certain degree before spinning as pointed out earlier in chapter 5.4.1. Especially since the 1% PVAm/PSf blend hollow fibre nr 2 should contain more PVAm than 1% PVAm/PSf blend hollow fibre nr 1 if this theory is correct, as this fibre was spun last. This is apparent as 1% PVAm/PSf blend hollow fibre nr 2 has a much higher selectivity than 1% PVAm/PSf blend hollow fibre nr 1 when the sweep flow rate was increased, indicating more selective PVAm content. The process selectivity approaches the membrane selectivity as the sweep flow rate is increased. This is because when the driving forces are larger than the value for the membrane selectivity, the main resistance is the permeation through the membrane and the process selectivity value approaches the membrane selectivity. This indicates that when the driving forces are sufficiently large, the overall selectivity is determined by the membrane itself and not the process conditions [16]. In figure 5.4.2.8 is the CO₂ purity of the blend membranes given as a function of the sweep flow rate. The lines are added only to see trends in the result.

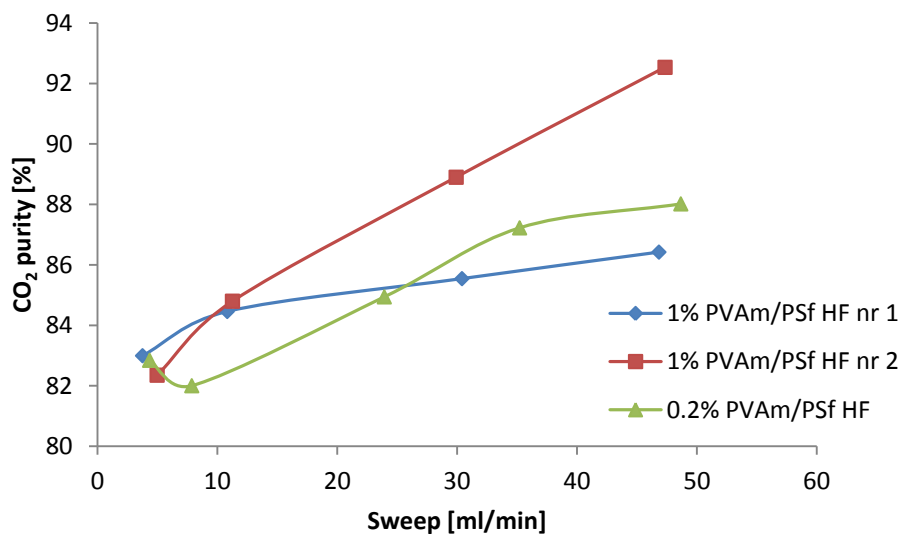


Figure 5.4.2.8: CO₂ purity for 1% PVAm/PSf blend hollow fibres coated two times with 5% PDMS as a function of the sweep flow rate

As expected does the 1% PVAm/PSf blend hollow fibre nr 2 give a much higher CO₂ purity in the permeate than the two other blend membranes. The reason for this is that the 1% PVAm/PSf blend hollow fibre nr 2 has a considerable higher CO₂/N₂ selectivity. The highest value is obtained at the highest sweep flow rate, and is a CO₂ purity of 93%. This is higher than the critical value of 90% [51], but the CO₂ permeance of this fibre is quite low. The CO₂ permeance is 0.05 m³(STP)/m² bar h with these conditions.

Influence of humidity

In figures 5.4.2.9-5.4.2.11 is the CO₂/N₂ selectivity for the blend membranes given as a function of the feed humidity.

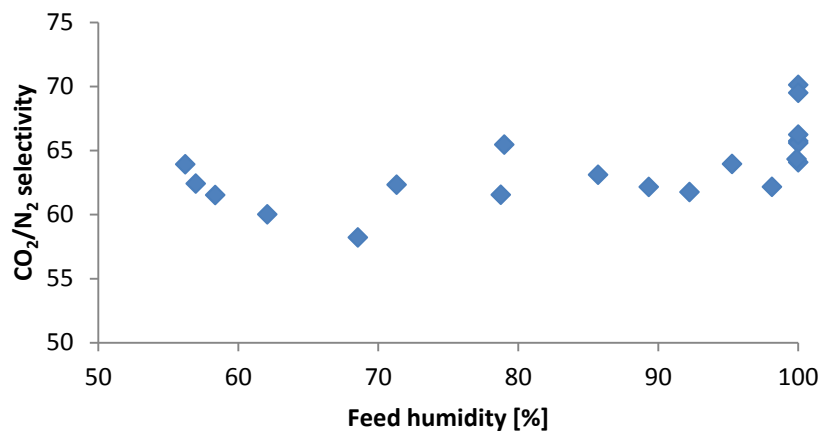


Figure 5.4.2.9: Influence of relative feed humidity on selectivity for 1% PVAm/PSf blend membrane nr 1 coated two times with 5% PDMS

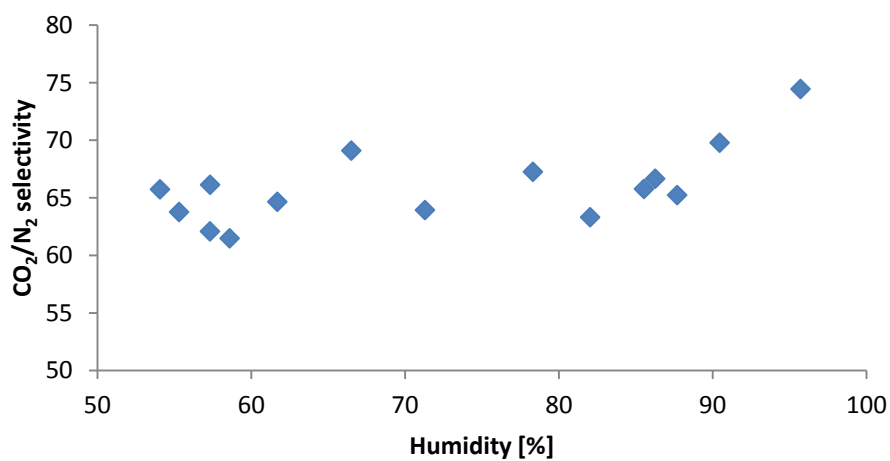


Figure 5.4.2.10: Influence of relative feed humidity on selectivity for 1% PVAm/PSf blend membrane nr 2 coated two times with 5% PDMS

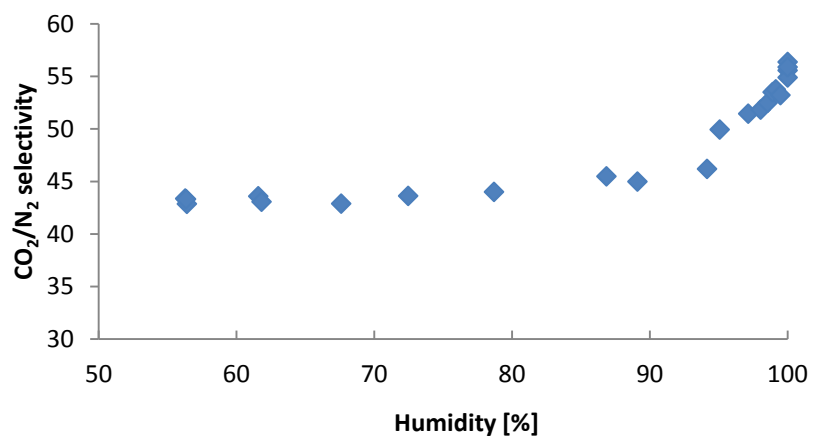


Figure 5.4.2.11: The influence of relative feed humidity on selectivity for 0.2% PVAm/PSf blend coated two times with 5% PDMS [11]

From figure 5.4.2.9 and 5.4.2.10 it can be seen that the CO₂/N₂ selectivity seems to change randomly with increased humidity for the 1% PVAm/PSf blend membranes, but a trend of increase may be observed after the relative humidity of the feed reached 85%. The 0.2% PVAm/PSf blend membrane [11] has a clearer increase in CO₂/N₂ selectivity as the humidity increases. CO₂ is transported through the membrane by both solution diffusion and facilitated transport by the PVAm. The CO₂ reacts with water to form bicarbonate (HCO₃⁻), and this bicarbonate forms a complex with PVAm in order to be transported through the membrane, as discussed in chapter 3.3.5. Because of this, an increase in selectivity was expected when the humidity was increased, as the permeance of CO₂ should increase while the permeance of N₂ should stay constant since N₂ only is transported by solution diffusion. It was expected a larger dependency on humidity for the PVAm/PSf blend membranes with 1% PVAm than for 0.2% PVAm. This is not the case. This may be related to the DSC curves from figures 5.4.1.4 and 5.4.1.5 where there were no traces of PVAm for the 1% PVAm/PSf blend membranes. The same happened for the specialization project, where PVAm was believed to be either retained by the filter during filtering, because of filter fouling, or to have separated causing a non-homogeneous mixture [11]. For the master thesis, the components were filtered before blending and after blending no filter was used, but the spinning was not performed immediately after the dope solution was prepared as the spinning rig was unavailable. Two hypotheses are equally valid. Either the polysulfone reacted with polyvinylamine due to the long mixing time before spinning, or the two polymers separated in two distinct regions, one rich in PVAm and one rich in PSf. Therefore it is possible that some fibres contained less PVAm than 1%, giving lower or no dependency of the feed humidity and lower CO₂/N₂ selectivity. As there was a trend towards increasing CO₂/N₂ selectivity when the relative humidity increases, is it also possible that the explanation of PVAm reacting with PSf is valid.

Influence of changing the stream configurations

As the blend membranes have an unknown distribution of the selective compound PVAm in the fibre, the separation properties when the feed was applied to the bore side of the fibre was tested. The permeation tests were done at 25 °C, 1.2 bar, sweep flow rate of 11 ml/min and 100% relative humidity of both sweep and feed gas. Table 5.4.2.3 shows the separation properties and CO₂ purity of 1% PVAm/PSf blend hollow fibre membrane nr 1 and nr 2 with inside-out permeation.

Table 5.4.2.3: The CO₂ and N₂ permeance, CO₂/N₂ selectivity and CO₂ purity for 1% PVAm/PSf blend fibre membranes with feed on the bore side

1% PVAm/PSf blend	CO₂ permeance [m³(STP)/m² bar h]	N₂ permeance [m³(STP)/m² bar h]	CO₂/N₂ selectivity	CO₂ purity [%]
nr 1	0.0915	0.0015	59	83
nr 2	0.0547	0.0011	49	81

The results shows that the CO₂/N₂ selectivity decreases from 70 to 59 for the 1% PVAm/PSf blend hollow fibre nr 1 and the CO₂/N₂ selectivity decreases from 63 to 49 for 1% PVAm/PSf blend hollow fibre nr 2 when the feed is applied to the bore side. The permeance is virtually unchanged for the 1% PVAm/PSf blend hollow fibre nr 1, while it is increased a bit for the 1% PVAm/PSf blend hollow fibre nr 2. The purity of the two fibres is almost the same, while the CO₂/N₂ selectivity is higher for the 1% PVAm/PSf blend membrane nr 1. This is as expected and discussed earlier in chapter 5.2.1. The results could indicate that the PVAm has a higher concentration on the outer surface of the membrane, but as this surface is coated two times with 5% PDMS, could the higher selectivity in the case of outside-in separation be

because the outer surface defects are covered while the inner defects are not. This could also explain the increased permeance for the 1% PVAm/PSf blend hollow fibre nr 2 when the experiment was done inside-out. These results indicate that it is most probable that the PVAm is quite uniformly distributed within the blend hollow fibres. This supports the theory that the PVAm and PSf have partially reacted during preparation of the dope solution. Another explanation can be that humid sweep and feed causes condensation of water on the bore side of the hollow fibre. When the feed humidity decreases, less water will condensate and this might increase the CO₂ permeance.

Summary of the PVAm/PSf blend membranes

It was attempted to successfully produce a 1% PVAm/PSf blend hollow fibre membrane, as this was not done successfully in the specialization project. During production of the blend polymer solution in the master thesis, no filtration was performed after blending the components as it was suspected that the selective PVAm was retained during filtration. In the specialization project the desired spinning conditions were not reached as most of the polymer solution was lost during filtration because of filter fouling [11]. In the master thesis, the desired spinning conditions were reached and by analysis by SEM the PVAm/PSf hollow fibre blend membranes showed a good morphology. When the 1% PVAm/PSf blend fibres were tested with DSC, no indication of PVAm was found. For gas permeation at different feed humidities the results showed a dependency of CO₂/N₂ selectivity on feed humidity, which is an indication of PVAm content in the 1% PVAm/PSf blend membranes. For the 0.2% PVAm/PSf blend membrane, a clear increase of CO₂/N₂ selectivity when the humidity was increased was shown, and it was expected that the tendency would be even stronger for the 1% PVAm/PSf blend membranes. The reasons for this not being the case could be separation of the blend since the polymer solution was idle for some time before spinning or that PVAm and PSf has reacted during preparation and storage of the dope solution. Another reason for the lower than expected dependency on humidity shown during gas permeation, could be condensation of water causing blockage in the hollow fibre as both feed and sweep was humid. On the other hand, the permeation tests with varying pressure and sweep flow rate gave higher CO₂/N₂ selectivity for the 1% PVAm/PSf blend membranes than the 0.2% PVAm/PSf blend membrane. This is a clear indication that selective PVAm is present in the 1% PVAm/PSf blend membranes as well, and has a large effect on the separation properties of the membrane. The CO₂/N₂ selectivity is high for the 1% PVAm/PSf blend membranes, where the highest value is 133 which gives a CO₂ purity of 93% in the permeate.

5.5 Comparison of the blend and composite membranes

In this chapter, the best PVAm/PSf composite membranes from the master thesis, as well as the best composite membrane produced in the specialization project will be compared with the best PVAm/PSf blend membranes. This is done in order to investigate if blend membranes are competitive with composite membranes with respect to separation properties. The spinning conditions and dope compositions for the compared blend and composite membranes are given in table 5.5.1.

Table 5.5.1: Dope composition and spinning conditions for the compared fibres in this chapter

Spinning condition	1% blend HF nr 1	1% blend HF nr 2	B	D	J
Dope composition [wt%]	32 PSF, 43 NMP, 15 THF, 1 PVAm, 9 Ethylene glycol		32 PSF, 58 NMP, 10 glycerol		
Dope flow rate [ml/min]	1	0.5	1	1	2
Bore fluid NMP/water [wt%]	80/20	80/20	80/20	80/20	80/20
Bore flow [ml/min]	0.65	0.32	0.65	0.65	1.3
Temperature [°C]	25	25	25	23	25
Air gap [cm]	28	28	61	27.2	61
Take-up speed [m/min]	8	8	16	8	20

5.5.1 Comparison of pressure influence

From the blend membranes, the 1% PVAm/PSf blend membrane nr 1 was chosen to be compared with the composite membranes, as this was the blend fibre that obtained the best separation properties when the pressure was increased. This blend membrane will be compared to the PVAm/PSf FSC composite membranes with B and D as support. In figure 5.5.1.1 and 5.1.1.2 are the CO₂ and N₂ permeance shown as function of pressure respectively. The lines are added only to see trends in the result.

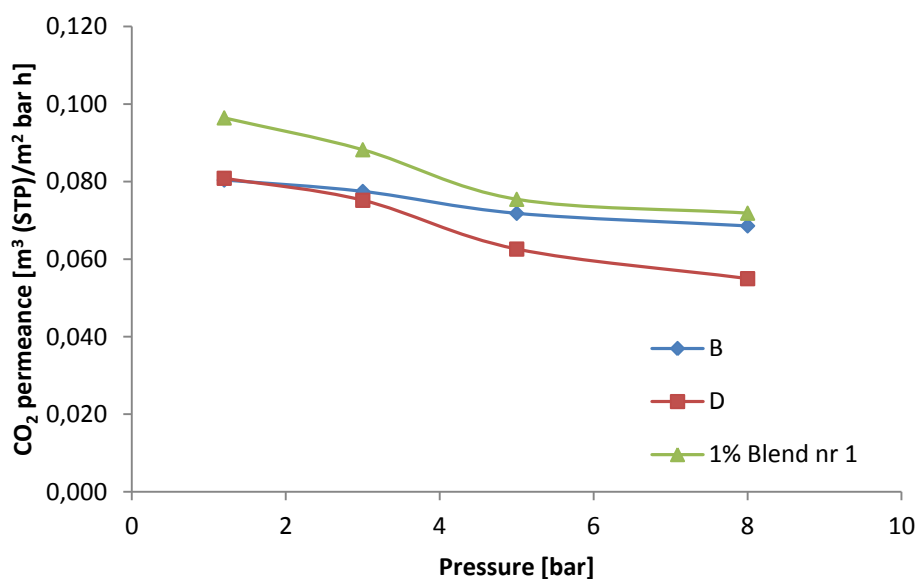


Figure 5.5.1.1: CO₂ permeance as a function of pressure for 1% PVAm/PSf blend nr 1 and PVAm/PSf FSC composite membrane with B and D as support

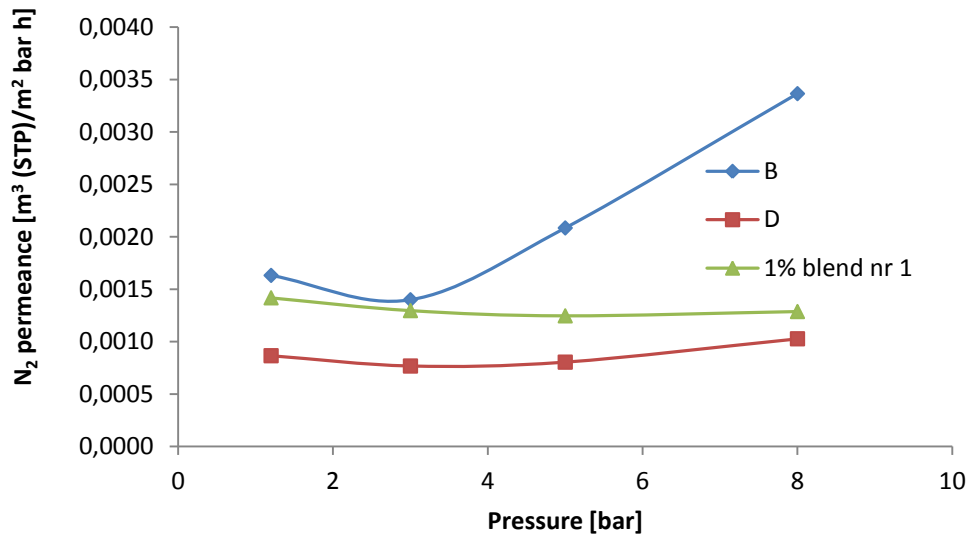


Figure 5.5.1.2: N_2 permeance as a function of pressure for 1% PVAm/PSf blend nr 1 and PVAm/PSf FSC composite membrane with B and D as support

The general trend for the CO_2 permeance shown in figure 5.5.1.1 is a decrease with increasing pressure as a consequence of carrier saturation, and the PVAm/PSf blend membrane has the exact same trend as the PVAm/PSf composite membrane with D as support. This could be a good indication of the presence of PVAm in the blend membrane and that facilitated transport occurs. The PVAm/PSf blend membrane is the membrane with highest CO_2 permeance, and the N_2 permeance is similar for the blend membrane and the composite fibre with D as the support, but the blend membrane has a more constant N_2 permeance, see figure 5.5.1.2. For the PVAm/PSf composite membrane with B as the support, the CO_2 permeance decreases with a slower rate with feed pressure, and this might be because the increased pressure has opened the sealed surface defects causing viscous flow or Knudsen diffusion transport mechanisms to become important. This is supported by the fact that the N_2 permeance for composite membrane B increases at a high rate when the pressure is increased, indicating that the surface defects are reopened. For the PSf hollow fibre B, the spinning conditions were quite extreme, with very high air gap, high take-up speed and low dope flow rate. This may have given an increased amount of surface defects caused by the high elongational stress experienced by the fibre. For PSf fibre D and the blend membrane, the spinning conditions were quite similar and more moderate, and it seems like these conditions were more suitable in order to produce membranes with few surface defects. In figure 5.5.1.3 are the CO_2/N_2 selectivity given as a function of the feed pressure. The lines are added only to see trends in the result.

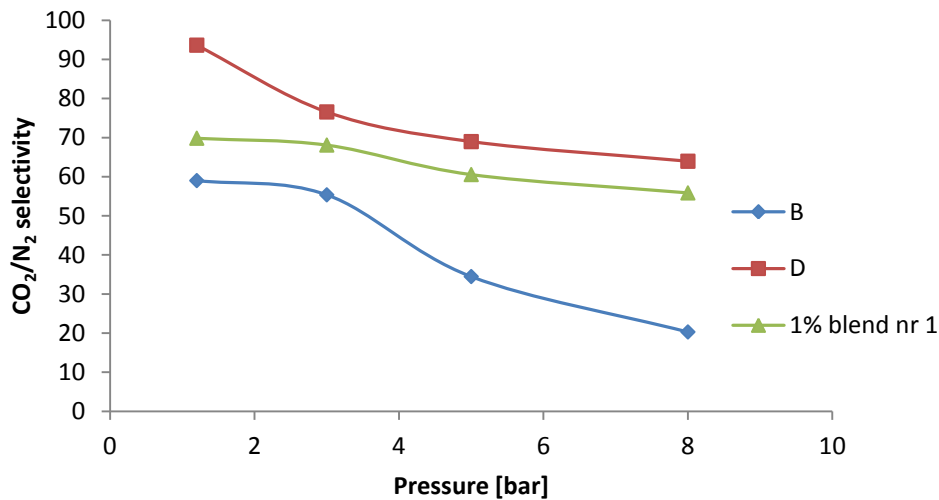


Figure 5.5.1.3: CO₂/N₂ selectivity as a function of pressure for 1% PVAm/PSf blend nr 1 and PVAm/PSf FSC composite membrane with B and D as support

From figure 5.5.1.3 it can be seen that the 1% PVAm/PSf blend membrane nr 1 and the PVAm/PSf FSC composite membrane with D as support also follows the same trend for CO₂/N₂ selectivity. The CO₂/N₂ selectivity decreases as the CO₂ permeance decreases because of carrier saturation while the N₂ permeance is approximately constant. The CO₂/N₂ selectivity decreases more rapidly for the composite membrane with D as support than for the blend membrane. This could be because the selective component is integrated in the structure of the blend membrane, and reopening of surface defects does not remove PVAm. This could make the blend membrane more resistant to high pressures than the composite membranes. The composite membrane with B as support has low CO₂/N₂ selectivity and a rapid decrease as the pressure increases. This is probably because of the high amount of surface defects and the reopening of the covered defects when the pressure becomes higher. In figure 5.5.1.4 is the CO₂ purity as a function of pressure given for the different membranes. The lines are added only to see trends in the result.

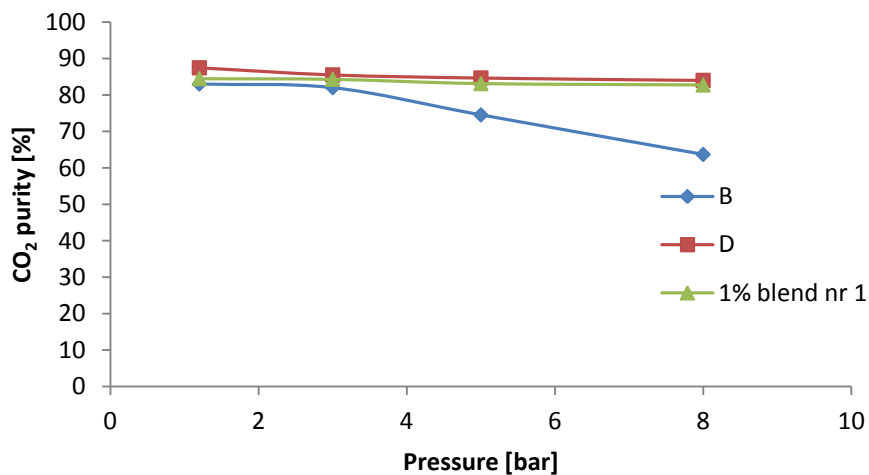


Figure 5.5.1.4: CO₂ purity as a function of pressure for 1% PVAm/PSf blend nr 1 and PVAm/PSf FSC composite membrane with B and D as support

The CO₂ purity of the 1% PVAm/PSf blend membrane nr 1 and the PVAm/PSf FSC composite membrane with D as the support are almost identical, as seen in figure 5.5.1.4, even though the CO₂/N₂ selectivity for PVAm/PSf FSC composite membrane with D as the

support is higher. The permeate purity increases fast with increasing driving forces up to a CO₂ purity around 80%. Above this value the CO₂ purity increases at much slower rates [36]. The CO₂ purity for the PVAm/PSf FSC composite membrane with B as support decreases rapidly with increased pressure. This is mostly because surface defects are reopened. None of the membranes obtain a CO₂ purity of 90%, which is the CO₂ purity absorption with amines gives [51]. To obtain a CO₂ purity above 90%, two-stage membranes are usually used. The CO₂ permeate purity obtained in one stage using the 1% PVAm/PSf blend nr 1 and the PVAm/PSf FSC composite membrane with D as support is approximately 90%. For many applications where CO₂ is captured, it is not necessary with purity above 90%, and in these processes could the membranes with the purities obtained here be a viable option.

5.5.2 Comparison of sweep flow rate influence

From the blend membranes, the 1% PVAm/PSf blend membrane nr 2 was chosen to be compared with the composite membranes, as this was the blend fibre that obtained the best separation properties when the sweep flow rate was changed. This blend membrane will be compared to the PVAm/PSf FSC composite membranes with D and J as support. In figure 5.5.2.1 and 5.5.2.2 are the CO₂ and N₂ permeance shown as function of sweep flow rate respectively. The lines are added only to point out the trends in the result.

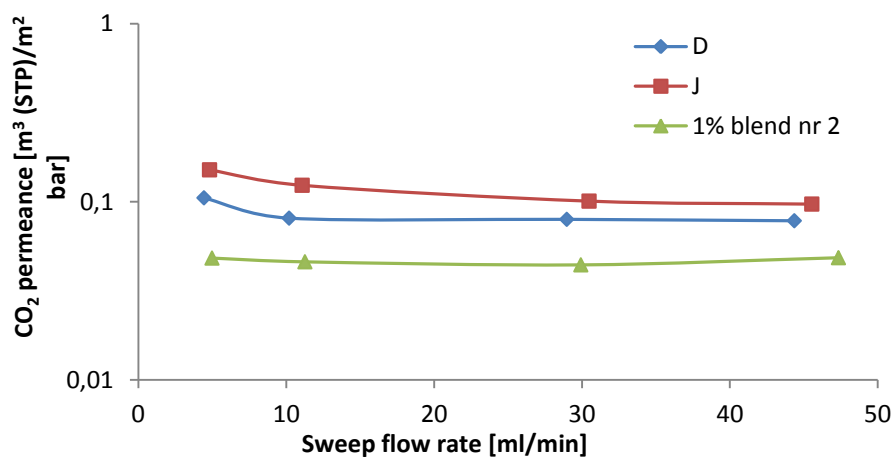


Figure 5.5.2.1: CO₂ permeance as a function of sweep flow rate for 1% PVAm/PSf blend nr 2 and PVAm/PSf FSC composite membrane with D and J as support

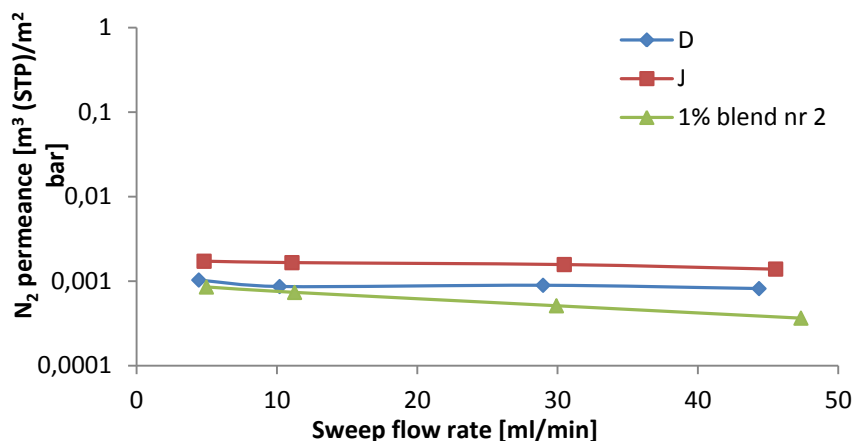


Figure 5.5.2.2: N₂ permeance as a function of sweep flow rate for 1% PVAm/PSf blend nr 2 and PVAm/PSf FSC composite membrane with D and J as support

From figure 5.5.2.1 it can be seen that the CO₂ permeance for the two composite membranes is decreasing when the sweep flow rate increases up to sweep flow rate 30 ml/min followed by a slight increase as the increased driving force overcome the effect of back diffusion. This may be due to back diffusion of the sweep gas as discussed earlier. For the blend membrane, the CO₂ permeance is almost constant at different sweep flow rates, while the N₂ permeance decreases a lot. The PVAm/PSf blend membrane nr 2 has lower CO₂ permeance than the two PVAm/PSf composite membranes, and the composite membrane with fibre J as support exhibits the highest permeance. The goal of increasing the CO₂ permeance from the composite membrane with D as support made in the specialization project was achieved by the composite membrane with J as support spun in the master thesis. Still, it was intended that the increase in CO₂ permeance for the J support should be even higher. In figure 5.5.2.3 is the CO₂/N₂ selectivity given as a function of the sweep flow rate. The lines are added only to see trends in the result.

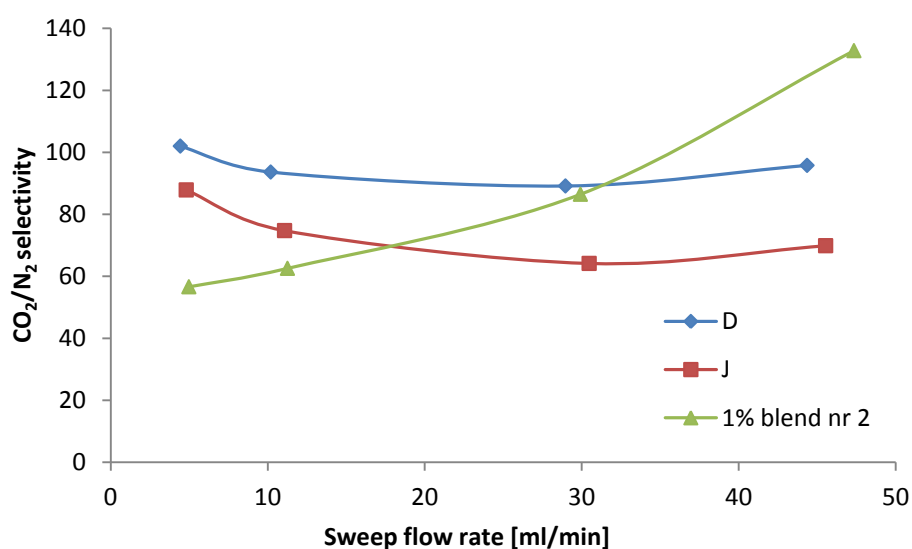


Figure 5.5.2.3: CO₂/N₂ selectivity as a function of sweep flow rate for 1% PVAm/PSf blend nr 2 and PVAm/PSf FSC composite membrane with D and J as support

From figure 5.5.2.3 it can be seen that the 1% PVAm/PSf blend membrane nr 2 has a large increase in CO₂/N₂ selectivity when the sweep flow rate increases. This is a normal response as an increase in sweep flow rate increases the driving forces. The CO₂/N₂ selectivity of the two PVAm/PSf composite membranes decrease at first when the sweep flow rate increases, but later starts to increase. This behaviour could indicate that when the sweep flow rate starts to increase, the back diffusion of sweep gas causes a decrease in CO₂/N₂ selectivity, but when the sweep flow rate increases even more, the increased driving forces becomes more important, and the CO₂/N₂ selectivity increases again. In figure 5.5.2.4 is the CO₂ purity as a function of pressure given for the different membranes. The lines are added only to see trends in the result.

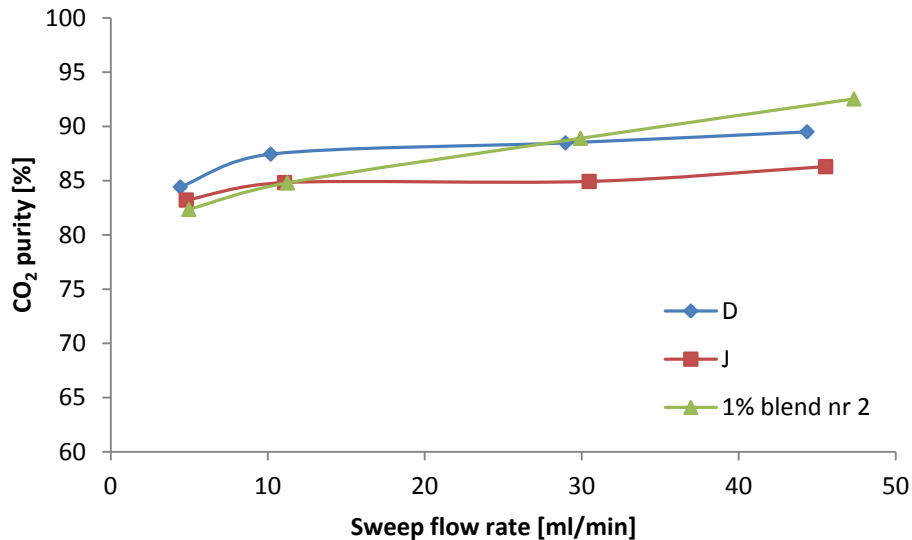


Figure 5.5.2.4: CO₂ purity as a function of sweep flow rate for 1% PVAm/PSf blend nr 2 and PVAm/PSf FSC composite membrane with D and J as support

The results from figure 5.5.2.4 show that the CO₂ purity for all the three membranes is quite similar and high. The permeate purity will increase at very slow rates above about 80% as mentioned earlier, and this can be seen by the fact that the CO₂/N₂ selectivity difference between the 1% PVAm/PSf blend nr 2 and the PVAm/PSf FSC composite membrane with D as support is 31, while the CO₂ purity difference is only 3% between these two fibres. The CO₂/N₂ selectivity and the CO₂ purity for the 1% PVAm/PSf blend membrane nr 2 is slightly higher than for the PVAm/PSf composite membranes, but the permeance is lower. This low permeance may be caused by condensation of the humid sweep and feed as the blend membrane inner diameter is much smaller as it is spun on 0.5 ml/min dope flow rate.

5.5.3 Summary

For the pressure tests does the 1% PVAm/PSf blend membrane nr 1 exhibit higher permeance than the two PVAm/PSf composite membranes, while for the sweep flow rate tests does the 1% PVAm/PSf blend membrane nr 2 show lower permeance than the PVAm/PSf composite membranes. This could be an indication that the morphology of the hollow fibre itself governs the permeance, and not the procedure of adding the selective material: blend membrane or a coated composite membrane. The CO₂/N₂ selectivity of the 1% PVAm/PSf blend membrane nr 1 is quite high and constant during the pressure tests, while the PVAm/PSf composite membranes experienced a slight decrease. This could indicate that by integrating the selective component into the structure of the hollow fibre, the membrane may become less vulnerable to opening of surface defects. For both the pressure and sweep flow rate tests, the 1% PVAm/PSf blend membranes show similar CO₂/N₂ selectivity and CO₂ purity, and by optimizing these membranes in order to increase permeance it is a good chance that PVAm/PSf blend membranes can compete with PVAm/PSf composite membranes. In figure 5.5.3.1 are the membranes that obtained the best CO₂/N₂ selectivity presented (1% PVAm/PSf blend fibre nr 2) and CO₂ permeance (PVAm/PSf composite fibre with J as support) compared with results from literature and Helberg's master thesis at 1.22 bar, 25 °C and 100% relative humidity. The CO₂/N₂ selectivity is shown as a function of CO₂ permeance. The fibres presented by Sandru, M., et al [36] and Helberg [12] are PSf fibres coated with PVAm.

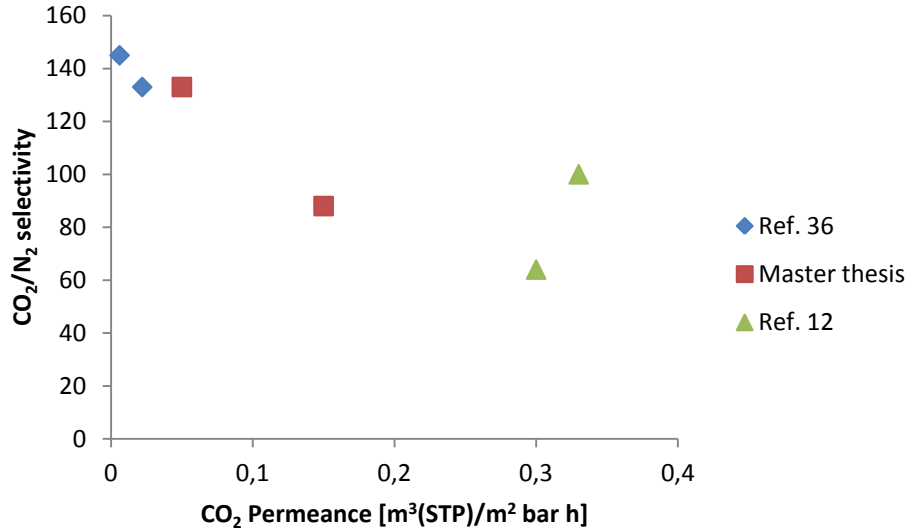


Figure 5.5.3.1: CO₂/N₂ selectivity as a function CO₂ permeance for the fibres from the master thesis with best separation properties compared with results from literature and Helberg's master thesis

The obtained results in this master thesis lies between the values obtained by Sandru, M. et al [36] and the values obtained by Helberg [12] as seen in figure 5.5.3.1. The CO₂/N₂ selectivity is lower than reported by Sandru, M., et al [36], while the CO₂ permeance is higher. Compared to Helberg [12] is the CO₂/N₂ selectivity similar or slightly higher, while the CO₂ permeance is much lower. For the second point from Helberg [12], is a dry sweep gas used, while the first point has utilized a sweep with 100% relative humidity. The dry sweep has lead to an increase in both CO₂/N₂ selectivity and CO₂ permeance. This might be related to the condensation of water in the pores and on the bore side of the hollow fibres which leads to blockage as mentioned earlier. This indicates that it can be useful for further testing to reduce the relative humidity of the sweep gas. The general trend is that an increase in CO₂ permeance causes a decrease in the CO₂/N₂ selectivity for the PVAm/PSf hollow fibre membranes.

5.6 Uncertainties

Uncertainties exist in all measurements due to instrumental and human errors. For example the thickness measurements done in SEM, the gas permeation test done by the gas chromatograph and the measurements done by DSC. This report covers primarily a comparative study and the same setups or instruments have been used for all the samples. In the cases where the same apparatuses have been used, the errors in the apparatus become less important. In order to quantify the uncertainty in the results, the standard deviation may be used. The standard deviation corresponds to a confidence interval including approximately 68% of the measurements [54]. To calculate the standard deviation for a set of data, equation 5.6.1 is used.

$$\sigma = \sqrt{\frac{1}{N} \sum_{i=1}^N (x_i - \bar{x})^2} \quad [54] \quad (5.6.1)$$

Where σ is the standard deviation, N is number of measurements, x_i is the value of measured variable i and \bar{x} is the arithmetic mean of all the measured variables [54]. The standard deviation for CO₂ permeance, CO₂/N₂ selectivity and CO₂ purity is calculated for the PVAm/PSf FSC composite membrane with J as support at 1.2 bar, 11 ml/min sweep flow rate, temperature at 25°C and feed and sweep flow at 100% relative humidity. It is assumed that the standard deviation is similar for the other membranes, and it is only calculated for this

membrane to show the trend. The measurement values that are considered are the values obtained after steady state is reached. In equation 5.6.2 the standard deviation for the CO₂/N₂ selectivity is given.

$$\sigma_S = \sqrt{\frac{1}{4}((78 - 75)^2 + (78 - 75)^2 + (72 - 75)^2 + (71 - 75)^2)} = 3 \quad (5.6.2)$$

In equation 5.6.3 the standard deviation for the CO₂ purity is calculated.

$$\sigma_{pur} = \sqrt{\frac{1}{4}((85 - 85)^2 + (85 - 85)^2 + (84 - 85)^2 + (84 - 85)^2)} = 0.7 \quad (5.6.3)$$

From equation 5.6.2 it can be seen that the CO₂/N₂ selectivity has a standard deviation that is much higher than the standard deviation for the CO₂ purity. This shows again that the CO₂ purity does not change considerably with change in selectivity above a certain value, and that the uncertainty in the results for CO₂ purity is very small. In equation 5.6.4 is the standard deviation for the CO₂ permeance shown.

$$\sigma_p = \left(\frac{1}{4}((0.128 - 0.124)^2 + (0.129 - 0.124)^2 + (0.119 - 0.124)^2 + (0.118 - 0.124)^2)\right)^{\frac{1}{2}} = 0.005 \quad (5.6.4)$$

Human influence is a source of error in approximately all the results. The experiment was carried out by one person. This helps to reduce the uncertainty as one person tends to be inaccurate in measurements the same way each time. For instance might one person consequently make a too high estimate when measuring the permeate gas velocity with a soap bubble meter, while another person might consequently underestimate the same velocity. Each of them will get results suitable for comparing different permeances, but together the deviations in the measurements may be large. The standard deviation for the bubble meter measurements on the PVAm/PSf FSC composite membrane with J as support, with the same conditions as used for the standard deviation calculations earlier in this chapter, is calculated by equation 5.6.5.

$$\sigma = \left(\frac{1}{6}((5.28 - 5.29)^2 + (5.31 - 5.29)^2 + (5.34 - 5.29)^2 + (5.32 - 5.29)^2 + (5.25 - 5.29)^2 + (5.22 - 5.28)^2)\right)^{\frac{1}{2}} = 0.04 \quad (5.6.5)$$

When the fibres were dip coated, the fibres were taken up by the solution manually. The withdrawal speed was kept constant as far as possible. The film formation on the membrane is influenced by the withdrawal speed, and higher speed gives a thicker layer. This is a large contribution to uncertainty as there was no real control of how fast the hollow fibre was withdrawn. The equation for the thickness of the coating layer was given in chapter 3.6.1, and the equation is cited her, see equation 5.6.6.

$$h_{\infty} = \frac{2}{3} \sqrt{\frac{\eta v}{\rho g}} \quad [5] \quad (5.6.6)$$

The maximum coating speed used was assumed to be approximately 2 times higher than the lowest coating speed. Using this assumption and equation 5.6.6 the difference in the thickness of the thickest and the thinnest possible coating layer could be calculated, see equation 5.6.7.

$$h_{max} = \frac{2}{3} \sqrt{\frac{\eta v_{max}}{\rho g}} = \frac{2}{3} \sqrt{\frac{\eta 2v_{min}}{\rho g}} = \frac{2}{3} \sqrt{\frac{\eta v_{min}}{\rho g}} \sqrt{2} \quad (5.6.7)$$

This gives the relationship between h_{max} and h_{min} , as shown in equation 5.6.8.

$$h_{max} = h_{min}\sqrt{2} \quad (5.6.8)$$

The difference between the thickest and the thinnest possible coating layer is then calculated as shown in equation 5.6.9.

$$\Delta h = h_{max} - h_{min} = h_{min}\sqrt{2} - h_{min} = (\sqrt{2} - 1)h_{min} = 41\%h_{min} \quad (5.6.9)$$

From equation 5.6.9 is it apparent that variance in the coating speed gives large differences in the coating layer thickness. Controlling this speed is therefore important in order to produce composite membranes with uniform coating layer thickness. As the coating speed was not measured, it was not possible to calculate a standard deviation for this value. Beside these errors, the biggest source of error might be that two different spinning rigs were used. One of the spinning machines were used for the very first time, and different factors such as a new spinneret, new take-up system and other factors were affecting the spinning procedure in an unknown way. The high number of surface defects obtained using the new spinning machine relative to the old one, may partly be attributed to these factors.

Chapter 6: Conclusion

6.1 PSf support

One of the main goals of this master thesis was to enhance the CO₂ permeance of the PVAm/PSf FSC composite membrane. Before proceeding with spinning of new hollow fibres, a 29% PSf hollow fibre support spun by Helberg was coated twice with 5% PDMS. The gas permeation results were compared with the results of the best 32% PSf support coated two times with 5% PDMS produced during the specialization project. This testing was performed to see if a lower PSf concentration of 29% PSf produced hollow fibres having higher CO₂ permeance. On the contrary, the 29% fibre exhibited very low CO₂ permeance and CO₂/N₂ selectivity. The low CO₂ permeance probably occurred as the 29% fibre was very vulnerable for back diffusion of sweep gas, as the structure had a large number of holes and thin fibre walls.

Another attempt to optimize the PSf support was performed by changing the spinning conditions. The air gap and take-up speed was increased, based on the results obtained by Ragne Helberg. These spinning conditions were believed to give a porous PSf hollow fibre without macrovoids, as the increased elongational stress applied to the hollow fibre would cause the polymer chains to align more tightly and remove all solvent, to prevent it from creating pockets of solvent inside the fibre. From the gas permeation tests, the PSf fibres coated two times with 5% PDMS exhibited high CO₂ permeance of about 0.22-0.23 m³(STP)/(m² bar h), except for one fibre that obtained a CO₂ permeance of 0.08 m³(STP)/(m² bar h). This fibre having low CO₂ permeance was produced using the lowest air gap and take-up speed, which imply that the air gap and take-up speed is important regarding the permeance of the fibres. The results confirmed the trend reported earlier by Helberg that permeance increases with increasing air gap and take-up speed. All the fibres showed very low CO₂/N₂ selectivity from 4 to 17. This is attributed to the high amount of surface defects on the new spun hollow fibres. The surface defects are believed to be caused by the fact that the fibres are spun with perhaps too high air gap and too high take-up speed simultaneously. These factors increase the elongational stress, and the elongational stress became too large, so the top layer has been stretched causing holes in the surface. The hollow fibre spun using the lowest polymer dope flow rate of 1 ml/min, which further increases the elongational stress in addition to high air gap and take-up speed, had bigger holes and defects in the surface. This supports the theory that the application of too high elongational stress causes defects and holes in the surface. This fibre with the dope flow rate on 1 ml/min contains no macrovoids or very small holes, while the fibres with a dope flow rate of 2 ml/min has some fingerlike macrovoids in the structure. This indicates that the choice of dope flow rate is the most important parameter in order to produce hollow fibre membranes without macrovoids, compared to air gap and take-up speed.

6.2 PVAm/PSf FSC composite membrane

Composite membranes were prepared by coating the various PSf hollow fibres three times with 3% PVAm and one time with 5% PDMS. All the PVAm/PSf composite membranes produced during the master thesis exhibited lower values for CO₂/N₂ selectivity compared to the best obtained PVAm/PSf composite membrane from the specialization project using the same coating procedure. At 25°C, 1.2 bar and 100% relative humidity when the sweep flow rates were varied between 4 and 46 ml/min, the best PVAm/PSf composite membrane from the master thesis exhibited a CO₂ permeance between 0.15 and 0.10 m³(STP)/(m² bar h), a

CO₂/N₂ selectivity between 88 and 70 and a CO₂ purity (CO₂ permeate concentration) between 83% and 86%. The best PVAm/PSf composite membrane from the specialization project however, exhibited a slightly lower CO₂ permeance between 0.11 and 0.08 m³(STP)/(m² bar h), a CO₂/N₂ selectivity between 102 and 96 and a CO₂ purity between 87% and 90%. As the coating sequence was the same for the PVAm/PSf composite membranes, is it reasonable to believe that the difference in performance is caused by the difference in quality of the new PSf support and the PSf support produced in the specialization project. After coating with PVAm, the PVAm/PSf composite membranes produced in the master thesis experienced a large decrease in permeance by increasing feed pressure from 1.2 bar to 8 bar. The reason for this, in addition to saturation of carriers, could be that PVAm penetrated into the porous structure of the PSf support, thus preventing the gas molecules from permeating through the membrane. The penetration of PVAm into the PSf support was possible because of the large number of surface defects and holes on the surface of these PSf hollow fibre supports. These holes and defects are also believed to be a reason for the high permeance of the PSf supports before applying a selective PVAm coating layer. When tested at different pressures, the PVAm/PSf composite membrane produced in the master thesis experienced a big decrease in CO₂/N₂ selectivity from 59 at 1.2 bar to 20 at 8 bar. The reason for this is believed to be that increased pressure will reopen the previously sealed surface defects, this also showed by the fact that the N₂ permeance increases with increased pressure. It seems reasonable to conclude that the PSf support itself has a large impact on the separation properties of a FSC composite membrane, and that an optimally produced support is essential in order to successfully make a FSC composite membrane.

6.3 PVAm/PSf blend membrane

The work of increasing the PVAm concentration from 0.2% to 1% in the PVAm/PSf blend was continued during the master thesis. During the specialization project an attempt to produce 1% PVAm/PSf blend fibre membranes was not successful. The wanted result was an increase of PVAm polymer effect on the separation properties of the PVAm/PSf hollow fibres. During the master thesis, the spinning procedure was successful and the wanted spinning conditions were reached. From the DSC results, the 0.2% PVAm/PSf blend hollow fibres are very similar to the pure PSf curve, but it also has a small decrease in heat flow where pure PVAm melts. This indicates that the 0.2% PVAm/PSf blend consists of both PSf and PVAm. For the 1% PVAm/PSf DSC curve it was expected a curve that is even more similar to the pure PVAm curve, but the 1% PVAm/PSf curve was very similar to the pure PSf curve and showed no similarity to the pure PVAm curve. A reason for this result may be that PVAm and PSf had separated, because the dope solution stood idle for several days after it was prepared as the spinning rig was not available. This might have caused regions with more PVAm and regions with less or without PVAm. Another reason might be that the PVAm and PSf had reacted in the blend dope solution. This would cause the polymer blend to exhibit properties from both polymers. As the amount of PSf is much higher than the amount of PVAm, and PVAm is much more crystalline and has no clear glass transition could this explain why the DSC gives no indication of PVAm in the blend. During tests of the PVAm/PSf blend membranes with change in humidity, the 0.2% PVAm/PSf blend membrane showed a clear tendency of increasing the CO₂/N₂ selectivity as the relative humidity of the feed increased. This was expected since PVAm requires the presence of H₂O to transport CO₂. The 1% PVAm/PSf membrane however, showed a trend, but not as clear as for the 0.2% PVAm/PSf blend membrane. This result supports the theory of PVAm and PSf reacting, as the amino groups would have to be present for humidity to affect the CO₂ transportation. The results from gas permeation tests showed that the 1% PVAm/PSf blend membrane had better

separation properties than the 0.2% PVAm/PSf blend membrane. This indicates that PVAm is present in the 1% PVAm/PSf blend membrane as well, even though the DSC gave no clear evidence of PVAm. One of the 1% PVAm/PSf blend membrane exhibited a CO₂ permeance of 0.05 m³(STP)/(m² bar h) and a CO₂/N₂ selectivity from 57 to 133 when the sweep flow rate changed from 5 to 47 ml/min at 1.2 bar, 25°C and 100% relative humidity. For a pressure ranging from 1.2 bar to 8 bar, the 1% PVAm/PSf blend membrane exhibited a CO₂ permeance from 0.1 to 0.07 m³(STP)/(m² bar h) and a CO₂/N₂ selectivity from 70 to 56.

The PVAm/PSf blend membrane has lower CO₂/N₂ selectivity than the best PVAm/PSf composite membrane, when tested for pressure influence. During sweep tests, the 1% PVAm/PSf blend membrane obtained the best CO₂/N₂ selectivity. The good CO₂/N₂ selectivity obtained is a clear indication that PVAm is present in the membrane and has a positive effect. The results do not show a clear trend of which membranes that have the highest CO₂ permeance, a PVAm/PSf blend membrane or a composite membrane. It seems that the CO₂ permeance is mostly dependent on the morphology of hollow fibres rather than the preparation procedure (coating versus blending). In the attempt to optimize the hollow fibre, the CO₂ permeance increased but the CO₂/N₂ selectivity has been reduced.

Chapter 7: Further work

7.1 Optimizing the PSf hollow fibre support

The experiments of optimizing the PSf support were not completely successful, and must be continued. The PSf support is essential in order to get a good composite membrane. The air gap and the take-up speed were increased to higher values, based on initial spinning results using the old spinning machine. These results indicated that further increasing the air gap and take-up speed, would give a fibre with good porous morphology and a dense surface. But the hollow fibres obtained using the new high speed spinning machine shows that elongational stress induced by these spinning conditions probably were too high, so the top layer has been stretched causing holes and defects in the surface. For further work the air gap and take-up speed should be increased separately. The air gap should be increased gradually from 28 to 60 cm, with intermediate spinnings of PSf hollow fibres at for example 30 cm, 40 cm, 50 cm and 60 cm to find the optimal air gap while the take-up speed is kept at quite low values. The same procedure should be used for the take-up speed, with a gradual increase at for example 10 m/min, 15 m/min, 20 m/min and continue as high as possible without breaking the fibres. The dope flow rate should be kept at 1 ml/min because the fibres spun at this dope flow rate were the fibres with fewest macrovoids in the structure.

7.2 Further investigation of PVAm/PSf composite membrane

Due to the high amount of surface defects of the PSf hollow fibres coated in the preparation of PVAm/PSf composite membranes, some PVAm probably penetrated into the pores of the support, which reduced the permeance. This shows the importance of having a good support, and the importance of optimizing the spinning process. If the support is produced successfully without surface defects or holes and coated with PDMS, is it possible that the number of coatings with 3% PVAm could be reduced from three to two without impairing the CO₂/N₂ selectivity. This could enhance the permeance of the composite membrane and would save both time and the amount of PVAm used for coating. PVAm/PSf composite membranes should be tested both for sweep gas at 100% and 0% relative humidity, to see if the PVAm/PSf composite membranes experience an increase in the separation properties when the relative humidity of the sweep gas is decreased to 0%. A relative humidity of 0% for the sweep gas could enhance the separation properties of the membrane as this prevents blocking of pores due to condensation of water.

7.3 Further investigation of PVAm/PSf blend membrane

The 1% PVAm/PSf blend membrane spun in the master thesis yielded better separation properties than the 0.2% PVAm/PSf blend membrane, and it is apparent that adding more PVAm to the spinning dope has had a clear effect on the separation performance of the membranes. During the investigation of the blend composition by DSC, PVAm was not clearly detected, and this could indicate that the blend solution had been prepared too long in advance of spinning and that PVAm and PSf had separated before spinning. Another reason could be that the PSf and the PVAm has reacted in the polymer blend solution. When tested with humidity, a slight trend of increasing CO₂/N₂ selectivity with increasing relative humidity of the feed was detected. It should for further production of PVAm/PSf blend membranes be attempted to carry out the spinning process as quickly as possible after the blend spinning dope solution is completed, in order to investigate if any of the theories can be confirmed, or if there is a combination of both effects. When the optimal spinning conditions for production of the PSf support hollow fibre are found, a PVAm/PSf blend membrane

should also be produced using the optimal air gap and take-up speed to provide a PVAm/PSf blend membrane with better morphology which could give better separation properties. Also for the PVAm/PSf blend membranes, the effect on the separation properties when the relative humidity is decreased to 0% for the sweep gas should be investigated.

Chapter 8: References



1. United Nations Framework Convention on Climate Change, *Kyoto Protocol*, http://unfccc.int/kyoto_protocol/items/2830.php 21.05.2012 09:42, United Nations, 1998
2. Kim, T.-J., Uddin, M.W., Sandru, M., Hägg, M.-B., *The effect of contaminants on the composite membranes for CO₂ separation and challenges in up-scaling of the membranes*. Energy Procedia 2011. p. 737-744
3. Galán Sánchez, L.M., *Functionalized Ionic Liquids, Absorption Solvents for Carbon Dioxide and Olefin Separation*, 2008, Gildeprint.
4. Låg, M. et al., *Health effects of amines and derivatives associated with CO₂ capture*, 2011, Published by The Norwegian Institute of Public Health, Division of Environmental Medicine.
5. Mulder, M., *Basic principles of membrane technology*. Second edition 2003, Dordrecht: Kluwer Academic Publishers.
6. Powell, C.E. and G.G. Qiao, *Polymeric CO₂/N₂ gas separation membranes for the capture of carbon dioxide from power plant flue gases*. Journal of Membrane Science, 2006. p. 1-49.
7. Robeson, L.M., *Correlation of separation factor versus permeability for polymeric membranes*. Journal of Membrane Science, 1991. p. 165-185.
8. Robeson, L.M., *The upper bound revisited*. Journal of Membrane Science, 2008. p. 390-400.
9. Henis, J.M.S. and M.K. Tripodi, *Composite hollow fiber membranes for gas separation: the resistance model approach*. Journal of Membrane Science, 1981. p. 233-246.
10. Kim, T.-J., B. Li, & M.-B. Hägg, *Novel fixed-site-carrier polyvinylamine membrane for carbon dioxide capture*. Journal of Polymer Science Part B: Polymer Physics, 2004. p. 4326-4336.
11. Johannessen, P.-K., *Hollow fibre membrane preparation and investigations for CO₂ capture*. Specialization project, 2011, Norwegian University of Science and Technology, NTNU Trondheim
12. Helberg, R.M.L, *Hollow fiber membranes for CO₂ capture- PSf hollow fibers preparation*. Master thesis, 2010, Norwegian University of Science and Technology, NTNU Trondheim.
13. Pinnau, I., and Koros, W.J., *Relationship between Substructure and Resistance and Gas Separation Properties of Defect-Free Integrally Skinned Asymmetric Membranes*. Ing.Eng.Chem.Res, 1991. p. 1837-1840

14. Clausi, D.T., Mckelvey, S.A., Koros, W.J., *Characterization of substructure resistance in asymmetric gas separation membranes*. Journal of Membrane Science, 1999. p. 51-64
15. Sandru, M., *Development of a FSC membrane for selective CO₂ capture*. Doctoral thesis 2009. Department of Chemical Engineering, NTNU
16. Baker, R.W., *Membrane technology and applications*. 2004, McGraw-Hill
17. Widjojo, N., and Chung, T.-S., *Thickness and Air Gap Dependence of Macrovoid Evolution in Phase-Inversion Asymmetric Hollow Fiber Membranes*. Industrial & Engineering Chemistry Research, 2006. p. 7618-7626.
18. Smolders, C., et al., *MICROSTRUCTURES IN PHASE-INVERSION MEMBRANES .1. FORMATION OF MACROVOIDS*. Journal of Membrane Science, 1992. p. 259-275.
19. Strathmann, H., and Kock, K., *The formation mechanism of phase inversion membranes*. Desalination, 1977. p. 241-255
20. Peng, N., Chung, T.-S. and Wang, K.Y., *Macrovoid evolution and critical factors to form macrovoid-free hollow fiber membranes*. Journal of Membrane Science, 2008. p. 363-372.
21. Bird, R.B., Armstrong, R.C., and Hassager, O., *Dynamics of polymeric liquids*. Fluid mechanics, volume 1, second edition 1987, New York, Wiley
22. Bird, R.B., Stewart, W.E., and Lightfoot, E.N., *Transport Phenomena*. second edition 2002, New York, Wiley
23. Wang, D., Teo, W.K., and Li, K., *Preparation and characterization of high-flux polysulfone hollow fibre gas separation membranes*. Journal of Membrane Science, 2002. p. 247-256.
24. van de Witte, P., et al., *Phase separation processes in polymer solutions in relation to membrane formation*. Journal of Membrane Science, 1996. p. 1-31.
25. Aroon, M.A., et al., *Morphology and permeation properties of polysulfone membranes for gas separation: Effects of non-solvent additives and co-solvent*. Separation and Purification Technology, 2010. p. 194-202.
26. Ding, X., et al., *Fabrication Matrimid/polysulfone dual-layer hollow fiber membranes for CO₂/N₂ separation*. Journal of Membrane Science, 2008. p. 352-361
27. McKelvey, S.A., Clausi, D.T., and Koros, W.J., *A guide to establishing hollow fiber macroscopic properties for membrane applications*. Journal of Membrane Science, 1997. p. 223-232.
28. Tsai, H.A., et al., *Morphology control of polysulfone hollow fiber membranes via water vapor induced phase separation*. Journal of Membrane Science, 2006. p. 390-400.

29. Helberg, R.M.L, *Hollow fiber membranes for CO₂ capture- PSf hollow fibers preparation*. Specialization project 2010, Trondheim: Norwegian University of Science and Technology
30. Kapantaidakis, G.C., Koops, G.H., Wessling, M., *Effect of spinning conditions on the structure and the gas permeation properties of high flux polyethersulfonepolyimide blend hollow fibers*. Desalination, 2002. p 121-125.
31. Wallace, D.W., Staudt-Bickel, C., and Koros, W.J., *Efficient development of effective hollow fiber membranes for gas separations from novel polymers*. Journal of Membrane Science, 2006. p. 92-104
32. Qin, J., and Chung, T.S., *Effect of dope flow rate on the morphology, separation performance, thermal and mechanical properties of ultrafiltration hollow fiber membranes*. Journal of Membrane Science, 1999. p. 35-51
33. Aroon, M.A., Ismail, A.F., Montazer-Rahmati, M.M., Matsuura, T., *A mathematical analysis of hollow fiber spinning: Bore and dope velocity profiles in the air gap*. Journal of Membrane Science, 2009. p. 13-20
34. Rahbari-Sisakh, M., Ismail, A.F., and Matsuura, T., *Effect of bore fluid composition on structure and performance of asymmetric polysulfone hollow fiber membranes contactor for CO₂ absorption*. Separation and Purification Technology, 2011. p. 99-106
35. Qin, J.-J., and Chung, T.-S., *Effect of orientation relaxation and bore fluid chemistry on morphology and performance of polyethersulfone hollow fibers for gas separation*. Journal of Membrane Science, 2004. p. 1-9
36. Sandru, M., Haukebø, S.H., and Hägg, M.-B., *Composite hollow fiber membranes for CO₂ capture*. Journal of Membrane Science, 2009. p. 172-186.
37. Chen, H.Z., Xiao, Y.C and Chung, T.-S., *Multi-layer composite hollow fiber membranes derived from poly(ethyleneglycol)(PEG) containing hybrid materials for CO₂/N₂ separation*. Journal of Membrane Science, 2011. p. 211-220.
38. He, T., Frank, M., Mulder, M.H.V and Wessling, M., *Preparation and characterization of nanofiltration membranes by coating polyethersulfone hollow fibers with sulfonated poly(ether ether ketone) (SPEEK)*. Journal of Membrane Science, 2007. p. 62-72.
39. Burggraaf, A.J. & Cot, L. *Fundamentals of Inorganic Membrane Science and Technology*, 1996, Elsevier Science B.V
40. He, T., Mulder, M.H.V., Strathmann, H., and Wessling, M., *Preparation of composite hollow fibre membranes: co-extrusion of hydrophilic coatings onto porous hydrophobic support structures*. Journal of Membrane Science, 2002. p. 143-146.
41. Ji, P., et al., *Impacts of coatings condition on composite membrane performance for CO₂ separation*. Separation and purification technology, 2009. p. 160-167
42. Shieh, J.-J., Chung, T.-S., and Paul, D.R, *Study on multi-layer composite hollow fiber membranes for gas separation*. Chemical Engineering Science. 1998. p. 675-684

43. Kai, T et al., *Development of commercial-sized dendrimer composite membrane modules for CO₂ removal from flue gas*, Separation and Purification Technology, 2008, p 524-530
44. Chung, T.-S., et al., *Fabrication of multi-layer composite hollow fiber membranes for gas separation*. Journal of Membrane Science, 1999. p. 211-225.
45. Hwang, H.Y., et al., *The effect of operating condition on the performance of hollow fiber membrane modules for CO₂/N₂ separation*. Journal of Industrial and Engineering Chemistry, 2011. p. 205-211
46. Sandru, M., Kim, T-J., Hägg, M-B., *High molecular fixed-site-carrier PVAm membrane for CO₂ capture*. Desalination, 2008. p. 298-300
47. Painter, P. C & Coleman M. M., *Fundamentals of polymer science*. Second edition 1997, CRC Press
48. Geankoplis, C. J., *Transport processes and separation process principles*. Fourth edition 2003, New Jersey: Pearson Educations, Inc
49. Yampolskii, Y., and Freeman, B., *Membrane Gas Separation*. First edition 2010, Chichester, United Kingdom: John Wiley & Sons Ltd.
50. Yampolskii, Y., Pinnau, I., and Freeman, B., *Materials Science of Membranes for Gas and Vapor Separation*. 2006, Chichester, England: John Wiley & Sons, Ltd.
51. Hussain, A., Hägg, M.-B., *A feasibility study of CO₂ capture from flue gas by a facilitated transport membrane*. Journal of Membrane Science, 2009. p. 140-148
52. Li, N. et al., *Advanced Membrane Technology and Applications*. 2008, John Wiley & Sons
53. Dean, J.A. *The Analytical Chemistry Handbook*, McGraw Hill, Inc., 1995
54. Walpole, R.E., Myers, R.H., Myers, S.L., and Ye, K., *Probability & Statistics for Engineers & Scientists*. Eight edition 2006, Pearson International Edition

Appendix A: Risk assessment

NTNU	Hazardous activity identification process				Risikovurdering	Nummer	Dato	
					HMS-avd.	HMSRV2601	17.01.2012	
HMS					Godkjent av	Side	Erstatter	
						1		
Unit:					<i>Kjemisk prosess teknologi</i>	Date:	17.01.2012	
Line manager:					<i>Øyvind Gregersen</i>			
Participants in the identification process (including their function):					Petra-Kristine Johannessen			
Short description of the main activity/main process:					Gas permeation tests and production of hollow fibres			
ID no.	Activity/process	Responsible person	Laws, regulations etc.	Existing documentation	Existing safety measures	Comment		
1	Working with compressed gases at maximum 8 bars	Dr Marius Sandru		HSE datasheets, Instrument description	Safety valve.	At emergency shut-down, close gas cylinders and turn off electrical devices.		
2	Working with flammable liquids: Tetrahydrofuran and Hexan	Dr Marius Sandru		HSE datasheets description	Fire extinguisher, eye protection, lab coat, ventilation cabinet, emergency shower	Keep away from sources of ignition - No smoking. Take precautionary measures against static discharges.		
3	Working with liquid nitrogen	Dr Marius Sandru		HSE Datasheet	Lab coat, eye protection, gloves			
4	Working with toxic compounds: 1-Methyl-2-pyrrolidinone, Tetrahydrofuran, Hexane, Etylene glycol	Dr Marius Sandru		HSE Datasheets, International Chemical Safety Cards	Eye protection, lab coat, gloves, ventilation cabinet, emergency shower and eye wash.	Hexane is marked as a rep2 compound.		
	Spinning of fibre							
5	Water spill caused by too high pressure in the hoses	Dr Marius Sandru		HSE datasheets, Instrument	Wear non-slippery shoes	Clean up the spilled water		
6	Chaos of hoses and cables	Dr Marius Sandru		HSE datasheets, Instrument	Wear non-slippery shoes	Clean up the hoses and cables		
7	Wet floor	Dr Marius Sandru		HSE datasheets, Instrument	Wear non-slippery shoes	Clean up the spilled water		

Risk assessment



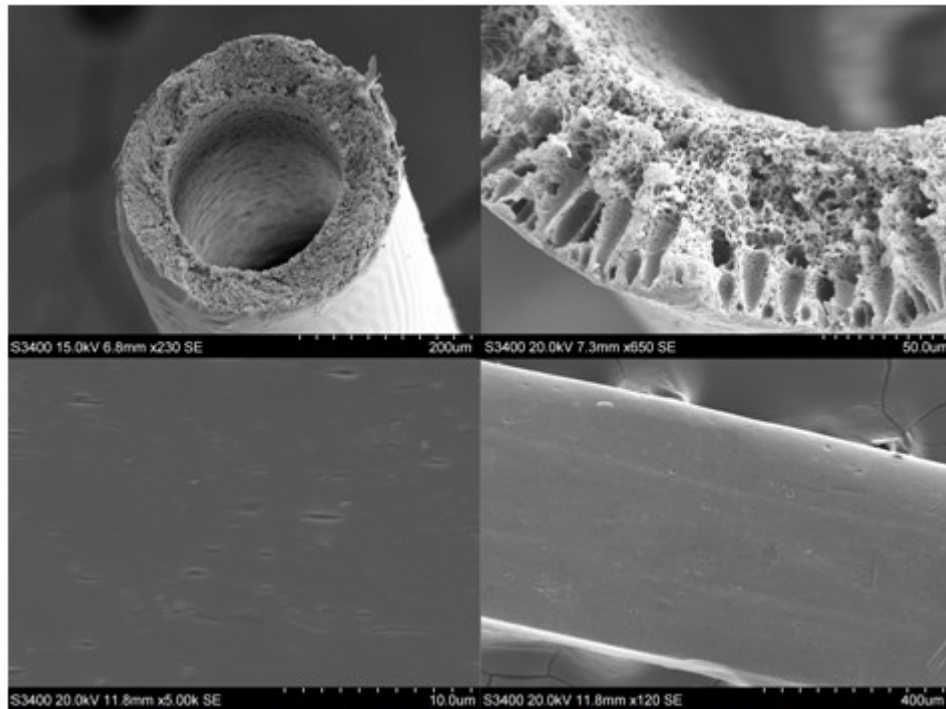
Unit: *Kjemisk prosess teknologi* **Date:** 17.01.2012
Line manager: *Øyvind Gregersen*
Participants in the identification process (including their function): *Petra-Kristine Johannessen*
Signature: Petra-Kristine Johannessen

ID no.	Activity from the identification process form	Potential undesirable incident/strain	Likelihood:	Consequence:				Risk value	Comments/status Suggested measures
			Likelihood (1-5)	Human (A-E)	Environment (A-E)	Economy/material (A-E)	Reputation (A-E)	Human	
1	Working with compressed gases at maximum 8 bars	Rapid pressure release	3	B				B3	At emergency shut-down, close gas cylinders and turn off electrical devices.
2	Working with flammable liquids: Tetrahydrofuran and Hexan	Fire	1	C				C1	Remove all sources of ignition. Beware of vapors accumulating to form explosive concentrations. Vapors can accumulate in low areas.
3	Working with liquid nitrogen	Frost injury	2	A				A2	Lab coat, gloves, eye protection
4	Working with toxic compounds: 1-Methyl-2-pyrrolidinone, Tetrahydrofuran, Hexane, Etylene glycol	Intoxication	2	C				C2	Wear respiratory protection. Avoid breathing vapors, mist or gas. Ensure adequate ventilation. Hand protection, skin and body protection.
Spinning of fibre									
5	Water spill caused by too high pressure in the hoses	Slip and fall	2	B				B2	Clean up the spilled water
6	Chaos of hoses and cables	Stumble and fall	3	B				B3	Clean up the hoses and cables
7	Wet floor	Slip and fall	3	B				B3	Clean up the spilled water

Minimal 1	Low 2	Medium 3	High 4
Once every 50 years or less	Once every 10 years or less	Once a year or less	Once a month or less
Grading	Human	Environment	Financial/material
E Very critical	May produce fatality/ies	Very prolonged, non-reversible damage	Shutdown of work >1 year.
D Critical	Permanent injury, may produce serious serious health damage/sickness	Prolonged damage. Long recovery time.	Shutdown of work 0.5-1 year.
C Dangerous	Serious personal injury	Minor damage. Long recovery time	Shutdown of work < 1 month
B Relatively safe	Injury that requires medical treatment	Minor damage. Short recovery time	Shutdown of work < 1week
A Safe	Injury that requires first aid	Insignificant damage. Short recovery time	Shutdown of work < 1day

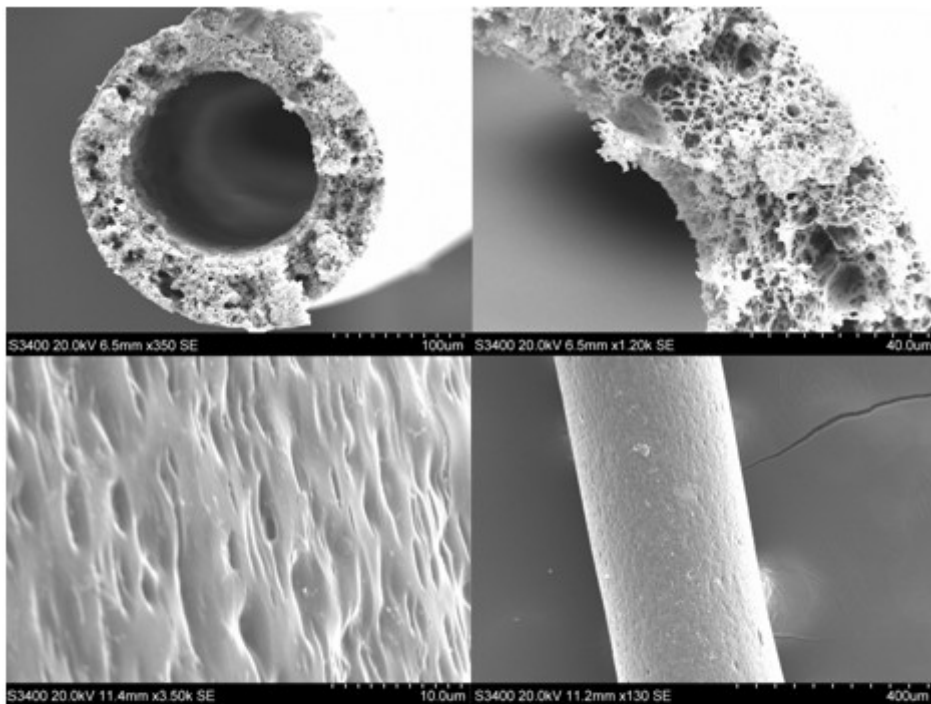
Appendix B: SEM pictures

B.1 SEM pictures for spinning 1 (Blend membranes)



*Dope 32 wt% PSf, 43 wt% NMP, 15 wt% THF, 1 wt% PVAm in 9 wt% ethylene glycol
dope flow rate 1 ml/min, Bore 80/20 NMP/Water, bore flow rate 0.65 ml/min, Temperature 25 °C,
Air gap 28 cm, take up speed 8 m/min*

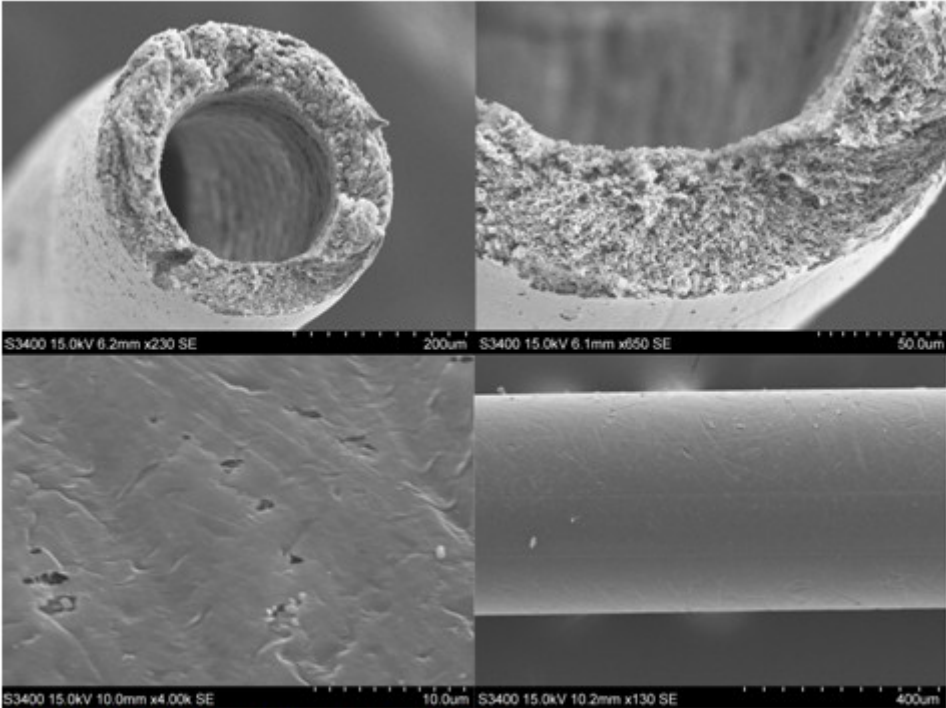
Figure B.1.1: SEM pictures 1% PVAm/PSf blend hollow fibre nr1



*Dope 32 wt% PSf, 43 wt% NMP, 15 wt% THF, 1 wt% PVAm in 9 wt% ethylene glycol
dope flow rate 0.5 ml/min, Bore 80/20 NMP/Water, bore flow rate 0.32 ml/min, Temperature 25 °C
Air gap 28 cm, take up speed 8 m/min*

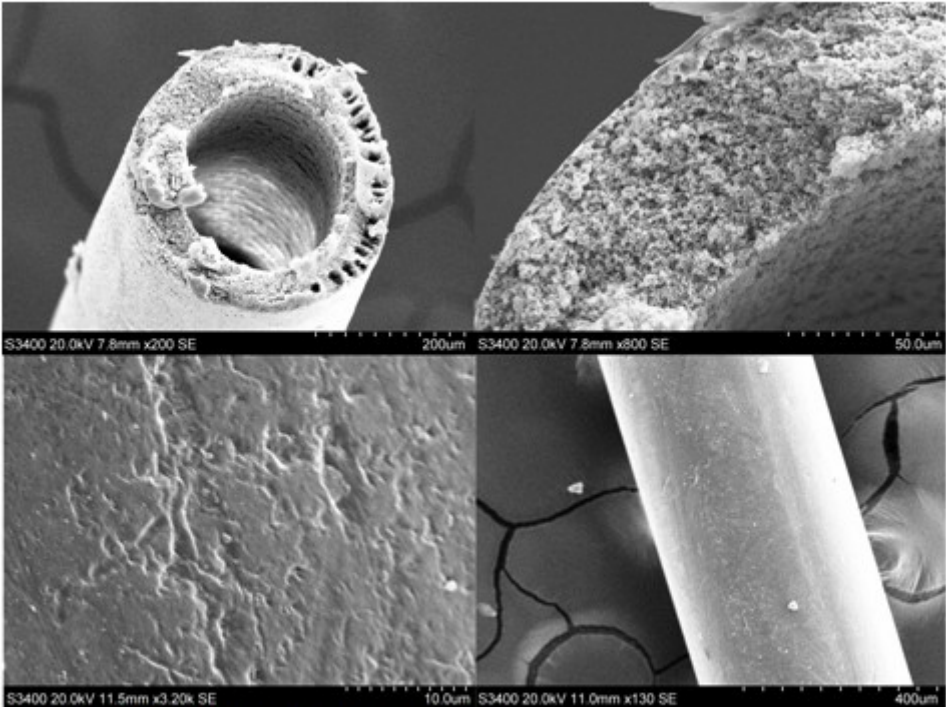
Figure B.1.2: SEM pictures 1% PVAm/PSf blend hollow fibre nr 2

B.2 SEM pictures for spinning 2 (PSf support)



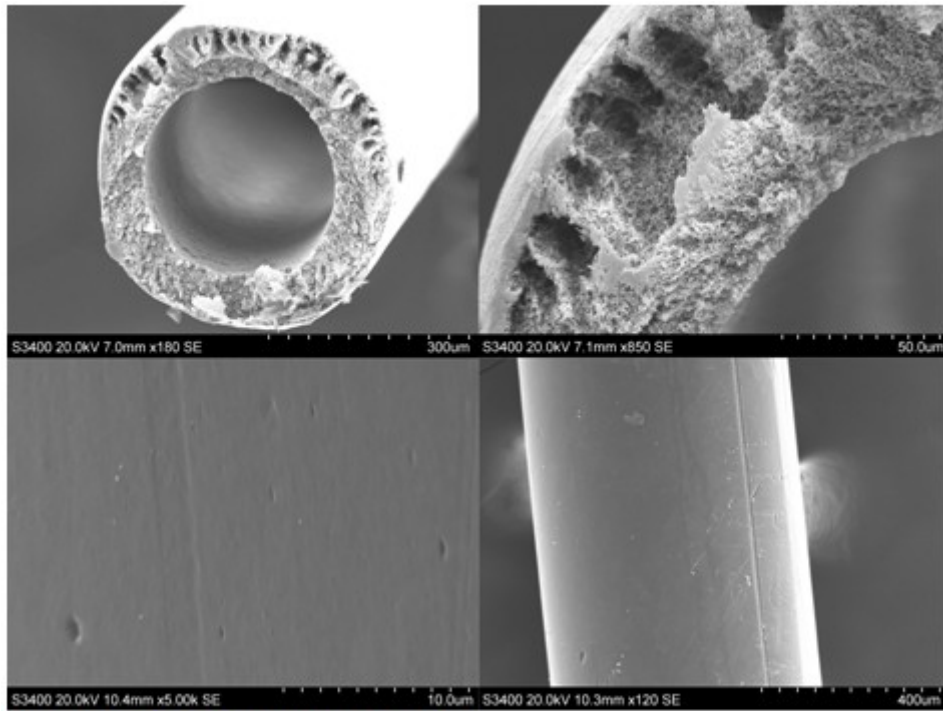
*Dope 32 wt% PSf, 58 wt% NMP, 10 wt% glycerol
dope flow rate 1 ml/min, Bore 80/20 NMP/Water, bore flow rate 0.65 ml/min, Temperature 25 °C,
Air gap 61 cm, take up speed 16 m/min*

Figure B.2.1: SEM pictures of PSf fibre B



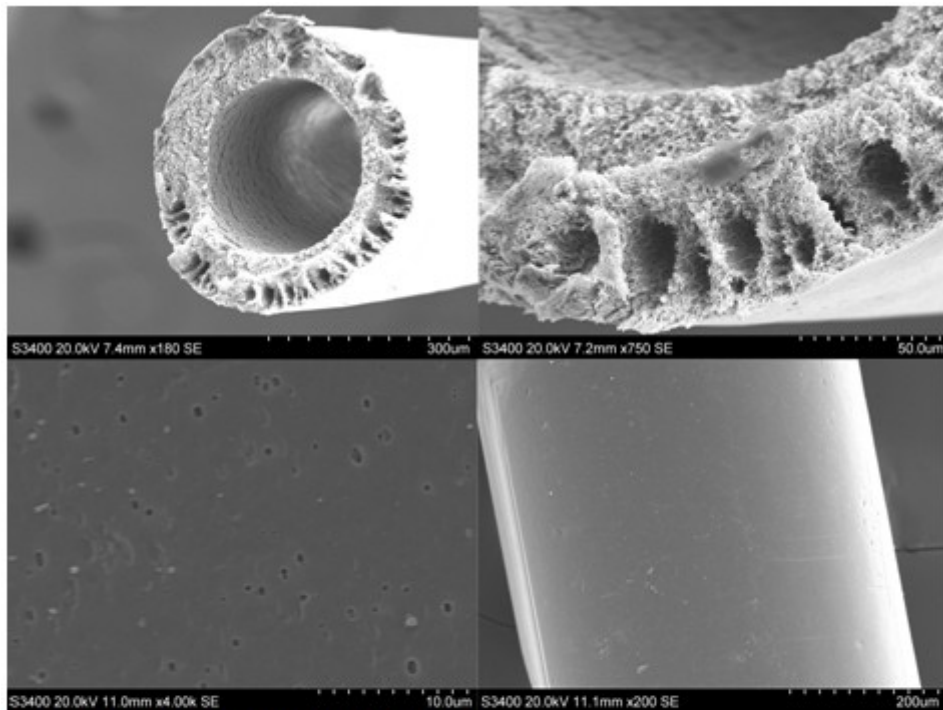
*Dope 32 wt% PSf, 58 wt% NMP, 10 wt% glycerol
dope flow rate 2 ml/min, Bore 80/20 NMP/Water, bore flow rate 1.3 ml/min, Temperature 25 °C,
Air gap 61cm, take up speed 20 m/min*

Figure B.2.2: SEM pictures of PSf fibre J



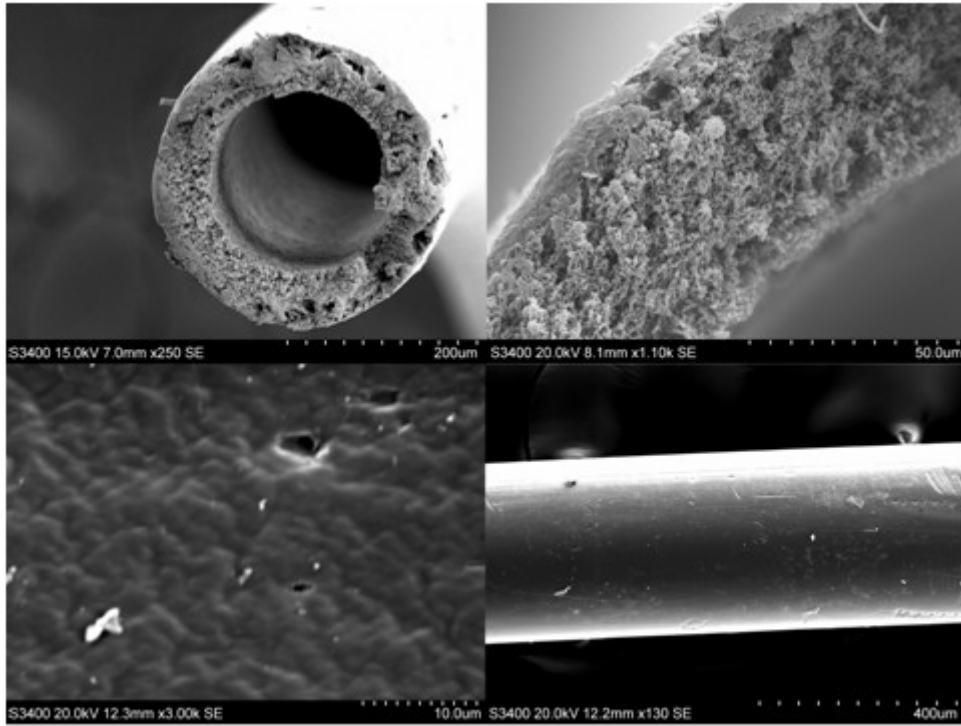
*Dope 32 wt% PSf, 58 wt% NMP, 10 wt% glycerol
dope flow rate 2 ml/min, Bore 80/20 NMP/Water, bore flow rate 1.3 ml/min, Temperature 25 °C,
Air gap 61cm, take up speed 10 m/min*

Figure B.2.3: SEM pictures of PSf fibre M



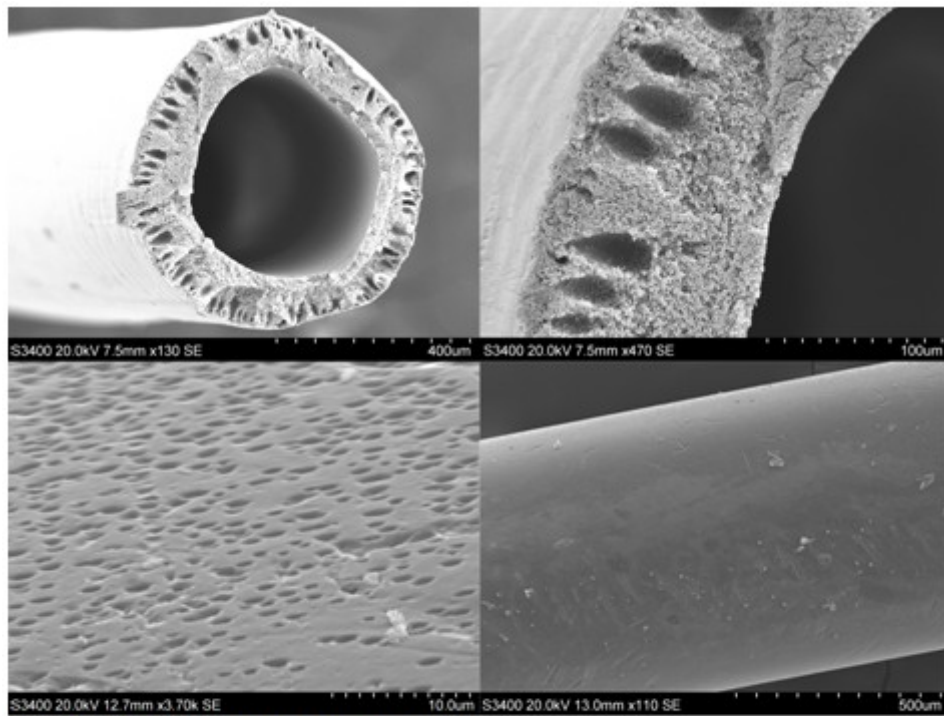
*Dope 32 wt% PSf, 58 wt% NMP, 10 wt% glycerol
dope flow rate 2 ml/min, Bore 80/20 NMP/Water, bore flow rate 1.3 ml/min, Temperature 25 °C,
Air gap 61cm, take up speed 14 m/min*

Figure B.2.4: SEM pictures of PSf fibre N



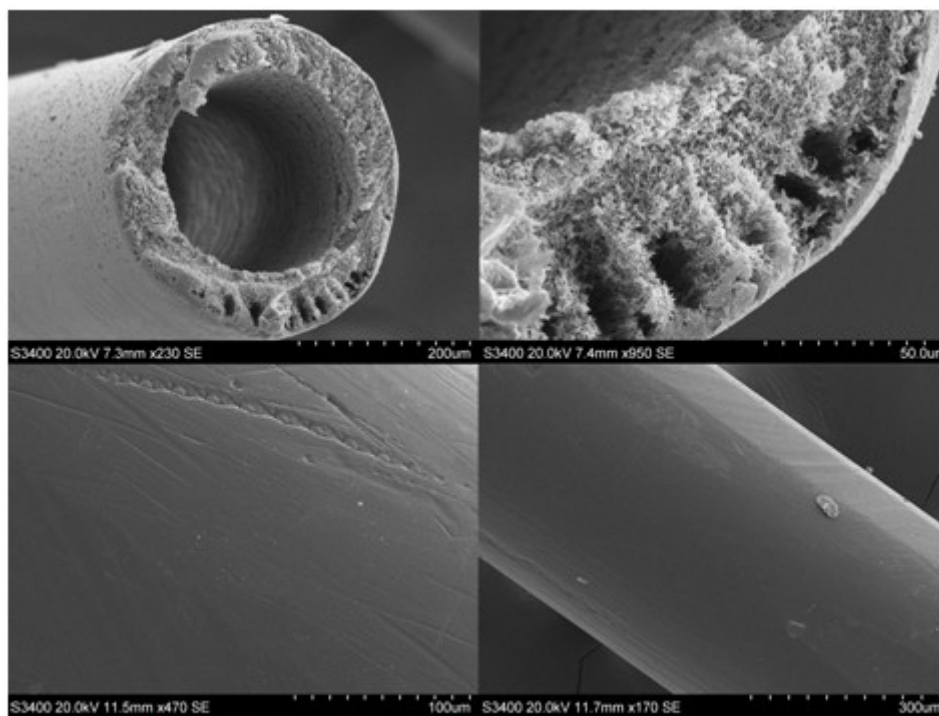
*Dope 32 wt% PSf, 58 wt% NMP, 10 wt% glycerol
dope flow rate 1 ml/min, Bore 80/20 NMP/Water, bore flow rate 0.65 ml/min, Temperature 25 °C,
Air gap 50 cm, take up speed 10 m/min*

Figure B.2.5: SEM pictures of PSf fibre O



*Dope 32 wt% PSf, 58 wt% NMP, 10 wt% glycerol
dope flow rate 2 ml/min, Bore 80/20 NMP/Water, bore flow rate 1.3 ml/min, Temperature 25 °C,
Air gap 50 cm, take up speed 8 m/min*

Figure B.2.6: SEM pictures of PSf fibre P



*Dope 32 wt% PSf, 58 wt% NMP, 10 wt% glycerol
dope flow rate 2 ml/min, Bore 80/20 NMP/Water, bore flow rate 1.3 ml/min, Temperature 25 °C,
Air gap 61 cm, take up speed 18 m/min*

Figure B.2.7: SEM pictures of PSf fibre W